Jason W. Rueter. A MULTIVARIATE APPROACH TO ESTABLISH HABITAT CLASSIFICATIONS IN A CORAL REEF ECOSYSTEM USING LANDSAT 7 SATELLITE IMAGERY AT TURNEFFE ATOLL, BELIZE, CENTRAL AMERICA. (Under the direction of Dr. Joseph J. Luczkovich). Department of Biology, April 2004.

The use of multivariate cluster and discriminant function analysis of ground truth data and LANDSAT 7 satellite imagery (23 May 2000) was examined to classify tropical marine habitats at Turneffe Atoll, Belize. Ground truth data were obtained using SCUBA, digital video and the global positioning system in June 2000 and July 2001. Ground truthing was done by swimming along eleven 150- to 300-meter transect lines located on the southeastern side of the atoll and videotaping bottom habitat from 1.5 m above the bottom at 30-meter intervals (126 sites). The still images were displayed on a 21cm x 29 cm flat-screen monitor, overlaid with a 20-cell grid (5.25 cm x 5.80 cm cells), and % cover of seven bottom cover classes was computed. Using hierarchical cluster analysis of water depth and habitat percent cover data, the 126 sites were grouped into three distinct habitat clusters (sand, seagrass and coral reef habitats). A discriminant analysis of the sites was performed using LANDSAT digital values in enhanced thematic mapper (ETM+) Bands 1, 2, 3, and 4 (the only ones that penetrate water) as predictors of habitat cluster membership. When predicting the habitat class of the sites used for training, coral reef areas were correctly classified 100%, seagrass areas 80 %, and sand dominated areas 77 % of the time. Using the classification function from the discriminant analysis, the LANDSAT 7 image was recoded to create a habitat map of the region surrounding Turneffe Atoll, showing coral reef, seagrass, and sand-dominated regions.

Using the recoded map, new ground truth sites were visited in 2002 to record depth and benthic classification. The recoded map had an overall accuracy of 60% and a τau coefficient of 52.47%. Such maps can be used to identify essential fish habitat areas and study changes in habitat area over time.

A MULTIVARIATE APPROACH TO ESTABLISH HABITAT CLASSIFICATIONS IN A CORAL REEF ECOSYSTEM USING LANDSAT 7 SATELLITE IMAGERY AT TURNEFFE ATOLL, BELIZE, CENTRAL AMERICA.

A Thesis

Presented to

The Faculty of the Department of Biology

East Carolina University

In Partial Fulfillment

of the Requirements for the Degree

Master of Science in Biology

By

Jason Walter Rueter

March 2004

A MULTIVARIATE APPROACH TO ESTABLISH HABITAT CLASSIFICATIONS IN A CORAL REEF ECOSYSTEM USING LANDSAT 7 SATELLITE IMAGERY AT TURNEFFE ATOLL, BELIZE, CENTRAL AMERICA.

by

Jason Walter Rueter

APPROVED BY:

DIRECTOR OF THESIS

Joseph J. Luczkovich, Ph. D.

COMMITTEE MEMBER

Gerhard W. Kalmus, Ph. D.

COMMITTEE MEMBER

Roger A. Rulifson, Ph. D.

COMMITTEE MEMBER

Yong Wang, Ph. D.

Chair of the Department of Biology:

Ronald J. Newton, Ph. D.

Interim Dean of the Graduate School:

Paul D. Tschetter, Ph. D.

Acknowledgements

I would like to sincerely thank Dr. Joseph J. Luczkovich for all that he has done for me from getting me into the Graduate program through the completion of this thesis. I would also like to thank Dr. Gerhard Kalmus and the Biology Graduate Department for their generous help in making this thesis possible. Dr. Roger Rulifson, and Dr. Yong Wang have been very generous with their support and guidance in this thesis and throughout my years in school.

I would also like to thank Eden Garcia and the Institute of Marine Science at Belize University for their assistance in this project. The facilities and the people at IMS went above and beyond time and again with their support. In addition, the staff at ECU's dive safety office headed by Steve Sellers was extremely helpful in providing needed equipment and training for this thesis. I would also like to thank the numerous undergraduate and graduate students as well as Dr. Peter Sale's Mesoamerican Barrier Reef Initiative group who helped with data collection and gave their support to me throughout this thesis.

Finally, I would like to thank my parents, Curtis and Carol Rueter, for their years of support, without which none of this would have been possible. I would also like to thank my grandparents, Barbara and Charles Tillman, and my aunt and uncle, Sandra and Richard Goodman, for their financial support and belief in me.

Thank you to all of you who helped, I am forever indebted.

Table of Contents

List of Tables

List of Figures

Introduction

Background

Fisheries biologists would like to measure the amount of available essential habitat that fish use as spawning, feeding and shelter sites (Baird 1999, Rubec *et al.* 1999). Maps of the benthic habitats in coastal areas are important so that coastal planners and managers can monitor changes in habitats over time, ecologists can understand the natural habitat associations of continuously varying communities of organisms, and develop marine protected areas and coastal zone management plans (McField *et al.* 1996). In tropical coastal zones, the main aquatic habitat type is coral reefs and their associated seagrass and mangrove habitats. The habitat maps are widely regarded to be an essential data source for coastal management planning and establishing marine protected areas (Cendrero 1989, McNeill 1994, Kenchington and Claasen 1998). In addition, ecologists want to have such maps to understand habitat distribution on large areal extents so that they can understand habitat associations of organisms, examine the influence of habitat on animal abundance and distribution patterns, and plan biological sampling programs (Aronson and LeFloc'h 1996). In tropical coastal ecosystems, habitat patterns and animal associations must be discerned over areas that are hundreds of square kilometers. With such areal extent, it is useful to establish habitat patterns and community associations in small regions, and then extrapolate these associations to a large area plotted on a map.

One approach to delimit habitat is to use satellite remote sensing to study the benthic cover available as fish habitat. This approach is especially useful in the clear waters of the tropics and on coral reefs, where visible wavelengths of light penetrate the waters and the reflectance from the bottom can be measured by a satellite sensor (Lyzenga 1981, Jupp *et al.* 1985, Luczkovich *et al.* 1993). Not only do these images cover large geographic areas, but also repetitive images can be captured consistently over time (Luczkovich *et al.* 1991, Holden and LeDrew 1999). Mumby *et al.* (1999) reported that satellite remote sensing techniques are cost-effective and accurate in studying coral reefs as compared with aerial photography data sources. In their study, the authors concluded that LANDSAT thematic mapper (TM) satellite digital data were found to be more cost effective and less time consuming to acquire and process than using airborne sensors (Mumby *et al.* 1999). Landsat TM is also significantly more accurate than other satellite sensors (overall accuracy 73%) for mapping at coarse descriptive resolution (i.e. four habitat classes; sand, coral, algae, seagrass) (Mumby *et al.* 1997). However it is not clear how many habitat classes are biologically relevant in such a study. Habitat classifications that are discernable from satellite imagery may not correspond to useful habitat classifications that are used differently by fishes or other mobile organisms.

This study is an attempt to characterize and map available fish habitat from space along the coastal reefs of Belize for ultimate use in developing marine protected areas (MPA) and coastal zone management plans. I will attempt to derive biologically relevant habitat classes from the underlying bottom habitat (using digital video ground truthing) and relate them to Landsat ETM+ digital data to use in habitat classification over a larger area. Multivariate cluster and discriminant function analysis (DFA) of ground truth data and LANDSAT 7 satellite imagery were used to classify tropical marine habitats at Turneffe Atoll, Belize (Figure 1). The objectives of this study were (1) to obtain ground-truth data of benthic habitats and depth using underwater digital video and (2) to assess the similarity of the habitats statistically using optimization cluster analysis to define natural habitat classes; (3) to use Landsat 7 satellite data as a predictor of the benthic habitat classes as defined by the cluster analysis in objective (2) in a discriminant function analysis; and (4) to ground-truth predictions of the discriminant function analysis so that prediction accuracy of the Landsat data can be estimated for this habitat map in Belize.

Belize was chosen as the study site of this project for several reasons. Belize is home to the second largest barrier reef system in the world and the only barrier reef system in the Western hemisphere. It is also a rapidly growing nation that relies heavily on the reefs for sustenance as well as tourism, but is increasingly under pressure from coastal development, coral reef bleaching events, pollution, and habitat destruction (McField et al. 1996). The tourism industry accounted for 20.6 % of the Gross Domestic Product in 1998 and 19.3 % in 1999 (Belize Audubon Society).

The Turneffe Atoll island chain, where this study took place, is currently under consideration for marine protected area (MPA) status, has a history of research, and is home to several current projects including a Bonefish and Tarpon Unlimited (www.tarbone.org) project as well as the Mesoamerican Barrier Reef Initiative (Sale *et al.* 2001).

Figure 1. Map of Central America and the Caribbean showing the location of Belize (www.geographynetwork.com).

LANDSAT and Enhanced Thematic Mapper (ETM+)

LANDSAT 7 is a U.S. satellite used to acquire remotely sensed images of the Earth's surface. It was launched on April 15, 1999 from Vandenberg Air Force Base in California as part of the National Aeronautic and Space Administration's (NASA) Earth Observing System (EOS)(Landsat.gsfc.nasa.gov). Landsat 7 collects 532 scenes/day from an orbit of 705 km above the Earth's surface at an inclination of 98.2° and has a revisit period (of the same location on the Earth) every 16 days. The satellite is equipped with an Enhanced Thematic Mapper+ (ETM+). The ETM+ consists of advanced, multispectral scanners with eight bands designed to achieve higher image resolution, sharper spectral separation, improved geometric fidelity and greater radiometric accuracy and resolution than previous sensors. Landsat ETM+ data are sensed in eight spectral bands simultaneously. Bands 1-5 and 7 have a resolution of 30 x 30 m while band 6 has a resolution of 60 x 60 m. Band 8, a panchromatic band has a resolution of 15 m x 15m (Table 1). The spectral characteristics of each band can also be seen in Table 1.

Using Landsat satellite data for coral reef monitoring has many advantages. The Landsat 7 satellite imagery and images obtained from its predecessors (Landsat 4 & 5) have been investigated by a number of researchers since their launches to examine their usefulness and effectiveness in mapping and monitoring coastal and aquatic environments (e.g., Luczkovich *et al.* 1993, Holden and LeDrew 1999, Mumby *et al.*, 1999, Andrefouet *et al.* 2001). This tool will become important to fisheries managers, environmentalists, and ecologists in monitoring degradation to essential fish habitats (EFH) and ensuring compliance with the Sustainable Fisheries Act (SFA). By mapping coastal habitats and comparing them over time, degradation, preservation, and recovery can be noted and further analyzed. This study hopes to show that Landsat satellite data can be used to classify and monitor these large areal extents in Belize with a known level of accuracy.

Table 1. The spectral characteristics and resolution of the Enhanced Thematic Mapper (ETM+) bands.

Thematic Mapper Band	Spectral Range (μm)	Resolution (m)	Water penetration
1	0.45 to 0.515	30 x 30	Yes
2	0.525 to 0.605	30 x 30	Yes
3	0.63 to 0.690	30 x 30	Yes
4	0.75 to 0.90	30 x 30	Some
5	1.55 to 1.75	30 x 30	No
6	10.40 to 12.5	60 x 60	No
7	2.09 to 2.35	30 x 30	No
Pan (8)	0.52 to 0.90	15 x 15	Yes

Materials and Methods

Site Description and Remote Sensing

Belize is located just south of Mexico on the Caribbean Sea. Turneffe Atoll is the largest of three offshore atolls in Belize and consists of more than 200 cayes. Specific sites that were visited in June 2000 and July 2001 for ground-truthing were near Soldier (87°47'43.4" W and 17°19'16.1" N) and Calabash Cayes (17°16'55.2" W and 17°16'55.2" N), which are islands in the shallow lagoonal waters along the windward edge of Turneffe Atoll (Figure 2). Soldier Caye is located to the north and is separated from Calabash Caye by a wide channel with a sandy bottom (the sand flat area, 17°17'47.6" W and 87°48'32.9" N), which was also used for ground-truthing. Cut Finger Reef (17°16'02.0" W and 87°49.09.6" N), located at the southern end of Calabash Caye, was a fourth ground-truthing site (Figure 3). At each of these four study sites, transects ranging in size from 150-300 meters were surveyed using SCUBA and a digital video camera. Depth of transects ranged from 0.6 – 11.0 m and was measured by a diver positioned on the bottom with a Suunto Vyper dive computer. These sites were chosen after a preliminary examination of the satellite imagery indicated that bottom cover changed dramatically over the length of these transects, and thus provided the maximum range of bottom reflectance as detected by the Landsat sensor. Specific transect lines depended upon accessibility to the sites as well as wave and weather conditions. In addition, travel to distant parts of the atoll in 2000 and 2001 was limited due to boat and fuel resources.

The image used in this study is a LANDSAT 7 image of the coastal region of Belize acquired on 23 May 2000 (Figure 2; Scene ID: L71019048_04820000523; WRS Path 019, Row 048).

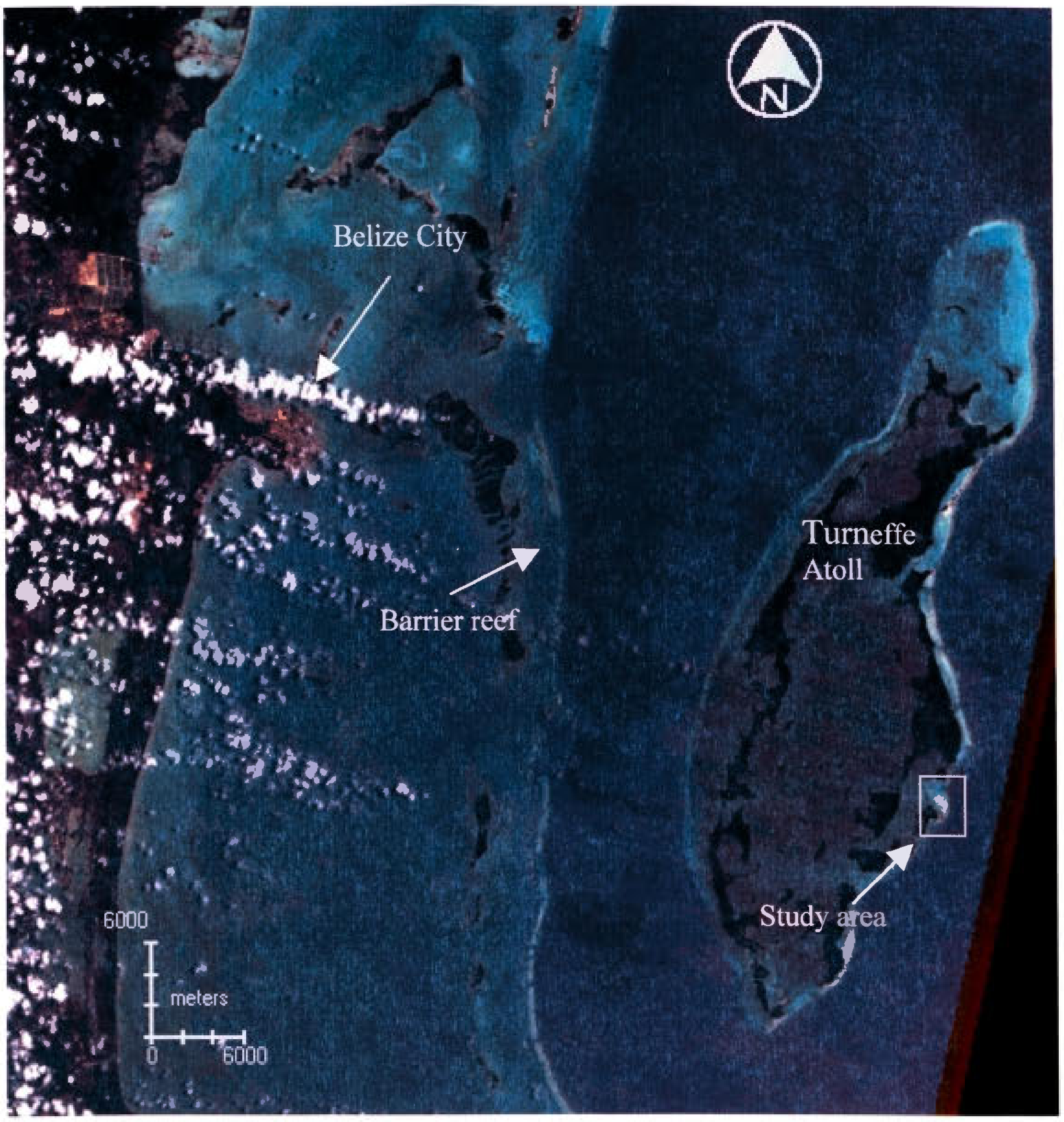

Figure 2. The coastal area of Belize, showing Belize City, the barrier reef system, and Turneffe Atoll, LANDSAT 7 scene L71019048_04820000523, shown in the true color image of ETM+ bands 1 (red), 2 (green), and 3 (blue) with the windward Cayes and the study areas used for ground-truthing.

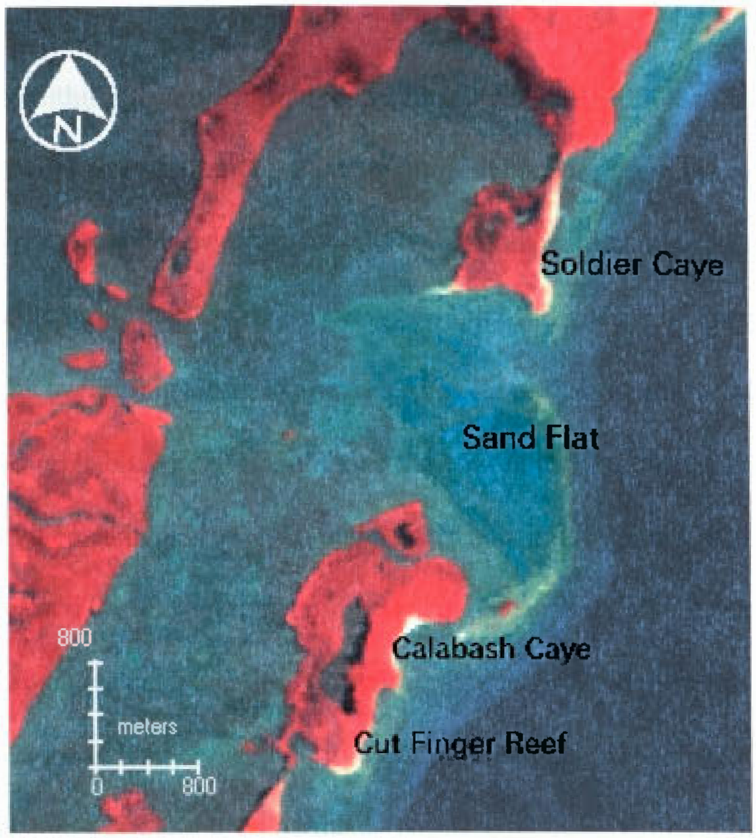

Figure 3. Area of interest close up view of the study area, showing the windward cayes and the study areas used for ground-truthing in 2000 and 2001 shown in false color bands 1, 2, and 4.

Ground-truthing

Ground-truthing data were gathered in June 2000, July 2001 and 2002. The June 2000 data were used as a preliminary assessment of the feasibility of the project. This data was used in conjunction with the July 2001 data to construct a habitat classification model using multivariate statistical analyses. Ground truth images of the sea bottom were obtained by swimming along 11 transect lines located at the four study sites and videotaping bottom habitat from 1.5 m above the bottom at 30 m intervals using a Sony PC 100 digital video camera in a Mako underwater housing (Figure 4, 126 locations). Positions along each transect were determined using a Garmin GPS 12 receiver held at the water surface above each location. Accuracy of the GPS receiver was ±15m RMS at the time because the Selective Availability was off during the period of this study. The Selective Availability is a tool used by the department of Defense to alter the accuracy of GPS receivers by up to 100m. Geo-referencing of the image itself was done using ERDAS and known land references at the University of Belize campus and the dock at the research center on Calabash Caye and Carry Bow Caye. Still images were taken from the digital video for each 30-m location along a transect, which placed each image in a separate LANDSAT pixel. Images were acquired from the video using a Sony® Ilink ™ video system and DV gate capture software for still pictures®. The still images were displayed on a 21cm x 29 cm flat-screen monitor, overlaid with a 20-cell grid (5.25 cm x 5.80 cm cells), and each cell assigned to one of seven bottom cover types (Figure 5). The cover types were sandy bottoms, seagrass meadows, macro-algae, hard coral, soft coral, dead coral covered with coraline algae, or small rubble fragmented from the main rock formations. Percentage cover of each bottom cover type in each still video image was computed by counting cells assigned to each bottom cover type using the formula:

% cover = (# cells of bottom cover type / 20) x 100.

Those cells that contained more than one bottom cover type were judged by eye to determine the dominant benthic cover type in that cell.

The bottom cover types (Figure 5) were the only ones observed in the shallow water areas around Calabash Caye. The organisms composing the seven cover types were not resolved to lower taxonomic levels to allow for rapid video analysis. Lower taxonomic levels of the benthic organisms may have been possible from the video, but was unlikely to produce a different clustering of habitats at a level that would be discernable in Landsat imagery, so was beyond the scope of this analysis. Video images for 90 of the 126 ground truth stations can be viewed in the accompanying CD (Appendix 3). The remaining 36 stations were collected in the preliminary study in July 2000, and the images have been lost, however the ground-truth data is still accounted for.

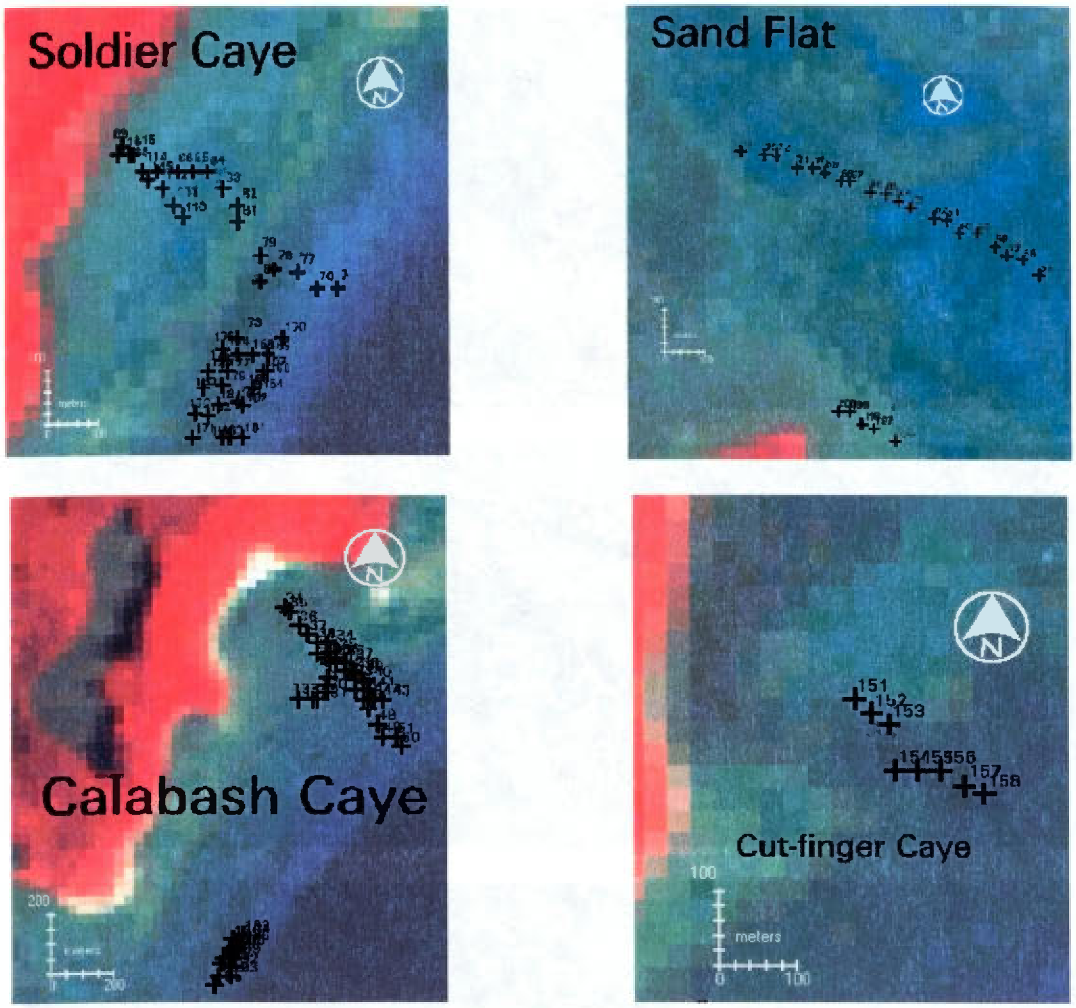

Figure 4. Transect locations at the two Cayes as well as the sand flat between Calabash and Soldier Caye, and Cut-finger reef south of Calabash.

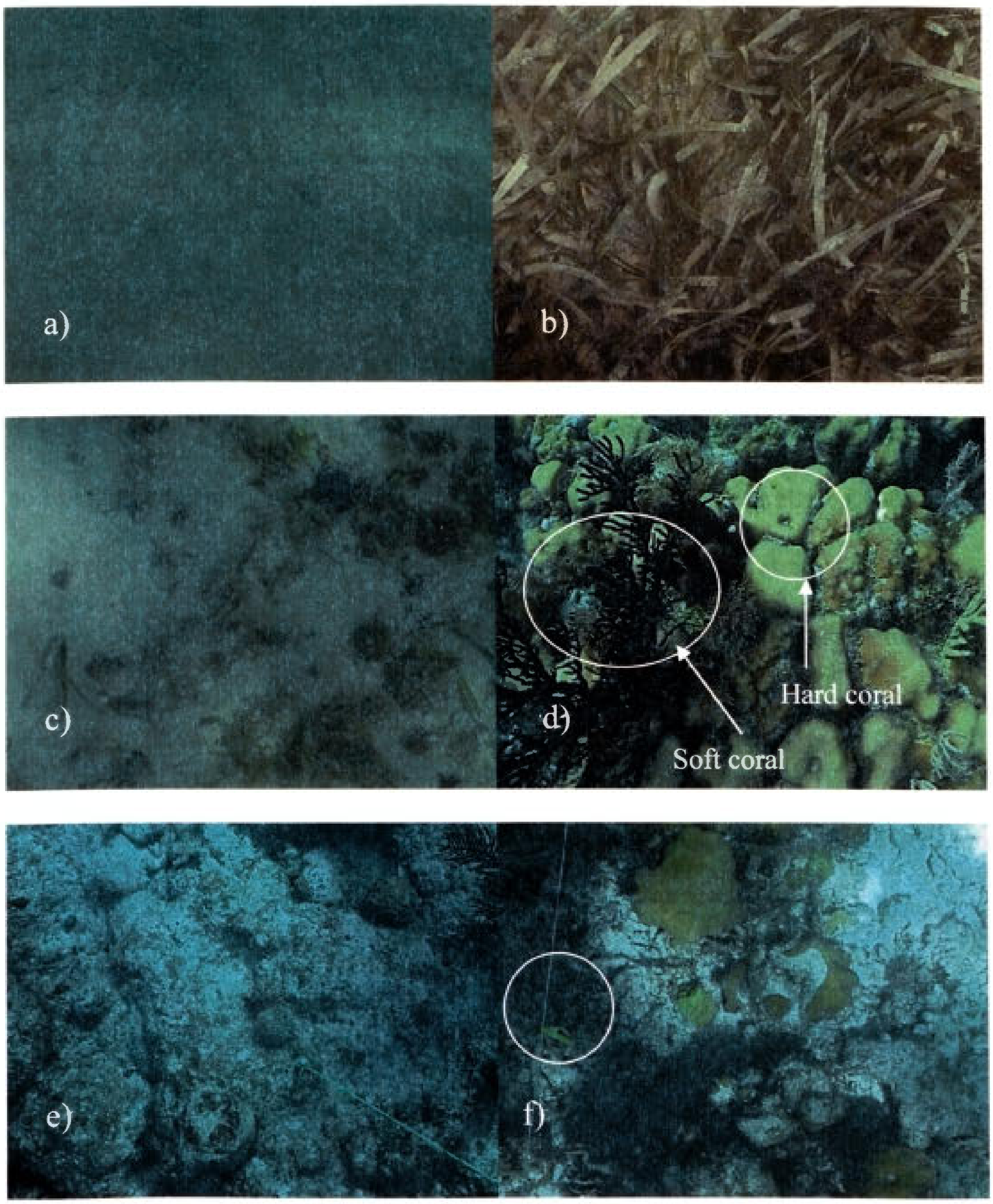

Figure 5. The 7 bottom cover types (a) sand, (b) seagrass, (c) foliose algae, (d) hard coral and soft coral, (e) coraline algae on dead coral, and (f) rubble.

Habitat Classification using Optimization Clustering

Cluster analysis is a multivariate statistical procedure that can find natural groups in a similarity matrix. Using an optimization cluster analysis (UCINET verion 5.78, Borgatti *et al.*, 1999), the 126 locations were grouped based on similarity (Pearson correlation) of water depth and percentage bottom cover data obtained from video of the seven bottom types. The Pearson correlation was computed as a similarity measure among stations; the water depth and percentage bottom cover were used as variables to compute the correlations. A 126 x 126 matrix with a Pearson correlation coefficient in each cell of the matrix was created. The optimization clustering strategy is divisive, and divides the station matrix into two or more user-defined groups, in which similarity is greatest within a group, as judged by the average similarity within groups. This cluster analysis was repeated for group sizes 2 up to 10. Group sizes >10 were not considered, because there were only 7 bottom cover types visible from the video. An R^2 measure (a measure of within to between group variation) was examined after each division.

Discriminant Function Methodology

Discriminant Function Analysis (DFA) is a multivariate approach that allows prediction of group membership based on a training set of independent variables. In this study, group membership in the habitat classes determined from the groud-truthing video surveys was predicted from Landsat digital pixel values derived from each site visited (the training set). A DFA derives linear combinations of the independent variables (Landsat bands) that will discriminate between the *a priori* defined groups (habitat types) in such a way that the misclassification error rates are minimized by maximizing the between group variance relative to the within-group variance. A subset of the ground truth sites were used as a training set for a discriminant function; only 78 sites were strongly associated with definable bottom classes. These aggregated bottom classes included sites with varying degrees of percent cover of the bottom cover classes. The coral reef habitat class for example, included the soft coral, hard coral, live rock, and rubble bottom cover types identified previously.

The next step was to predict the habitat classes (cluster groups) from the Landsat data (training set) using a discriminant function. A discriminant function analysis was derived using data from Landsat bands 1, 2, 3, and 4 at the 78 sites identified as representative of habitat type classes.

Classification of the LANDSAT 7

Using a conditional statement with parameter values acquired from the canonical scores (Appendix 2) given by the discriminant function analysis, the ETM+ images were classified into one of five image classes (land, sand, seagrass, coral reef, and deep ocean). Figure 6 shows the steps involved with this classification. The land and deep ocean bottom types were determined by analyzing areas of the map whose scores fell outside of those determined to be sand, seagrass, or reef and identifying known geographical features. To determine boundaries for those habitats whose scores overlap, the averaging method of the canonical scores was used as described by Dillon and Goldstein (1984).

Ground Truthing the Accuracy of the Discriminant Function at New Sites on Turneffe

In July 2002, additional ground-truth data were gathered to assess the accuracy of the habitat classification model at sites away from the ones used in the training set. Sites were chosen at random within new quadrants that contained a diversity of bottom reflectance patterns. Five areas were selected (1590 m x 1200m) along the coastal areas of Turneffe Atoll. Sites for the new quadrants were areas of interest to the Mesoamerican Barrier Reef Systems project currently under way in the western Caribbean and were located on both the windward and leeward sides of the Atoll (Sale *et al.*) Individual sites within a quadrant were determined by Microsoft Excel random number generator and were located with the Garmin GPS 12 receiver. Each site was classified by determining bottom cover and depth measurements using SCUBA and snorkeling and was videotaped for further analysis. The percentage accuracy of the predicted habitat types versus the observed habitat type was calculated using user accuracy, classification accuracy, and the Tau coefficient (Mumby *et al.*, 1997). Tau (τ) is calculated from:

$$T = \frac{P_0 - P_r}{1 - P_r}, \text{ where } P_r = \frac{1}{N^2}\sum_{i=1}^{m} n_i * x_i$$

Po = overall accuracy; m = number of habitats, i = ith habitat, N = total number of sites, n_i = row total for habitat i, and x_i = diagonal value for habitat (i.e., number of correct assignments for habitat i).

User accuracy is the ability of the discriminant function to accurately predict habitat classification membership and is defined as (number of sites in each habitat class observed/ number of sites in each habitat class expected) x 100. Classification accuracy is a measure of how well sites are classified for each habitat type and is defined as (number of sites classified correctly expected/ total number of sites of all classes observed) x 100. In other words user accuracy examines predicted versus observed where classification accuracy examines observed versus predicted. The Tau coefficient is a statistic that is readily interpretable, permits hypothesis testing, and accounts for chance agreement within the matrix (Ma and Redmond, 1995). A τ of 0.80 indicates that 80% more pixels were classified correctly than would be expected by chance alone (Mumby *et al.* 1997).

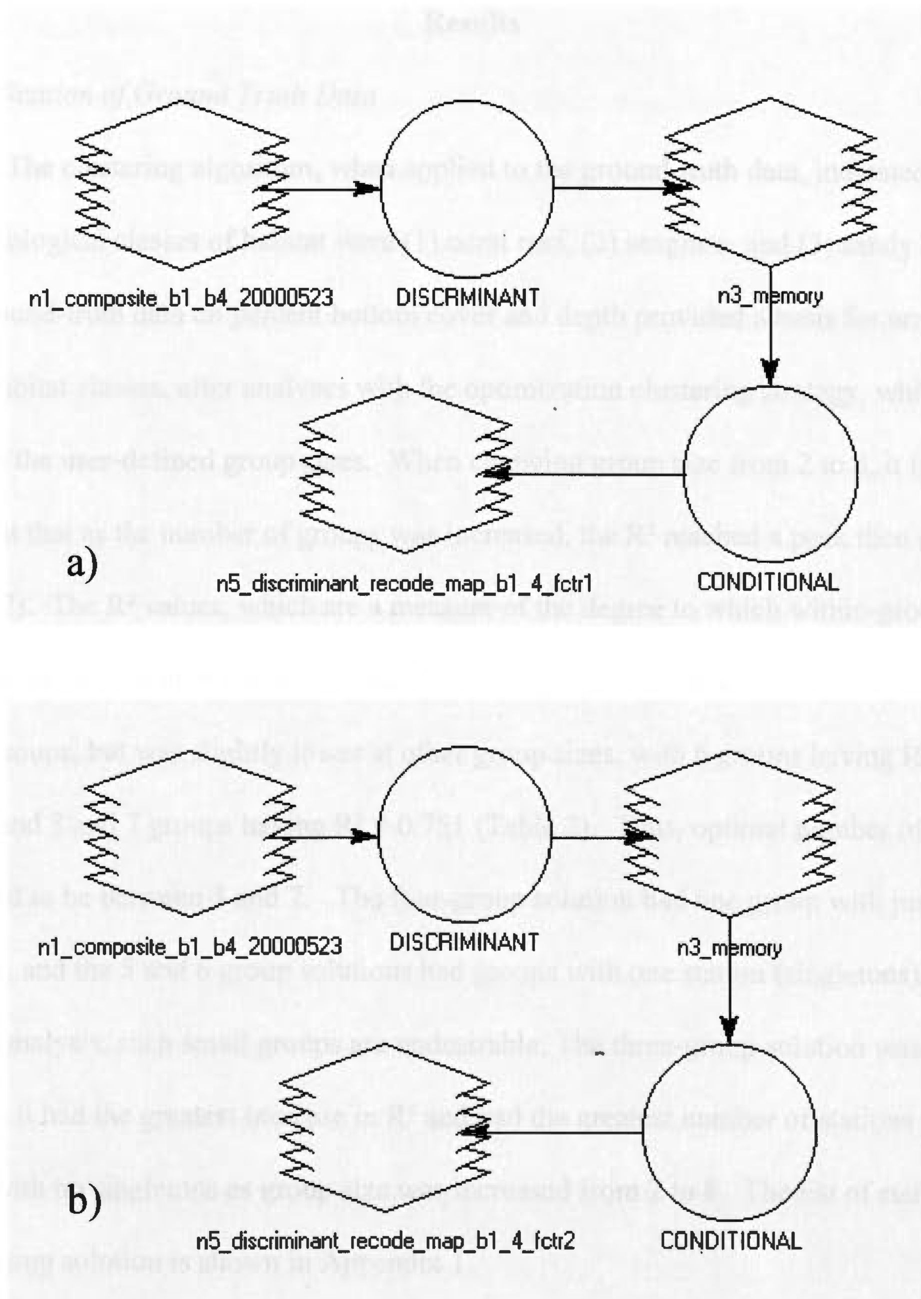

Figure 6. The Model Maker design implemented in the reclassification of the LANDSAT image for factor 1 (a) and factor 2 (b).

Results

Classification of Ground Truth Data

The clustering algorithm, when applied to the ground-truth data, indicated that the main biological classes of habitat were (1) coral reef, (2) seagrass, and (3) sandy bottom. The ground-truth data on percent bottom cover and depth provided a basis for arriving at these habitat classes, after analyses with the optimization clustering strategy, while varying the user-defined group sizes. When changing group size from 2 to 8, it is apparent that as the number of groups was increased, the R^2 reached a peak then declined (Table 2). The R^2 values, which are a measure of the degree to which within-group to between-group variance was maximized for each group size, peaked at $R^2 = 0.758$ for 4 and 5 groups, but was slightly lower at other group sizes, with 6 groups having $R^2 = 0.757$, and 3 and 7 groups having $R^2 = 0.751$ (Table 2). Thus, optimal number of groups appeared to be between 3 and 7. The four-group solution had one group with just three stations, and the 5 and 6 group solutions had groups with one station (singletons). In cluster analysis, such small groups are undesirable. The three-group solution was chosen because it had the greatest increase in R^2 and had the greatest number of stations per group with no singletons as group size was increased from 2 to 8. The list of stations in the 3-group solution is shown in Appendix 1.

The stations within each group in the three-group solution were characterized as to the average [± one standard error of the mean (s.e.m.)] percent cover of each bottom type and depth. These three groups are hereafter called sand, seagrass and coral reef biological habitats. The 64 stations in group 1 (sand) had an average of 66.0 (± 2.49) %

cover of sand bottom, with an average depth of 2.60 (± 0.22) m. The 11 stations in group 2 (seagrass) had mostly seagrass (mean = 82 ± 8.76 % cover) with an average depth of 1.8 (± 0.52) m. The 51 stations of group 3 (coral-reef) had mostly coraline-algae-covered dead reef (mean = 51.3 ± 3.17 % cover), but also significant amounts of hard coral (21.8 ± 2.29 % cover) and soft coral (21.7 ± 2.25 % cover) covering the bottom. This group also occurred in the deepest water (mean = 4.99 ± 0.26 m). Thus, after grouping the 126 locations along the 11 transects at the four ground-truth sites in the cluster analysis, three main habitat classes were identified as sand, seagrass, or coral reef.

Discriminant Function Analysis

For the discriminant function analysis, a subset of the ground-truth stations was selected as being good representatives of these three habitat types. These 78 stations were used to define the training set, because of their high percent cover for each dominant bottom cover type. The remaining locations were omitted from later analysis, as they represent transaction habitats between the three primary habitat type clusters.

These 78 stations with clearly identifiable habitat classifications (sand, seagrass, and reef) were then used as a training set in a discriminant function analysis to predict image classes from LANDSAT 7 digital values in ETM+ bands 1, 2, 3, and 4. The results produced a canonical discriminant function (CFF1 and CFF2) with two factors:

$$CFF1 = 0.014(TM\ 1) + 0.039(TM\ 2) + 0.023(TM\ 3) + 0.487(TM\ 4) - 26.187.$$

$$CFF2 = 0.084(TM\ 1) - 0.027(TM\ 2) - 0.026(TM\ 3) - 0.836(TM\ 4) + 21.488$$

where TM x is ETM+ band x.

The large coefficients in these functions for ETM+ band 4 are due to the fact that this band (near infrared) has low digital values due to the lack of water penetration by infrared wavelengths. The canonical scores of each site in the 78-member training set were computed using these equations (Appendix 2), and plotted using the habitat classes derived from cluster analysis as plotting symbols for each station (Figure 7). The canonical scores of stations mostly fall into three distinct clouds of points showing good discrimination among habitats. However, there are some stations that plot outside the 95% confidence ellipse in the other classes. The canonical scores can then be turned into an *a posteriori* probability that gives the likelihood of the object belonging to each of the habitats. In terms of user accuracy, which is the ability of the DFA to accurately predict habitat classification membership, Landsat digital values from coral reefs were correctly classified 100%, from seagrass pixels 80 %, and from sand pixels 77 % of the time (Table 3).

In terms of classification accuracy, the observed sand areas were placed into the correct classification 96% of the time, the seagrass locations were correctly classified 73% of the time, and coral reef locations were correctly classified 88% of the time. Overall accuracy of the discriminant function was 88.5% and the Tau (τ) coefficient, which corrects the overall accuracy because some classifications are likely to be correct by chance alone, was slightly lower at 81.25%. Thus, the discriminant function gives an overall highly accurate classification of habitats for the training set.

Table 2. The R^2 values for groups of stations ranging from 2 to 10 user-defined groups.

User-defined group number	R^2	Comments
2	0.698	2 large groups
3	0.751	Smallest has 11 stations
4	0.758	Group 4 has only 3 stations
5	0.758	Group 5 is a singleton
6	0.757	Group 6 is a singleton
7	0.751	3 singleton groups; 1 two-station group
8	0.747	5 singleton groups
9	0.732	5 singleton groups; 1 two-station group
10	0.744	7 singleton groups

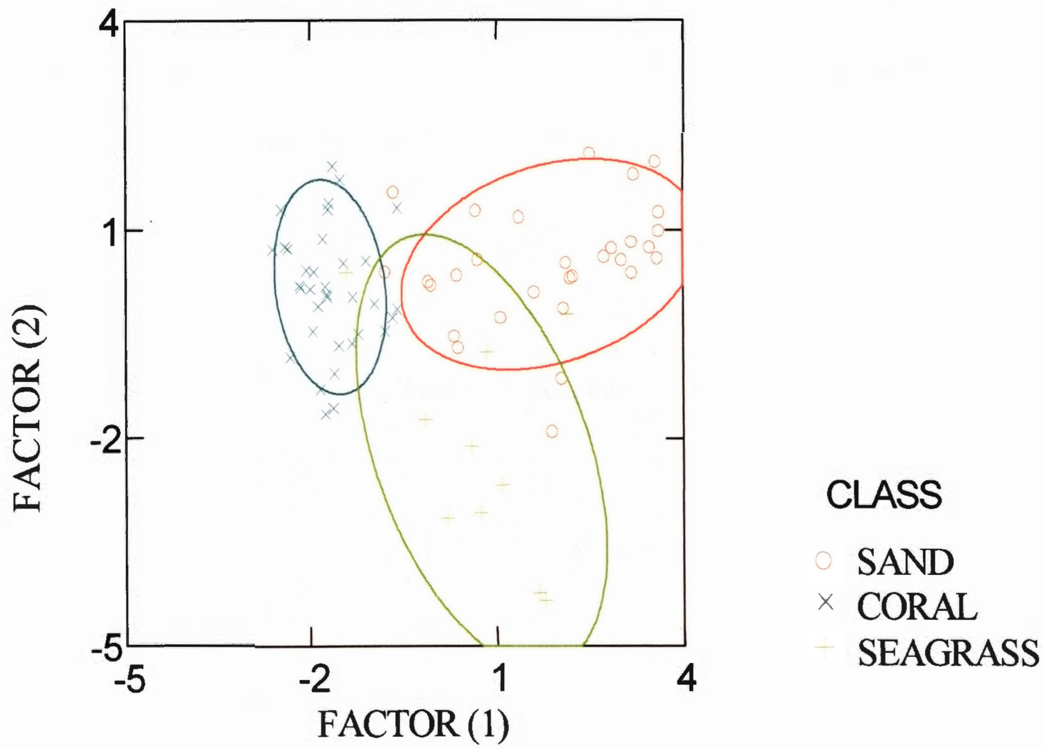

Figure 7. Canonical scores plot showing the grouping of scores for each of the three habitat types. Each point represents one station included in the training set. The ellipse is a 95% confidence ellipse.

Table 3. Classification error matrix of the discriminant function based on training data with the number of stations in each classification. Expected habitat based on DFA factor 1. Overall accuracy = 88.5%; Tau (τ) coefficient = 81.25%.

	Observed habitat in underwater video				
Habitat type	Sand	Seagrass	Coral reef	Row total	User accuracy (%)
Sand	23	3	4	30	77
Seagrass	1	8	1	10	80
Coral Reef	0	0	38	38	100
Column total	24	11	43		
Classification Accuracy (%)	96	73	88		

LANDSAT 7 Image Recoding

The LANDSAT 7 image was recoded to create a habitat map of the region surrounding Turneffe atoll, showing coral reef, seagrass, and sand habitats as well as the terrestrial and open ocean areas of the atoll. The Model Maker function of ERDAS™ was used along with the discriminant function canonical scores computed for every pixel. Conditional values for the Model Maker Function were derived from the canonical scores of the training set (Dillon and Goldstein 1984) that placed each Landsat 7 pixel value into one of five classes (open ocean, coral, seagrass, sand, and terrestrial). There are two additional habitat classes in this model (open ocean and terrestrial classes) because these represented areas that were beyond my ground-truthing sample areas (deeper than 11 m or on land). Separate Model Maker processes were carried out for each factor of the discriminant function, which produced two recoded maps representing factor 1 (Figure 8) and factor 2 (Figure 9). The factor 1 map is most useful upon examination of the features within this map. One can see that blue areas are deep ocean, cyan-coded areas are coral reef, green areas are seagrass beds, yellow areas are sand flats, and red is land. Factor 1 appears to be greatly influenced by ETM+ band 4, which is important in identifying the island, and by ETM+ band 2, which would have the best ability to detect shallow water. Factor 2, however, does very little in delineating and identifying habitats. The apparent disturbance from wave and wind action in the aquatic areas can be readily discerned in this image.

Figure 10 is a close-up of the recoded map shown in Figure 8 (from the DFA factor 1), with transects that were ground-truthed at Calabash Caye overplotted with the individual GPS waypoints shown. In this figure it appears that there is a small sand flat area adjacent to the land that leads into a seagrass bed, then into the coral reef, and finally out to open ocean. It appears to be most useful to examine individual waypoints and their habitat classifications with the recoded maps based on factor (Figure 8 and 10) compared to ground truth data. For example, compare Figure 10 to Figure 4 (lower left image of Calabash Caye) and one can see the transition described above in that false color image. Thus, the habitat recoding based on DFA factor 1 gives an intuitively satisfying map of a well-known section of Belize's coastal zone. However, this map needs verification in areas outside of the training set sites.

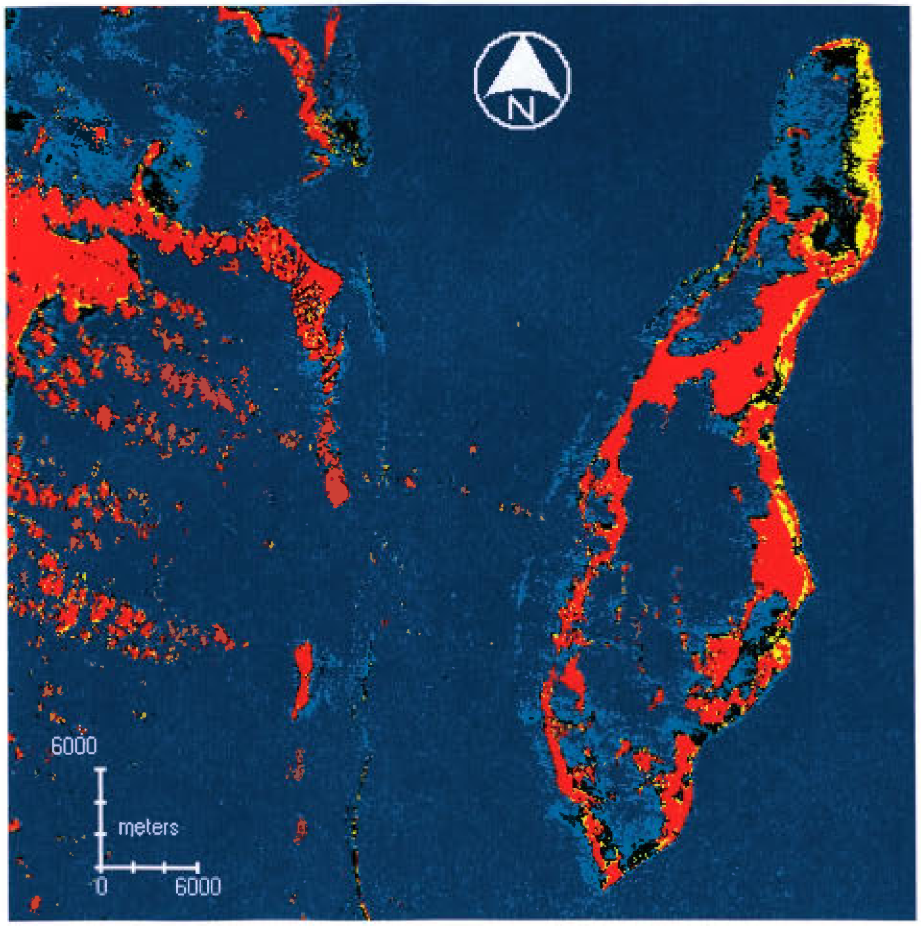

Figure 8. Discriminant Function Factor 1 used to recode Landsat image (Scene ID: L71019048_04820000523; WRS Path 019, Row 048) identifying 5 habitats. Color code: blue=deep water; cyan=coral reef; green=seagrass; yellow=sand bottom; red=land (or clouds).

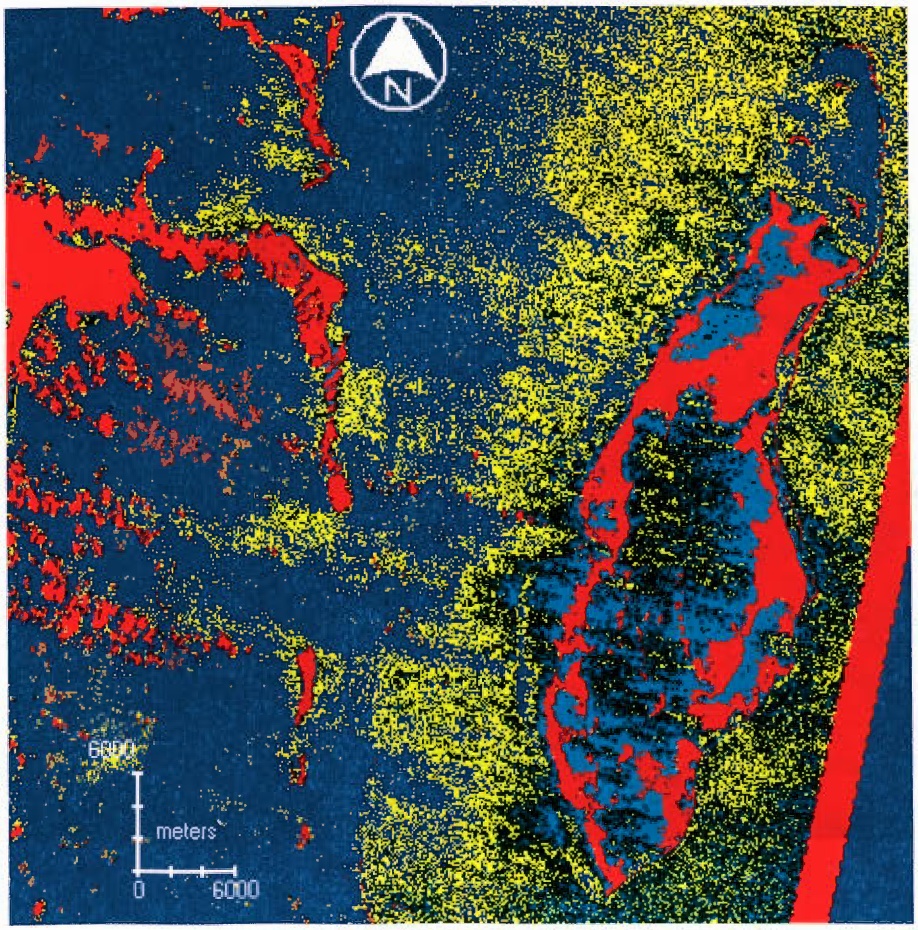

Figure 9. Discriminant Function Factor 2 used to recode Landsat image (Scene ID: L71019048_04820000523; WRS Path 019, Row 048). Color code: blue=deep water; cyan=coral reef; green=seagrass; yellow=sand bottom; red=land (or clouds).

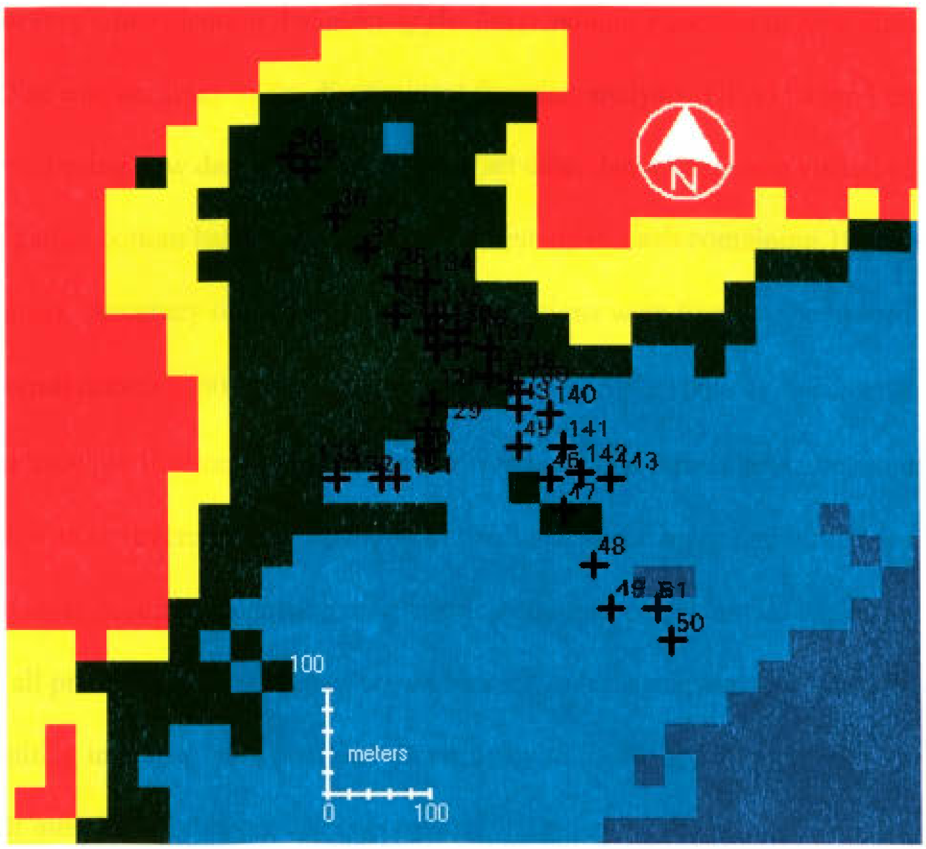

Figure 10. Close-up of Calabash Caye Transects in the recoded LANDSAT image. Color code: blue=deep water; cyan=coral reef; green=seagrass; yellow=sand bottom; red=land (or clouds).

Assessment of Classification Accuracy of the Discriminant Function at New Sites

The true accuracy of the discriminant function analysis (DFA) factor 1 can only be assessed using new data not in the training set data. New sites were visited in July 2002 to gather bottom habitat data at five different areas, each containing 10 points (Fig. 11, 70 sites). Accuracy of the DFA factor 1 predictions were found to be lower for new sites (overall accuracy 60 % and Tau (τ) coefficient 52.5 %; Table 4), because of an apparent misclassification of predicted coral reef areas that turned out to be seagrass. In addition, a more severe misclassification of predicted ocean areas that turned out to be seagrass areas occurred, and these misclassifications caused accuracies to decline overall. Indeed, all predicted habitat classes were observed to have seagrass habitats at least one site, resulting in a very low classification accuracy of 25 % for seagrass.

It must be pointed out that two new habitat categories exist (land and deep ocean) which were not present in the initial analysis of the training set (Table 3). Land and ocean image classifications were created out of a necessity to classify those pixels, which had values either less than or greater than the canonical scores for the three identified habitat classes. When these two classes are removed from the analysis, the overall accuracy improves to 67% and the Tau (τ) coefficient becomes 55.4% (Table 5). However, there is still a problem with misclassification of predicted seagrass areas into coral reef areas (71 % user accuracy for seagrass), and observed seagrass areas being classified as coral reef (42% classification accuracy for seagrass). Also, coral reef classified pixels turned out to be seagrass 40% of the time; thus, user accuracy was low for coral reef (60 %). It is apparent that seagrass and coral reef habitats were difficult to discriminate using Landsat 7 ETM+ data alone and this discriminant function analysis at these new sites.

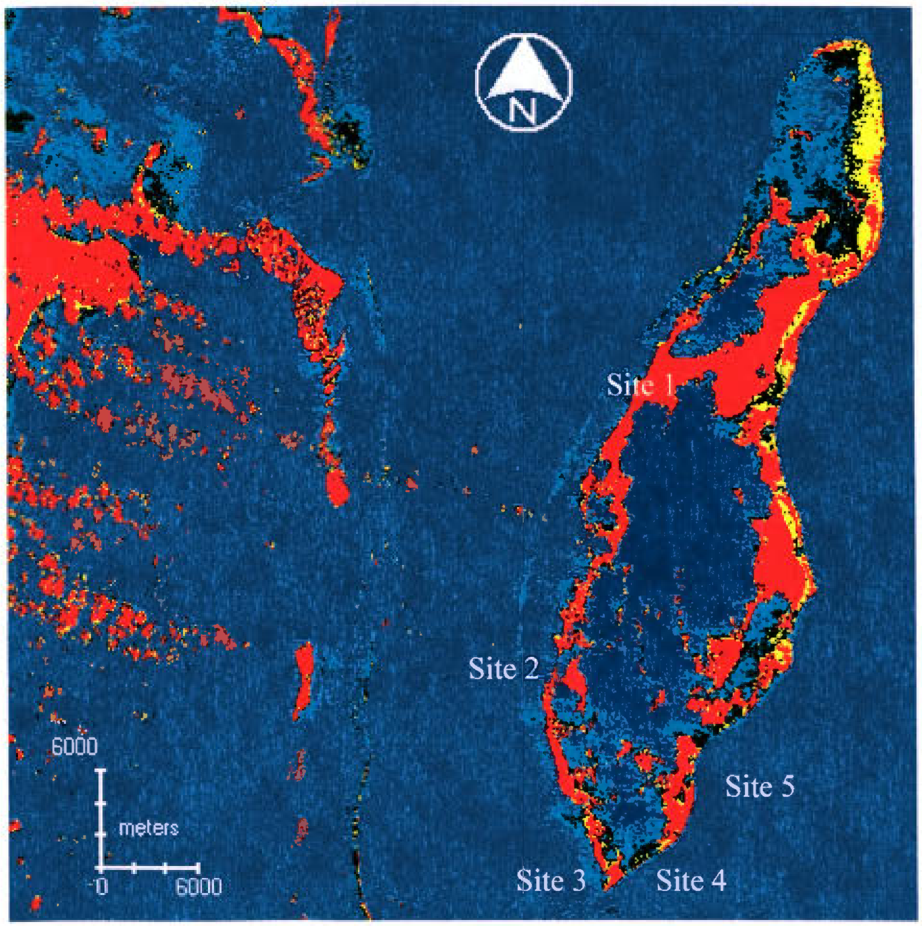

Figure 11. Factor 1 recoded map showing the location of the July 2002 ground-truthing sites. Color code: blue=deep water; cyan=coral reef; green=seagrass; yellow=sand bottom; red=land (or clouds).

Table 4. Error Matrix for new sites visited in July 2002 with the number of stations in each class. Expected habitat image class from DFA factor 1 versus observed habitat. Overall Accuracy = 60%; Tau Coefficient = 52.47%.

	Observed habitat in underwater video						
	Sand	Seagrass	Coral reef	Land	Ocean	Row total	User accuracy (%)
Sand	4	1	0	0	0	5	80
Seagrass	0	5	2	0	0	7	71
Coral Reef	0	6	9	0	0	15	60
Land	0	1	0	2	0	3	67
Ocean	0	7	3	0	10	20	50
Column total	4	20	14	2	10		
Classification accuracy (%)	100	25	64	100	100		

Table 5. Error Matrix for sites visited in July 2002 with the land and ocean classifications removed from the analysis with the number of stations in each class. Expected habitat image class from DFA factor 1 versus observed habitat class. Overall Accuracy = 67%; Tau Coefficient = 55.35%.

	Observed habitat while snorkeling or using SCUBA and in underwater video				
Habitat type	Sand	Seagrass	Coral reef	Row total	User accuracy (%)
Sand	4	1	0	4	80
Seagrass	0	5	2	7	71
Coral reef	0	6	9	15	60
Column total	4	12	11		
Classification accuracy (%)	100	42	82		

Concluding Remarks

I classified the coastal habitats of a small portion of the coastline of Belize based on Landsat 7 satellite imagery, videotaped ground-truth data, cluster analysis, and a discriminant function analysis (DFA). I used a discriminant function analysis with two factors to classify a Landsat image using pixel values alone and a training set. When the image was recoded using DFA factor 1, a map that identified 5 major habitat types was produced with an overall accuracy of 81% for the training set, but fell to 67 % for new sites away from the training set sites. This technique appears to be a useful and inexpensive means to detect and monitor tropical coastal ecosystem habitats. In contrast, the second DFA factor appears to be affected by the characteristics of ETM+ band 4 and the near infrared wavelengths in water, and not habitat. These wavelengths only penetrate water to a depth of a few centimeters and tend to detect surface disturbances, such as wave action, causing the fanning pattern seen in the factor 2 map (Figure 10). When the factor 2 map is examined closely with respect to habitat distribution in known areas, there is no intuitive relationship observed, in spite of the apparent discrimination observed for training set seagrass sites with this factor in the canonical scores plot (Figure 7). Therefore, for the purposes of this study, the map produced by factor 2 is of no use for habitat classification.

My method, using a discriminant function multivariate statistical technique, achieved relatively accurate habitat classifications: the lowest user accuracy is 77 % correct classification (sand) in the training set and 60 % (coral) in the new area data set. However, the method suffers from low classification accuracy for seagrass (42 %).

Practically, this method will under-estimate the distribution of seagrass habitats, which is an essential fish habitat that must be studied in other ways. However, coral reef areas will be mapped with relatively high accuracy (100 % classification accuracy at the training set sites, and 82 % at new sites), making it an excellent method for delimiting coral-reef fish habitat.

The verification process carried out in July 2002 in areas outside of the training set was essential in rigorously testing the accuracy of the discriminant function factor 1 to predict habitat type. The accuracy at the new sites visited was considerably lower than when using the training set data. Although other researchers have published map accuracy estimates of 77% for Landsat data (Mumby *et al.* 1997), this is the first time that a model created on a training set was tested against sites outside of the training set. My map accuracy results exceed that of Mumby *et al.* (1997) for predicting correctly the training set, but are slightly lower when used on sites outside the training set. As more researchers attempt to use their models on areas outside of their training sets, a better understanding of the ability of this method or other methods to correctly map habitats will be gained.

A number of explanations can be suggested to explain this difference in accuracy rates between training set data and the results of the July 2002 ground-truth data collected at sites outside the training set. The first of these concerns the inclusion of sites on the leeward side of the Atoll. It has been shown that the leeward side of the Belizean Atolls tends to have higher turbidity than the windward side due to the surface circulation in the western Caribbean that is dominated by the Caribbean current, which approaches the

Belize continental margin from the east (James and Ginsburg 1979). This water movement washes through the islands while moving east picking up loads of sediment, which are deposited on the leeward side. If site 2, which was a heavily sedimented seagrass bed in water 3.4 -10 m deep on the leeward side, is removed from the assessment, the accuracy of the discriminant function improves greatly (overall accuracy = 75 % and Tau (τ) = 69.25 %; Table 6). Improvements can be noted in the classification accuracy of seagrass, which improved to 50%. However, this is not satisfactory, as all coastal habitats need to be classified and we must accept that sedimentation and turbidity will occur in some areas and will remain a problem. But, by dropping this site, the model still had difficulty in identifying deep water coral reef at other sites and classified them as open ocean or seagrass (64 % classification accuracy).

Another explanation for the reduction in accuracy deals with the depths of the sites visited in July 2002 compared to those used in the training set. Sites in 2002 ranged from 0.30 m to extremely deep water (>1000 m), whereas sites used for the initial training set ranged in depth from 0.6 m to 11.0 m. The sites selected in the July 2002 work that were deeper than 11.0 m would cause sunlight to attenuate during penetration and reflection, lowering the albedo in the visible wavelengths and all of the associated Landsat ETM+ band's digital values. This would have the effect of causing misclassification of observed coral reef and seagrass habitat types as predicted deep-water habitats. When deep-water sites (> 11.0 m) are removed from the analysis, the accuracy of the discriminant function again increases (overall accuracy = 77 %, Tau (τ)= 73.4 %; Table 7). Coral reef and sand habitats are correctly classified > 82 % of the time, but there is still a low classification accuracy for seagrass habitats (42 %), which are misclassified as coral reef habitats. Therefore, given the limitations of the Landsat satellite's ability to sense visible light wavelengths in deep water, my recommendation for the application of this method is to restrict its use to windward reefs that are in depths less than 11.0 m.

A third explanation for low accuracy is the elimination of problem (mixed) pixels in the training set data. Stations that were deemed to be a mixed pixel were eliminated in establishing the training data. In the July 2002 data these pixels are present, but are not eliminated from the analysis. This would cause lower percent accuracy for the overall analysis due to the percent cover data of these stations.

A fourth possible explanation for the low accuracy of the predictions is that the habitats may have changed over the time between when the Landsat image was acquired (23 May 2000) and when the ground truth surveys were done. The surveys at the new sites away from the training set areas were done more than two years later in July 2002. If the bottom habitats changed over time, for example, if seagrass grew over the bottom in a deep water area between May 2000 and July 2002, the predictions of the DFA factor 1 model would have been in error. Although I cannot assess this source of error at the sites visited in the locations away from the Calabash Caye, I can say that the habitats near Calabash Caye did not change noticeably between June 2000 and July 2002, so I suspect that this is not a major source of classification error.

Other concerns in the general use of this approach are that it is limited to scenes with low cloud cover and with good water visibility. An additional concern for the general use of this approach is that there is no guarantee that the canonical discriminant functions derived can be applied without correction to new images with different radiometric gain values (which are listed in LANDSAT calibration parameter files of every image). Entering a correction factor for the image gain factor into the Imagine Model Maker function when recoding the images using the discriminant function can standardize differences among images. If this image gain correction were done so that two images taken at different places or times were radiometrically balanced, then LANDSAT digital values could be converted into habitat classes by my method. With these corrections, coastal managers and ecologists could reclassify LANDSAT scenes in tropical coastal areas for use as rough biological habitat maps. Such maps would be inexpensive to prepare, and would save a tremendous amount of labor and money in performing habitat surveys for fish population estimates, habitat area measurements, and establishment of coastal marine protected areas. Such habitat maps would be based on a classification of biological (percent bottom cover and depth) data not radiometric data from Landsat imagery alone, making my approach biologically meaningful. In addition, if combined with change detection methods (Michalek *et al.* 1991), this approach can be used to monitor habitat boundary shifts over time. This is potentially an important tool for ecologists and coastal managers to monitor change in habitat areal coverage over time.

Table 6. Error Matrix for new sites visited in July 2002 without site 2. Expected Habitat Based on Discriminant Function versus observed habitat. Overall Accuracy = 75%; Tau Coefficient = 69.25%.

	Observed habitat in underwater video						
	Sand	Seagrass	Coral reef	Land	Ocean	Row total	User accuracy (%)
Sand	4	1	0	0	0	5	80
Seagrass	0	5	2	0	0	7	71
Coral reef	0	3	9	0	0	12	75
Land	0	1	0	2	0	3	67
Ocean	0	0	3	0	10	13	77
Column total	4	10	14	2	10		
Classification accuracy (%)	100	50	64	100	100		

Table 7. Error Matrix for new sites visited in July 2002 removing sites with a depth > 11.0 m. Expected habitat based on discriminant function versus observed habitat. Overall Accuracy = 77%; Tau Coefficient = 73.40%.

	Observed habitat in underwater video						
	Sand	Seagrass	Coral reef	Land	Ocean	Row total	User accuracy (%)
Sand	4	1	0	0	0	5	80
Seagrass	0	5	2	0	0	7	71
Coral reef	0	5	9	0	0	14	64
Land	0	1	0	2	0	3	67
Ocean	0	0	0	0	10	10	100
Column total	4	12	11	2	10		
Classification accuracy (%)	100	42	82	100	100		

REFERENCES

Andrefouet, S., and Payri, C. 2001. Scaling-up carbon and carbonate metabolism of coral reefs using in-situ data and remote sensing. Coral Reefs 19 (3): 259-269.

Andrefouet, S., Muller-Karger, F. E., Hochberg, E. J., Chuanmin, H., and Carder, K. L. 2001. Change detection in shallow coral reef environments using Landsat 7 ETM+ data. Remote Sensing of Environment 78: 150-162.

Aronson, J., and Le Floc'h, E. L. 1996. Vital landscape attributes: missing tools for restoration ecology. Restoration Ecology 4 (4): 377-387.

Baird, R. C. 1999. Introduction. Fish Habitat: Essential fish habitat and rehabilitation. Proceedings of the Sea Grant symposium of fish habitat. AFS Bethesda, MD

Bonefish and Tarpon Unlimited. www.tarbone.org. March 2004.

Carriquiry, J. D., Cupul-Magana, A. L., Rodriguez-Zaragoza, F., and Medina-Rosas, P. 2001. Coral bleaching and mortality in the Mexican Pacific during the 1997-98 El Nino and prediction from a remote sensing approach. Bulletin of Marine Science 69 (1): 237-249.

Cendrero, A. 1989. Mapping and evaluation of coastal areas for planning. Ocean and Shoreline Management 12: 427-462.

Chauvaud, S., Bouchon, C., and Maniere, R. 1998. Remote sensing techniques adapted to high resolution mapping of tropical coastal marine ecosystems (coral reefs, seagrass beds and mangrove). International Journal of Remote Sensing 19 (18): 3625-3639.

Chuanmin, H., Muller-Karger, F.E., Andrefouet, S., and Carder, K.L. 2001. Atmospheric correction and cross-calibration of LANDSAT 7 ETM+ imagery over aquatic environments: a multiplatform approach using SeaWiFS/MODIS. Remote Sensing of Environment 78: 99-107.

Dillon, W. R., and Goldstein, M. 1984. Multivariate Analysis, Methods and Applications. Wiley, New York.

Foody, G. M., and Boyd, D. S. 1999. Fuzzy mapping of tropical land cover along an environmental gradient from remotely sensed data with an artificial neural network. Journal of Geographical Systems 1: 23-35.

Geography network. March 8, 2004. **www.geographynetwork.com**. Environmental System Research Institute (ESRI).

Hardisky, M. A., Gross, M. F., and Klemas, V. 1986. Remote sensing of coastal wetlands. Bioscience 36 (7): 453-459.

Hochberg, E. J., and Atkinson, M. J. 2000. Spectral discrimination of coral reef benthic communities. Coral Reefs 19 (2): 164-171.

Holden, H., and LeDrew E. 1998. Spectral discrimination of healthy and non-healthy corals based on cluster analysis, principal components analysis, and derivative spectroscopy. Remote Sensing of Environment 65 (2): 217-224.

Holden, H., and LeDrew, E. 1998. The scientific issues surrounding remote detection of submerged coral ecosystems. Progress in Physical Geography 22 (2): 190-221.

Holden, H. and LeDrew, E. 1999. Hyperspectral identification of coral reef features. International Journal of Remote Sensing 20 (13): 2545-2563.

James, N. P., and Ginsburg, R. K. The geological setting of Belize reefs. The seaward margin of Belize barrier and atoll reefs. Blackwell Scientific Publications. Oxford.

Kenchington, R. A., and Claasen, D. R. 1998. Australia's Great Barrier Reef-management technology. Proceedings of Symposium on remote Sensing of the Coastal Zone, Gold Coast, Queensland. Department of Geographic Information, Brisbane, VA2.1-VA2.9.

Lubin, D., Li, W., Dustan, P., Mazel, C. H., and Stamnes, K. 2001. Spectral signatures of coral reefs: Features from space. Remote Sensing of Environment 75 (1): 127-137.

Luczkovich, J. J., Wagner, T. W., and Stoffle, R. W. 1993. Discrimination of coral reefs, seagrass meadows, and sand bottom habitat types from space: A Dominican-Republic case study. Photogrammetric Engineering and Remote Sensing 59 (3): 385-389.

Lyzenga, D. R. 1981. Remote sensing of bottom reflectance and water attenuation parameters in shallow water using aircraft and Landsat data. International Journal of Remote Sensing 2 (1): 71-82.

Ma, Z. and Redmond, R. L. 1995. Tau coefficients for accuracy assessment of classification of remote sensing data. Photogrammetric Engineering and Remote Sensing 61: 435-439.

McField, M., Wells, S., and Gibson, J. (eds.) 1996. State of the Coastal Zone Report, Belize, 1995, Coastal Zone Management Programme, Government of Belize, Belize City, Belize, pp. 255, June, 1996.

McNeill, S. E. 1994. The selection and design of marine protected areas: Australia as a case study. Biodiversity Conservation 3: 586-605.

Menges, C. H., Hill, G. J. E., and Ahmad, W. 1998. Landsat TM data and potential feeding grounds for threatened marine turtle species in northern Australia. International Journal of Remote Sensing 19 (6): 1207-1221.

Michalek, J. L., Wagner, T.W., Luczkovich, J. J., and Stoffle, R. W. "Multispectral change vector analysis for monitoring coastal marine environments", Photographic Engineering & Remote Sensing, Vol. 59, No. 3, pp. 381-384, March 1993.

Mumby, P. J., Clark, C. D., Green, E. P., and Edwards, A.J. 1998. Benefits of water column correction and contextual editing for mapping coral reefs. International Journal of Remote Sensing 19 (1): 203-210.

Mumby, P. J., Green, E. P., Edwards, A. J., and Clark, C. D. 1999. The cost-effectiveness of remote sensing for tropical coastal resources assessment and management. Journal of Environmental Management 55 (3): 157-166.

Mumby, P. J., and Harborne, A. R. 1999. Development of a systematic classification scheme of marine habitats to facilitate regional management and mapping of Caribbean coral reefs. Biological Conservation 88 (2): 155-163.

Mumby, P. J., Green, E. P., Edwards, A. J., and Clark, C. D. 1997. Coral reef habitat-mapping: how much detail can remote sensing provide? Marine Biology 130 (2): 193-202.

Mumby, P. J., Raines, P. S., Gray, D. A., and Gibson, J. P. 1995. Geographic information-systems - A tool for integrated coastal zone management in Belize. Coastal Management 23 (2): 111-121.

Mumby, P. J. 2001. Beta and habitat diversity in marine systems: a new approach to measurement, scaling and interpretation. Oecologia 128: 274-280.

NASA. March 8, 2004. http://landsat.gsfc.nasa.gov/

O'Regan, P. R. 1995. The use of contemporary information technologies for coastal research and management-a review. Journal of Coastal Research 12 (1): 193-204.

Phinney, J. T., Muller-Karger, F., Dustan, P., and Sobel, J. 2001. Using remote sensing to reassess the mass mortality of *Diadema antillarum* 1983-1984.Conservation Biology 15 (4), 885-891.

Rigol, J. P., and Chica-Olmo, M. 1998. Merging remote-sensing images for geological environmental mapping: application to the Cabo de Gata-Nijar Natural Park, Spain. Environmental Geology 34 (2/3): 194-202.

Rubec, P. J., Bexley, J. C. W., Norris, H., Coyne, M. S., Monaco, M. E., Smith, S. G., and Ault, J. S. 1999. Suitability modeling to delineate habitat essential to sustainable fisheries. . Fish Habitat: Essential fish habitat and rehabilitation. Proceedings of the Sea Grant symposium of fish habitat. AFS Bethesda, MD.

Sale, P. F., Chavez, E. A., Hatcher, B. G., Mayfield, C., and Ciborowski, J. H. 2001. Guidelines for developing a regional monitoring and environmental information system. Conservation and sustainable use of the Mesoamerican barrier reef system (MBRS) in Mexico, Belize, Guatemala, and Honduras.

Stoffle, R. W., Halmo, D. B., Wagner, T. W., and Luczkovich, J. J. 1994. Reefs from space: Satellite imagery, marine ecology, and ethnography in the Dominican-Republic. Human Ecology 22 (3): 355-378.

Smits, P. C. 2001. Combining supervised remote sensing image classifiers based on individual class performances. Lecture Notes in Computer Science 2096: 269-278.

Appendix A. Ground-Truthing Data for the 126 Stations.

Waypoint	Latitude N	Longitude W	Depth (m)	% Sand	% Seagrass	% Algae	% Hard Corals	% Soft Corals	% Coraline Algae "live rock"	% Rubble
110	17'19'12.0	87'47'39.4	1.83	70	30	0	0	0	0	0
111	17'19'12.8	87'47'40.1	1.83	90	10	0	0	0	0	0
112	17'19'13.6	87'47'41.0	2.13	65	5	30	0	0	0	0
113	17'19'14.3	87'47'41.4	2.74	85	0	0	0	0	0	15
114	17'19'14.8	87'47'42.2	2.44	60	0	30	0	10	0	0
115	17'19'15.4	87'47'43.1	1.52	70	25	5	0	0	0	0
116	17'19'15.9	87'47'43.9	0.91	0	100	0	0	0	0	0
126	17'16'49.1	87'48'34.0	2.74	30	30	0	5	20	15	0
127	17'16'48.6	87'48'34.4	3.05	45	0	25	5	25	0	0
128	17'16'47.2	87'48'34.3	3.35	50	0	30	5	15	0	0
129	17'16'46.3	87'48'34.4	3.35	60	0	15	0	20	0	5
130	17'16'45.3	87'48'34.8	3.05	0	0	0	20	20	60	0
131	17'16'44.6	87'48'35.5	3.66	40	5	0	10	25	20	0
132	17'16'44.4	87'48'36.3	3.66	40	0	0	15	20	25	0
133	17'16'44.5	87'48'37.5	3.35	30	0	0	20	25	15	10
134	17'16'50.6	87'48'34.9	2.74	50	50	0	0	0	0	0
135	17'16'50.0	87'48'34.4	2.74	65	35	0	0	0	0	0
136	17'16'49.3	87'48'33.7	2.74	70	30	0	0	0	0	0
137	17'16'48.6	87'48'32.9	2.74	55	45	0	0	0	0	0
138	17'16'48.0	87'48'32.1	2.44	0	0	5	0	0	90	5
139	17'16'47.4	87'48'31.3	3.35	40	0	0	55	5	0	0
140	17'16'46.5	87'48'30.9	3.35	0	0	0	20	25	55	0
141	17'16'45.7	87'48'30.2	4.27	0	0	0	25	0	75	0
142	17'16'45.1	87'48'29.5	4.88	60	0	0	25	0	0	0
143	17'16'44.5	87'48'28.8	5.18	0	0	0	35	30	45	15
151	17'16'02.0	87'49'09.6	2.44	0	100	0	0	0	0	0
152	17'16'01.3	87'49'08.8	2.13	55	45	0	0	0	0	0

Appendix A. Ground-Truthing Data for the 126 Stations.

Waypoint	Latitude N	Longitude W	Depth (m)	% Sand	% Seagrass	% Algae	% Hard Corals	% Soft Corals	% Coraline Algae "live rock"	% Rubble
153	17'16'00.6	87'49'08.1	1.22	0	0	0	20	10	70	0
154	17'15'59.7	87'49'07.6	1.83	0	0	0	0	20	80	0
155	17'15'59.3	87'49'06.6	2.74	0	0	0	85	0	15	0
156	17'15'58.5	87'49'05.8	4.27	0	0	0	5	50	45	0
157	17'15'58.2	87'49'04.9	4.88	0	0	0	45	25	30	0
158	17'15'57.7	87'49'04.1	3.96	0	0	0	15	0	85	0
170	17'19'04.7	87'47'33.2	6.10	0	0	0	35	10	55	0
169	17'19'03.8	87'47'33.6	6.71	0	0	0	5	5	90	0
168	17'19'03.6	87'47'34.3	5.18	0	0	0	35	15	50	0
167	17'19'02.7	87'47'34.1	5.18	50	0	25	10	15	0	0
166	17'19'02.5	87'47'33.8	6.40	0	0	5	15	0	80	0
165	17'19'01.6	87'47'34.6	7.01	0	0	0	0	20	80	0
164	17'19'01.8	87'47'35.0	5.18	0	0	20	5	45	30	0
163	17'19'01.1	87'47'35.7	4.88	0	0	0	15	20	65	0
162	17'18'00.6	87'47'35.4	4.88	0	0	0	25	5	70	0
161	17'18'59.6	87'47'35.4	5.79	0	0	0	30	25	45	0
160	17'18'59.8	87'47'36.3	5.18	15	0	0	15	45	25	0
159	17'18'58.8	87'47'36.4	5.49	25	0	15	10	20	30	0
173	17'19'05.1	87'47'35.7	3.66	0	0	0	20	40	40	0
174	17'19'03.9	87'47'35.5	4.27	20	0	0	10	10	60	0
175	17'19'04.2	87'47'36.6	3.66	0	0	0	20	40	40	0
176	17'19'03.4	87'47'37.0	3.35	0	0	0	10	50	40	0
177	17'19'02.9	87'47'36.4	3.35	0	0	0	70	25	5	0
178	17'19'02.1	87'47'36.8	3.66	0	0	0	10	30	60	0
179	17'19'02.3	87'47'37.6	3.96	0	0	0	20	15	65	0
180	17'19'01.5	87'47'38.1	3.66	65	0	5	0	15	15	0
181	17'19'00.9	87'47'37.1	4.57	0	0	0	35	35	30	0

Appendix A. Ground-Truthing Data for the 126 Stations.

Waypoint	Latitude N	Longitude W	Depth (m)	% Sand	% Seagrass	% Algae	% Hard Corals	% Soft Corals	% Coraline Algae "live rock"	% Rubble
182	17'19'00.2	87'47'37.5	4.57	0	0	0	10	0	90	0
172	17'19'00.3	87'47'38.3	3.96	0	0	0	30	15	55	0
171	17'18'59.7	87'47'38.8	3.96	0	0	0	0	40	60	0
183	17'16'19.2	87'48'43.6	8.84	0	0	0	25	30	45	0
185	17'16'18.3	87'48'43.9	8.84	10	0	0	25	25	40	0
186	17'16'18.7	87'48'44.7	7.01	0	0	0	15	15	55	20
187	17'16'17.8	87'48'45.1	6.71	0	0	0	25	25	50	0
188	17'16'17.5	87'48'44.2	8.53	10	0	0	30	30	40	0
189	17'16'16.7	87'48'44.7	7.32	0	0	0	5	50	25	20
190	17'16'17.0	87'48'45.5	5.79	0	0	0	25	25	15	0
191	17'16'16.2	87'48'46.1	6.10	0	0	0	40	40	10	0
192	17'16'15.7	87'48'45.1	7.01	0	0	0	35	35	30	0
193	17'16'14.7	87'48'45.1	7.62	0	0	0	5	55	15	25
194	17'16'14.8	87'48'46.2	6.40	5	0	0	40	35	20	0
195	17'16'13.8	87'48'46.4	6.71	10	0	0	35	35	0	40
196	17'17'28.4	87'48'32.1	1.22	5	95	0	0	0	0	0
197	17'17'29.4	87'48'33.9	1.22	45	40	15	0	0	0	0
198	17'17'30.0	87'48'34.7	0.91	20	80	0	0	0	0	0
199	17'17'30.5	87'48'35.6	0.91	5	95	0	0	0	0	0
200	17'17'30.8	87'48'36.5	0.91	0	100	0	0	0	0	0
34	17'16'55.2	87'48'39.4	1.52	44	56	0	0	0	0	0
35	17'16'54.3	87'48'38.6	1.83	20	78	0	2	0	0	0
36	17'16'53.0	87'48'37.9	2.13	26	74	0	0	0	0	0
37	17'16'51.9	87'48'37.0	2.44	32	68	0	0	0	0	0
38	17'16'51.1	87'48'36.0	2.74	50	50	0	0	0	0	0
39	17'16'50.0	87'48'35.4	2.74	74	26	0	0	0	0	0
40	17'16'49.3	87'48'34.6	3.05	62	38	0	0	0	0	0

Appendix A. Ground-Truthing Data for the 126 Stations.

Waypoint	Latitude N	Longitude W	Depth (m)	% Sand	% Seagrass	% Algae	% Hard Corals	% Soft Corals	% Coraline Algae "live rock"	% Rubble
41	17'16'49.1	87'48'33.5	2.13	46	54	0	0	0	0	0
42	17'16'48.1	87'48'32.7	2.74	0	0	0	14	4	82	0
43	17'16'47.1	87'48'32.0	3.35	58	0	0	10	0	32	0
45	17' 16'45.8	87'48'31.3	3.96	42	0	0	0	14	0	20
46	17'16'44.6	87'48'30.6	4.27	40	0	0	0	12	18	30
47	17'16'43.5	87'48'30.2	4.88	50	0	0	10	8	6	26
48	17'16'42.2	87'48'29.2	5.79	4	0	0	28	0	68	0
49	17'16'40.9	87'48'28.5	6.10	0	0	0	32	4	64	0
50	17'16'39.8	87'48'26.5	10.36	72	0	0	0	6	0	11
51	17'16'40.8	87'48'27.3	7.32	4	0	0	22	0	60	14
55	17'17'41.9	87'48'20.0	1.22	100	0	0	0	0	0	0
56	17'17'42.6	87'48'21.4	1.22	88	0	12	0	0	0	0
57	17'17'43.2	87'48'22.5	1.22	88	0	12	0	0	0	0
58	17'17'43.9	87'48'23.7	1.52	97	0	3	0	0	0	0
59	17'17'44.4	87'48'25.3	0.91	97	0	3	0	0	0	0
60	17'17'44.9	87'48'26.6	0.91	97	0	3	0	0	0	0
61	17'17'45.5	87'48'27.8	0.91	98	0	2	0	0	0	0
62	17'17'46.1	87'48'29.0	1.22	91	0	9	0	0	0	0
63	17'17'46.6	87'48'30.3	0.91	94	0	6	0	0	0	0
64	17'17'47.3	87'48'31.5	1.52	64	36	0	0	0	0	0
65	17'17'47.6	87'48'32.9	1.83	72	24	4	0	0	0	0
66	17'17'48.1	87'48'34.1	1.52	60	40	0	0	0	0	0
67	17'17'48.5	87'48'35.3	1.52	78	22	0	0	0	0	0
68	17'17'49.0	87'48'36.4	1.52	66	34	0	0	0	0	0
69	17'17'49.4	87'48'37.7	1.52	56	44	0	0	0	0	0
70	17'17'49.7	87'48'39.0	1.52	74	26	0	0	0	0	0
71	17'17'50.0	87'48'40.2	1.22	80	20	0	0	0	0	0

Appendix A. Ground-Truthing Data for the 126 Stations.

Waypoint	Latitude N	Longitude W	Depth (m)	% Sand	% Seagrass	% Algae	% Hard Corals	% Soft Corals	% Coraline Algae "live rock"	% Rubble
72	17'17'50.4	87'48'41.5	0.91	62	32	0	0	0	0	0
73	17'17'50.8	87'48'43.0	0.91	80	20	0	0	0	0	0
74	17'17'51.1	87'48'44.5	1.52	20	80	0	0	0	0	0
75	17'19'07.4	87'47'29.2	8.23	99	0	1	0	0	0	0
76	17'19'08.0	87'47'30.4	7.01	80	0	20	0	0	0	0
77	17'19'08.6	87'47'31.9	4.27	12	0	0	12	28	48	0
78	17'19'09.1	87'47'33.2	3.35	8	0	0	12	0	80	0
79	17'19'10.0	87'47'34.3	1.83	4	0	0	26	16	54	0
80	17'19'10.8	87'47'35.0	1.52	84	0	0	0	8	0	8
81	17'19'11.8	87'47'35.5	1.52	62	0	0	2	0	22	14
82	17'19'12.9	87'47'35.8	2.74	38	0	0	0	8	0	54
83	17'19'13.6	87'47'36.7	3.66	100	0	0	0	0	0	0
84	17'19'14.5	87'47'37.7	0.91	77	10	0	0	5	0	8
85	17'19'14.5	87'47'38.7	1.83	76	8	0	6	2	8	0
86	17'19'14.6	87'47'40.0	2.44	92	0	0	0	8	0	0
87	17'19'14.9	87'47'41.2	2.44	74	0	0	0	8	18	0
88	17'19'15.3	87'47'42.5	1.83	40	0	20	0	0	0	40
89	17'19'16.1	87'47'43.4	0.61	0	100	0	0	0	0	0

Appendix A. Ground-Truthing Data for the 126 Stations.

Waypoint	Latitude N	Longitude W	Optimization Clustering Classification (3- group)	Band 1	Band 2	Band 3	Band 4	Band 5	Band 7	Band 8
110	17'19'12.0	87'47'39.4	1	186	148	101	36	49	40	63
111	17'19'12.8	87'47'40.1	1	178	141	91	36	47	40	61
112	17'19'13.6	87'47'41.0	1	185	144	92	37	47	41	59
113	17'19'14.3	87'47'41.4	1	170	131	90	36	47	40	56
114	17'19'14.8	87'47'42.2	1	174	132	91	38	48	40	56
115	17'19'15.4	87'47'43.1	1	169	128	89	38	48	40	58
116	17'19'15.9	87'47'43.9	2	148	118	93	39	50	42	55
126	17'16'49.1	87'48'34.0	1	160	117	84	36	47	39	52
127	17'16'48.6	87'48'34.4	1	157	116	85	35	47	40	53
128	17'16'47.2	87'48'34.3	1	154	111	83	35	48	40	53
129	17'16'46.3	87'48'34.4	1	154	111	83	35	48	40	51
130	17'16'45.3	87'48'34.8	3	151	111	82	35	48	41	53
131	17'16'44.6	87'48'35.5	1	147	108	82	35	47	39	52
132	17'16'44.4	87'48'36.3	1	148	110	83	35	48	39	52
133	17'16'44.5	87'48'37.5	1	149	110	83	35	47	41	51
134	17'16'50.6	87'48'34.9	1	166	125	87	35	47	41	55
135	17'16'50.0	87'48'34.4	1	161	120	87	35	47	41	53
136	17'16'49.3	87'48'33.7	1	161	119	84	36	47	41	54
137	17'16'48.6	87'48'32.9	1	158	116	83	35	50	39	50
138	17'16'48.0	87'48'32.1	3	148	109	82	35	46	41	54
139	17'16'47.4	87'48'31.3	1	146	108	82	35	46	39	47
140	17'16'46.5	87'48'30.9	3	148	105	81	34	46	39	52
141	17'16'45.7	87'48'30.2	3	144	102	78	35	46	39	49
142	17'16'45.1	87'48'29.5	1	144	103	80	35	46	40	48
143	17'16'44.5	87'48'28.8	3	143	100	79	35	46	40	47
151	17'16'02.0	87'49'09.6	2	147	106	82	34	47	39	51
152	17'16'01.3	87'49'08.8	1	147	106	82	34	46	39	49

Appendix A. Ground-Truthing Data for the 126 Stations.

Waypoint	Latitude N	Longitude W	Optimization Clustering Classification (3- group)	Band 1	Band 2	Band 3	Band 4	Band 5	Band 7	Band 8
153	17'16'00.6	87'49'08.1	3	134	97	82	34	46	38	50
154	17'15'59.7	87'49'07.6	3	130	95	81	35	45	39	49
155	17'15'59.3	87'49'06.6	3	127	93	79	35	46	40	50
156	17'15'58.5	87'49'05.8	3	128	93	80	35	46	39	46
157	17'15'58.2	87'49'04.9	3	127	92	79	34	45	41	48
158	17'15'57.7	87'49'04.1	3	131	91	78	35	46	38	44
170	17'19'04.7	87'47'33.2	3	161	99	76	34	45	38	50
169	17'19'03.8	87'47'33.6	3	154	99	77	34	46	40	48
168	17'19'03.6	87'47'34.3	3	154	99	77	34	46	39	49
167	17'19'02.7	87'47'34.1	1	160	101	78	34	46	38	49
166	17'19'02.5	87'47'33.8	3	160	101	78	34	46	39	44
165	17'19'01.6	87'47'34.6	3	155	99	77	34	46	39	47
164	17'19'01.8	87'47'35.0	3	155	99	77	34	46	39	47
163	17'19'01.1	87'47'35.7	3	143	96	77	33	45	38	45
162	17'18'00.6	87'47'35.4	3	143	96	77	33	45	37	46
161	17'18'59.6	87'47'35.4	3	149	98	78	34	46	39	48
160	17'18'59.8	87'47'36.3	3	149	98	78	35	45	39	46
159	17'18'58.8	87'47'36.4	3	138	95	76	35	47	39	46
173	17'19'05.1	87'47'35.7	3	142	101	79	34	45	38	50
174	17'19'03.9	87'47'35.5	3	142	100	78	34	46	38	48
175	17'19'04.2	87'47'36.6	3	138	100	78	34	45	39	49
176	17'19'03.4	87'47'37.0	3	138	100	78	33	42	37	48
177	17'19'02.9	87'47'36.4	3	133	96	75	33	42	37	46
178	17'19'02.1	87'47'36.8	3	136	95	77	33	42	37	44
179	17'19'02.3	87'47'37.6	3	138	99	78	33	43	37	49
180	17'19'01.5	87'47'38.1	1	138	99	78	34	47	41	47
181	17'19'00.9	87'47'37.1	3	135	96	77	35	46	39	48

Appendix A. Ground-Truthing Data for the 126 Stations

Waypoint	Latitude N	Longitude W	Optimization Clustering Classification (3- group)	Band 1	Band 2	Band 3	Band 4	Band 5	Band 7	Band 8
182	17'19'00.2	87'47'37.5	3	142	99	80	35	46	39	48
172	17'19'00.3	87'47'38.3	3	142	99	80	35	48	39	50
171	17'18'59.7	87'47'38.8	3	141	101	81	34	46	37	50
183	17'16'19.2	87'48'43.6	3	140	95	79	35	46	38	46
185	17'16'18.3	87'48'43.9	3	139	92	79	34	46	39	47
186	17'16'18.7	87'48'44.7	3	138	96	76	34	47	40	46
187	17'16'17.8	87'48'45.1	3	140	95	80	34	47	40	48
188	17'16'17.5	87'48'44.2	3	139	92	78	34	46	39	48
189	17'16'16.7	87'48'44.7	3	142	95	76	34	47	40	46
190	17'16'17.0	87'48'45.5	3	140	95	79	34	47	40	48
191	17'16'16.2	87'48'46.1	3	139	93	79	34	47	40	48
192	17'16'15.7	87'48'45.1	3	136	92	78	34	48	40	47
193	17'16'14.7	87'48'45.1	3	136	91	78	34	47	38	43
194	17'16'14.8	87'48'46.2	3	135	94	78	34	46	38	47
195	17'16'13.8	87'48'46.4	2[3]	136	93	78	34	46	39	48
196	17'17'28.4	87'48'32.1	2	162	134	80	36	48	40	48
197	17'17'29.4	87'48'33.9	1	148	121	109	36	49	40	55
198	17'17'30.0	87'48'34.7	2	148	120	102	36	50	42	58
199	17'17'30.5	87'48'35.6	2	151	119	102	37	49	38	60
200	17'17'30.8	87'48'36.5	2	144	114	100	37	48	41	55
34	17'16'55.2	87'48'39.4	1	141	108	100	37	48	40	54
35	17'16'54.3	87'48'38.6	2	138	109	89	37	49	40	53
36	17'16'53.0	87'48'37.9	2	145	111	87	36	48	40	53
37	17'16'51.9	87'48'37.0	1	162	122	85	36	48	40	54
38	17'16'51.1	87'48'36.0	1	164	122	85	36	47	40	56
39	17'16'50.0	87'48'35.4	1	160	119	87	36	49	40	54
40	17'16'49.3	87'48'34.6	1	161	120	85	35	47	41	53

Appendix A. Ground-Truthing Data for the 126 Stations.

Waypoint	Latitude N	Longitude W	Optimization Clustering Classification (3- group)	Band 1	Band 2	Band 3	Band 4	Band 5	Band 7	Band 8
41	17'16'49.1	87'48'33.5	1	160	117	87	36	47	39	52
42	17'16'48.1	87'48'32.7	3	153	111	84	35	50	41	53
43	17'16'47.1	87'48'32.0	1	149	106	81	35	46	39	48
45	17' 16'45.8	87'48'31.3	1	147	105	81	35	47	41	50
46	17'16'44.6	87'48'30.6	1	145	101	81	35	48	40	49
47	17'16'43.5	87'48'30.2	1	143	102	83	36	47	42	50
48	17'16'42.2	87'48'29.2	3	151	103	83	35	50	40	47
49	17'16'40.9	87'48'28.5	3	143	96	79	34	47	38	47
50	17'16'39.8	87'48'26.5	1	152	95	79	35	46	41	47
51	17'16'40.8	87'48'27.3	3	143	94	78	35	45	40	48
55	17'17'41.9	87'48'20.0	1	199	176	78	35	47	41	71
56	17'17'42.6	87'48'21.4	1	197	171	134	35	49	40	71
57	17'17'43.2	87'48'22.5	1	191	167	127	35	47	42	65
58	17'17'43.9	87'48'23.7	1	191	167	120	35	46	39	67
59	17'17'44.4	87'48'25.3	1	195	169	121	35	46	38	67
60	17'17'44.9	87'48'26.6	1	203	176	123	35	46	40	69
61	17'17'45.5	87'48'27.8	1	201	172	131	35	47	38	66
62	17'17'46.1	87'48'29.0	1	197	172	127	35	46	39	68
63	17'17'46.6	87'48'30.3	1	201	176	128	34	47	39	72
64	17'17'47.3	87'48'31.5	1	206	180	133	34	47	40	66
65	17'17'47.6	87'48'32.9	1	168	138	142	35	46	37	58
66	17'17'48.1	87'48'34.1	1	167	139	104	34	45	39	59
67	17'17'48.5	87'48'35.3	1	162	133	103	34	46	40	57
68	17'17'49.0	87'48'36.4	1	174	137	102	34	46	40	62
69	17'17'49.4	87'48'37.7	1	180	152	104	34	46	39	62
70	17'17'49.7	87'48'39.0	1	179	148	110	34	47	39	60
71	17'17'50.0	87'48'40.2	1	176	153	113	35	47	41	60

Appendix A. Ground-Truthing Data for the 126 Stations.

Waypoint	Latitude N	Longitude W	Optimization Clustering Classification (3- group)	Band 1	Band 2	Band 3	Band 4	Band 5	Band 7	Band 8
72	17'17'50.4	87'48'41.5	1	189	163	116	35	48	41	66
73	17'17'50.8	87'48'43.0	1	192	161	123	35	48	40	67
74	17'17'51.1	87'48'44.5	2	177	146	127	35	46	40	63
75	17'19'07.4	87'47'29.2	1	168	100	112	34	46	39	48
76	17'19'08.0	87'47'30.4	1	173	109	78	34	48	40	50
77	17'19'08.6	87'47'31.9	3	168	108	80	35	47	40	49
78	17'19'09.1	87'47'33.2	3	141	102	79	34	45	38	49
79	17'19'10.0	87'47'34.3	3	151	113	81	34	46	39	48
80	17'19'10.8	87'47'35.0	1	152	118	85	34	46	38	48
81	17'19'11.8	87'47'35.5	1	153	121	91	38	48	39	64
82	17'19'12.9	87'47'35.8	1	170	138	103	37	49	42	57
83	17'19'13.6	87'47'36.7	1	186	144	106	36	50	42	62
84	17'19'14.5	87'47'37.7	1	196	155	99	37	47	40	61
85	17'19'14.5	87'47'38.7	1	196	152	103	36	49	41	61
86	17'19'14.6	87'47'40.0	1	187	146	99	36	49	41	60
87	17'19'14.9	87'47'41.2	1	174	132	96	36	48	40	61
88	17'19'15.3	87'47'42.5	1	169	128	91	38	48	40	58
89	17'19'16.1	87'47'43.4	2	148	118	89	39	50	42	55

Appendix B. Canonical Scores of the 78 Stations Used in the Analysis.

Habitat	Case Number	Canonical score factor 1	Canonical score factor 2
1 (Sand)	1	2.235	0.334
	2	1.61	0.114
	3	1.075	-0.257
	4	1.892	-1.904
	7	-0.048	0.203
	8	0.33	-0.527
	47	0.385	-0.689
	48	-0.094	0.255
	52	2.513	2.089
	53	3.586	0.602
	54	3.179	0.389
	55	3.016	0.571
	56	3.176	0.827
	57	3.615	1.255
	58	3.613	0.989
	59	3.463	0.756
	60	3.216	1.792
	61	3.562	1.973
	62	2.045	-1.136
	63	0.701	0.577
	64	0.368	0.348
	65	0.675	1.274
	66	1.37	1.182
	67	2.083	-0.123
	68	2.736	0.618
	69	2.861	0.743
	71	-0.652	1.532
	75	-0.789	0.389
	76	2.192	0.315
	77	2.123	0.526
2 (Coral Reef)	6	-0.665	-0.26
	9	-0.787	-0.457
	10	-1.457	0.516
	11	-1.215	-0.496
	13	-1.951	-0.468
	14	-1.624	-1.56
	15	-1.755	-1.647
	16	-2.319	-0.841
	17	-1.838	-1.287
	18	-1.627	1.907
	19	-1.703	1.291

Appendix B. Canonical Scores of the 78 Stations Used in the Analysis.

	20	-1.703	1.291
	21	-1.515	1.715
	22	-1.689	1.375
	23	-2.466	1.284
	24	-2.466	1.284
	25	-1.791	0.872
	26	-1.304	0.036
	27	-1.748	0.173
	28	-1.868	-0.11
	29	-2.355	0.726
	30	-2.606	0.722
	31	-2.395	0.753
	32	-1.606	-1.062
	33	-1.317	-0.634
	34	-1.317	-0.634
	35	-1.715	0.037
	36	-1.528	-0.666
	37	-2.149	0.169
	38	-1.992	0.144
	39	-2.172	0.195
	40	-2.056	0.417
	49	-0.59	-0.143
	50	-0.96	-0.064
	51	-1.933	0.396
	72	-0.589	1.307
	73	-1.722	0.061
	74	-1.095	0.547
3 (Seagrass)	5	1.776	-4.337
	12	-1.408	0.378
	41	0.848	-0.754
	42	0.603	-2.118
	43	1.093	-2.674
	44	0.748	-3.073
	45	0.208	-3.154
	46	-0.147	-1.731
	70	2.144	-0.209
	78	1.683	-4.233

Appendix C. CD of Digital Images of the Ground-Truthing Stations.


wp_110.bmp

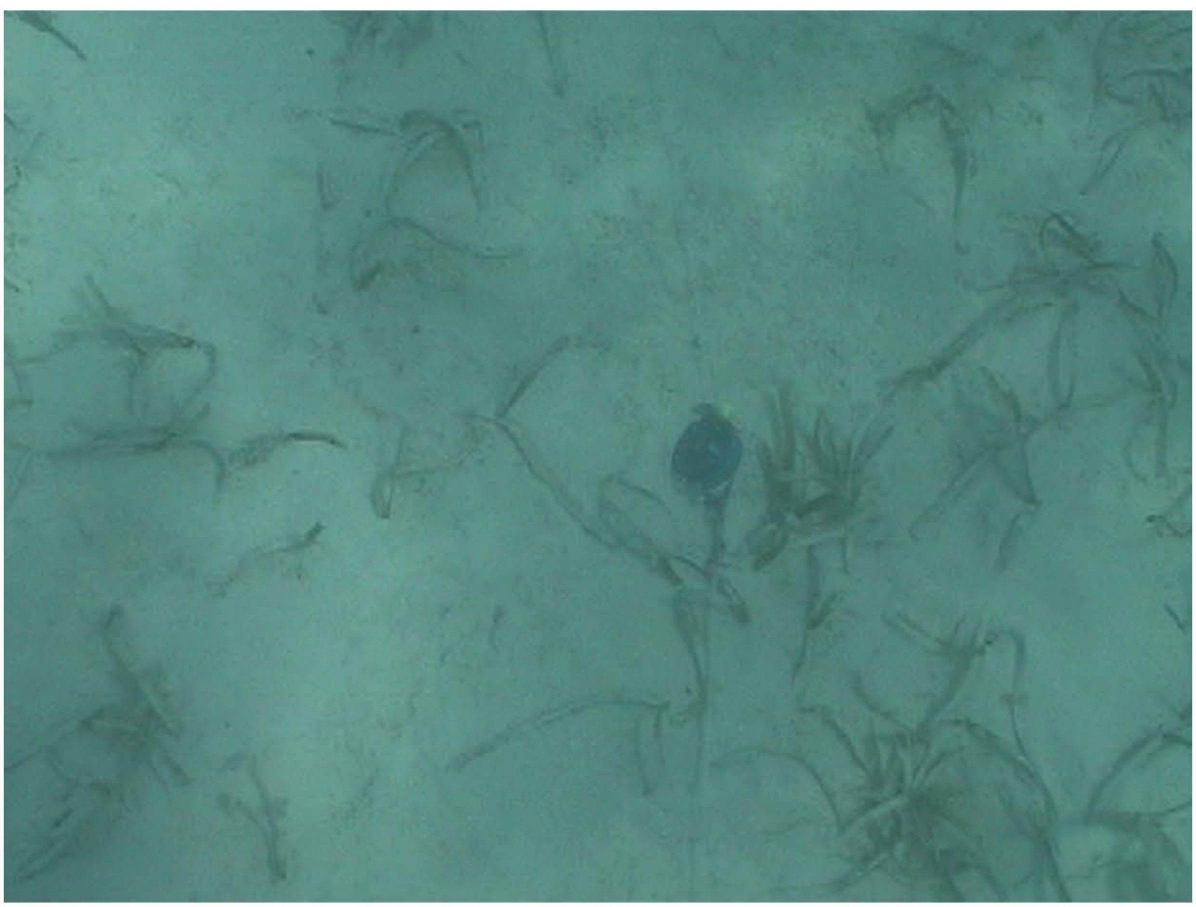
wp_111.bmp

wp_112.bmp

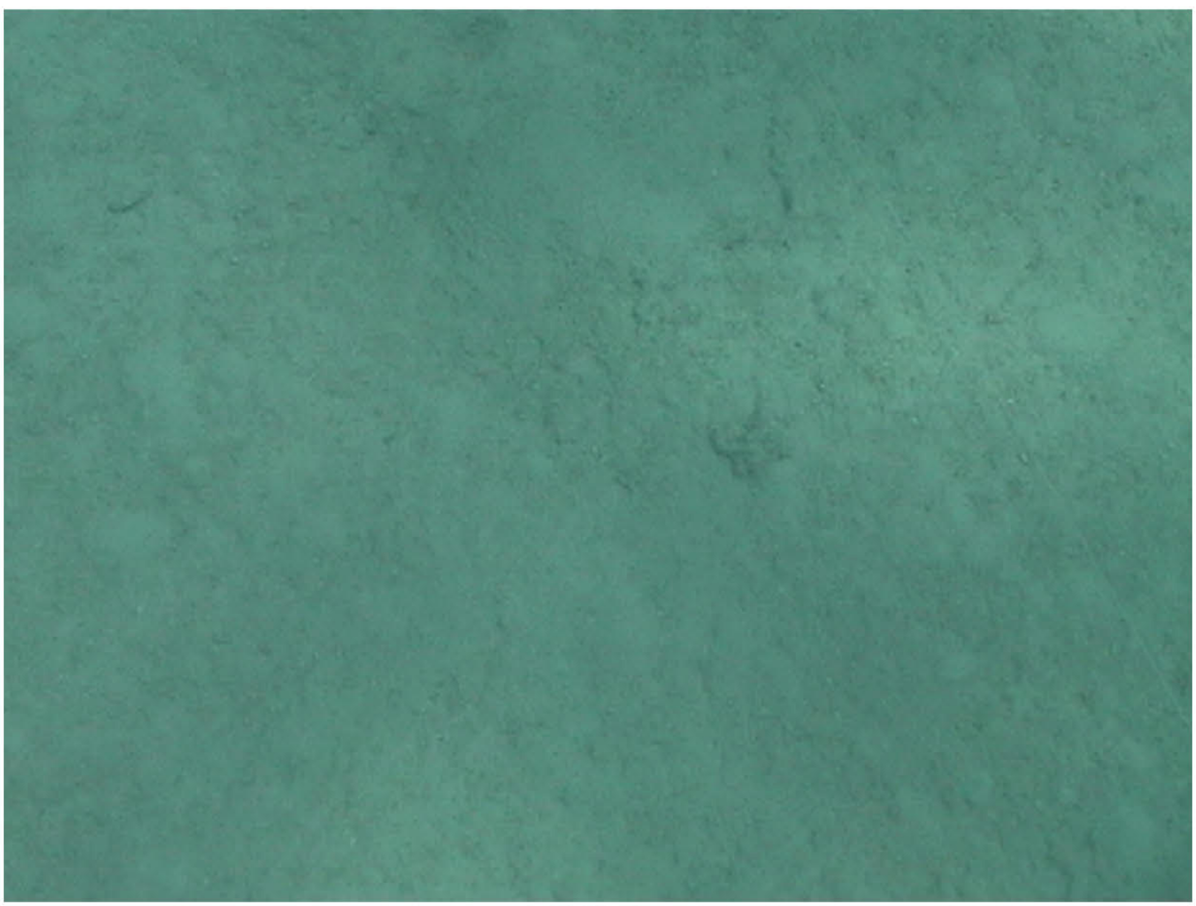

wp_112a.bmp

wp_113.bmp

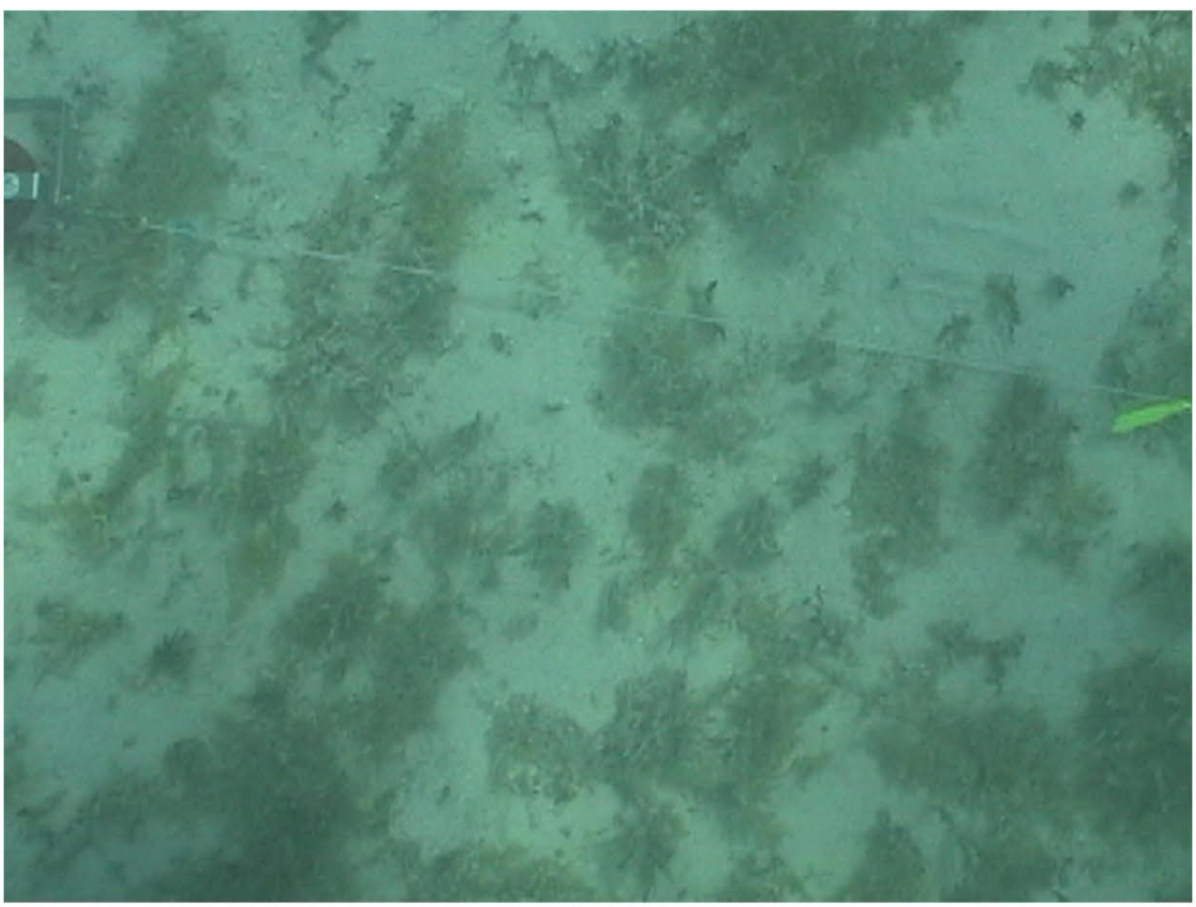
wp_114.bmp

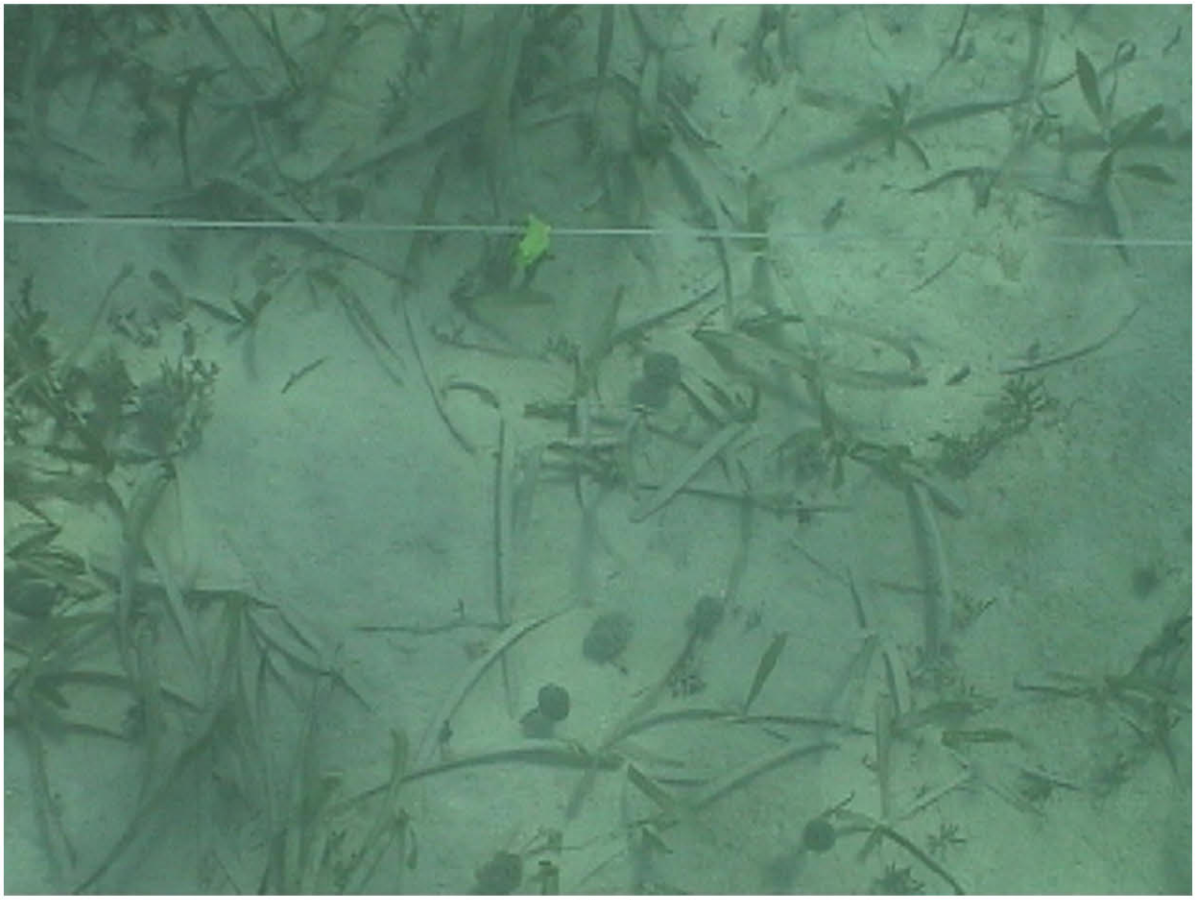
wp_115.bmp


wp_116.bmp

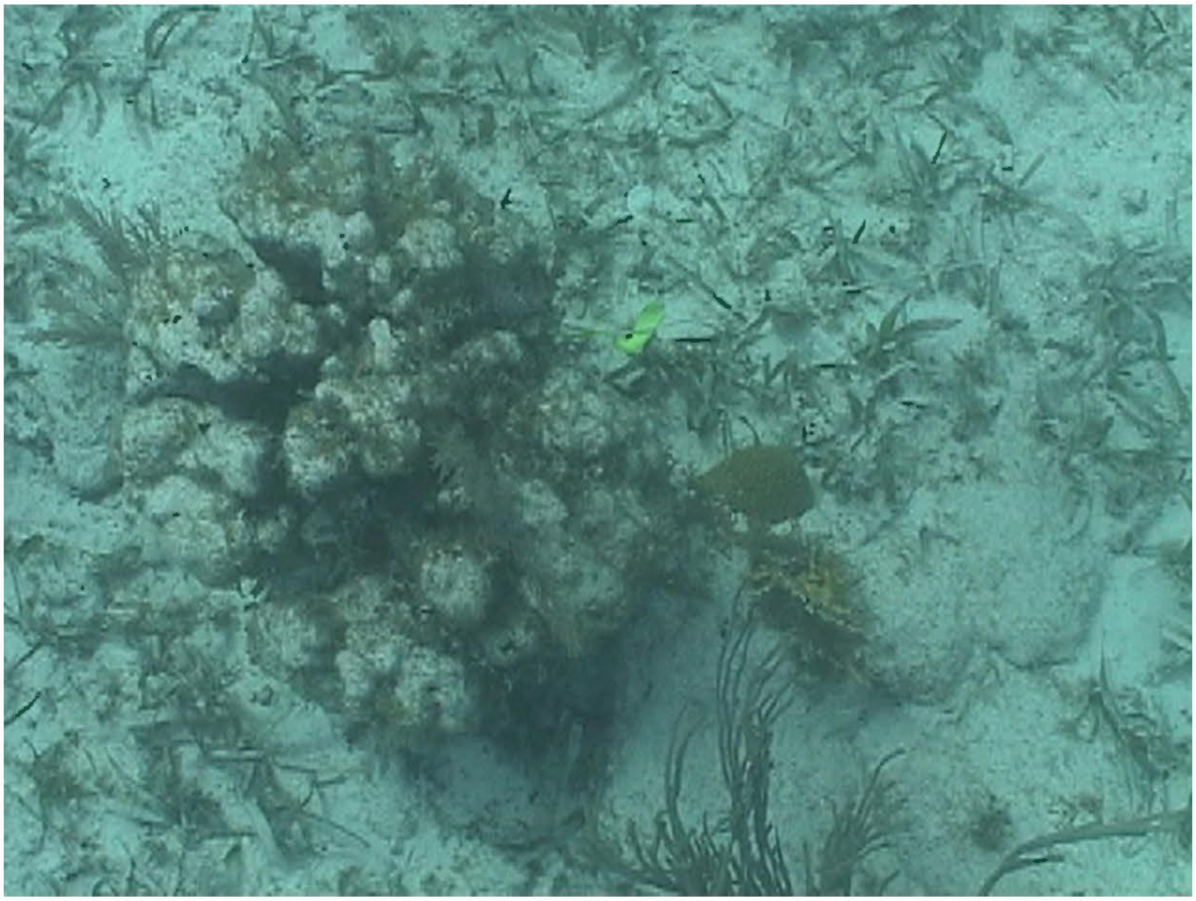

wp_126.bmp

wp_127.bmp

wp_128.bmp

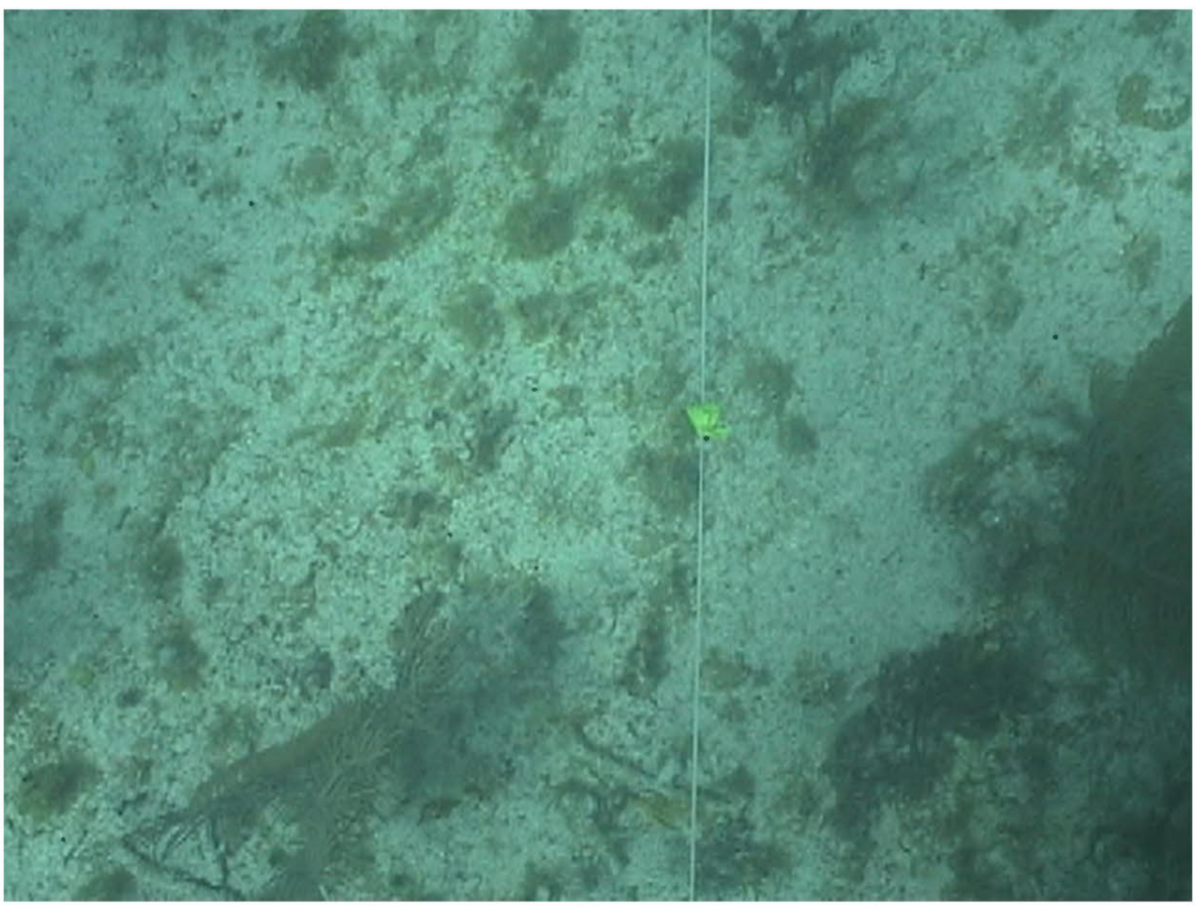

wp_129.bmp

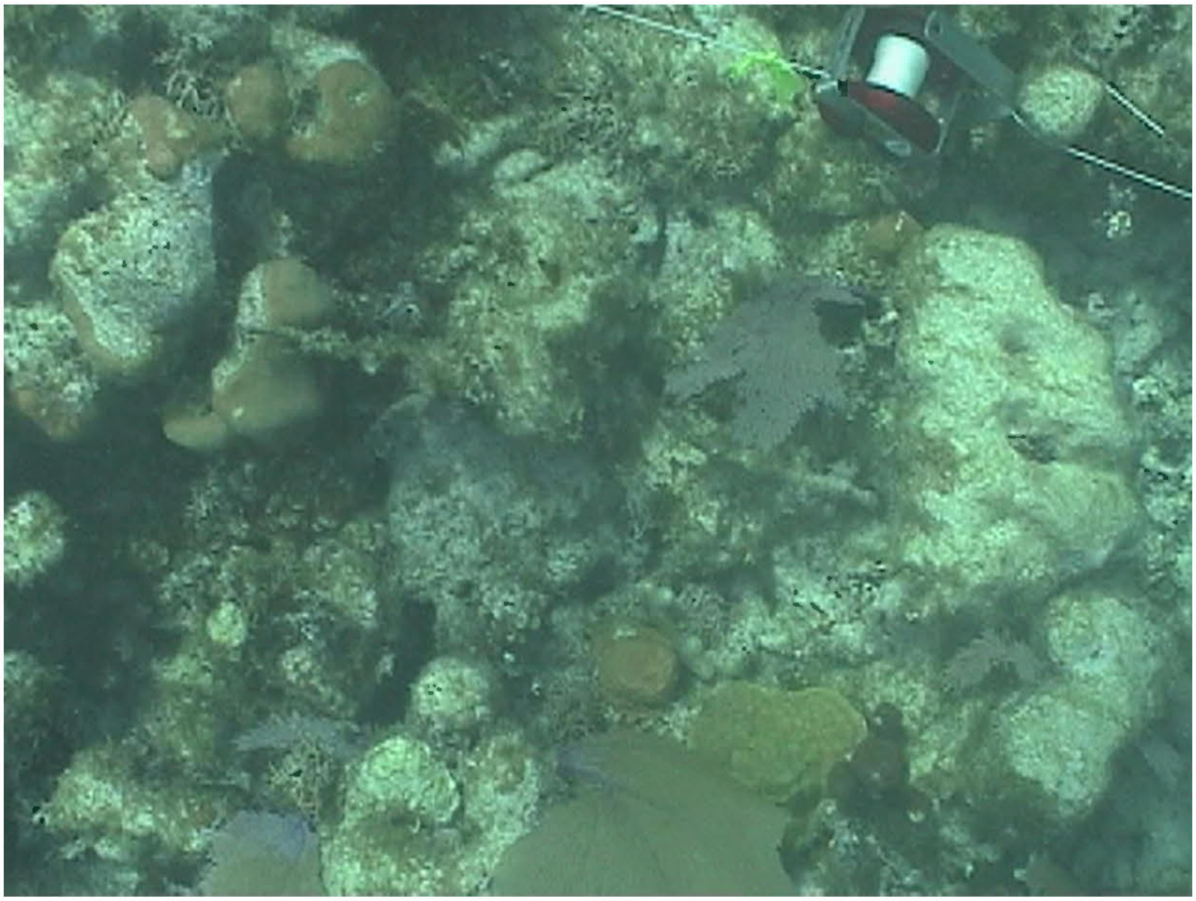
wp_130.bmp


wp_131.bmp

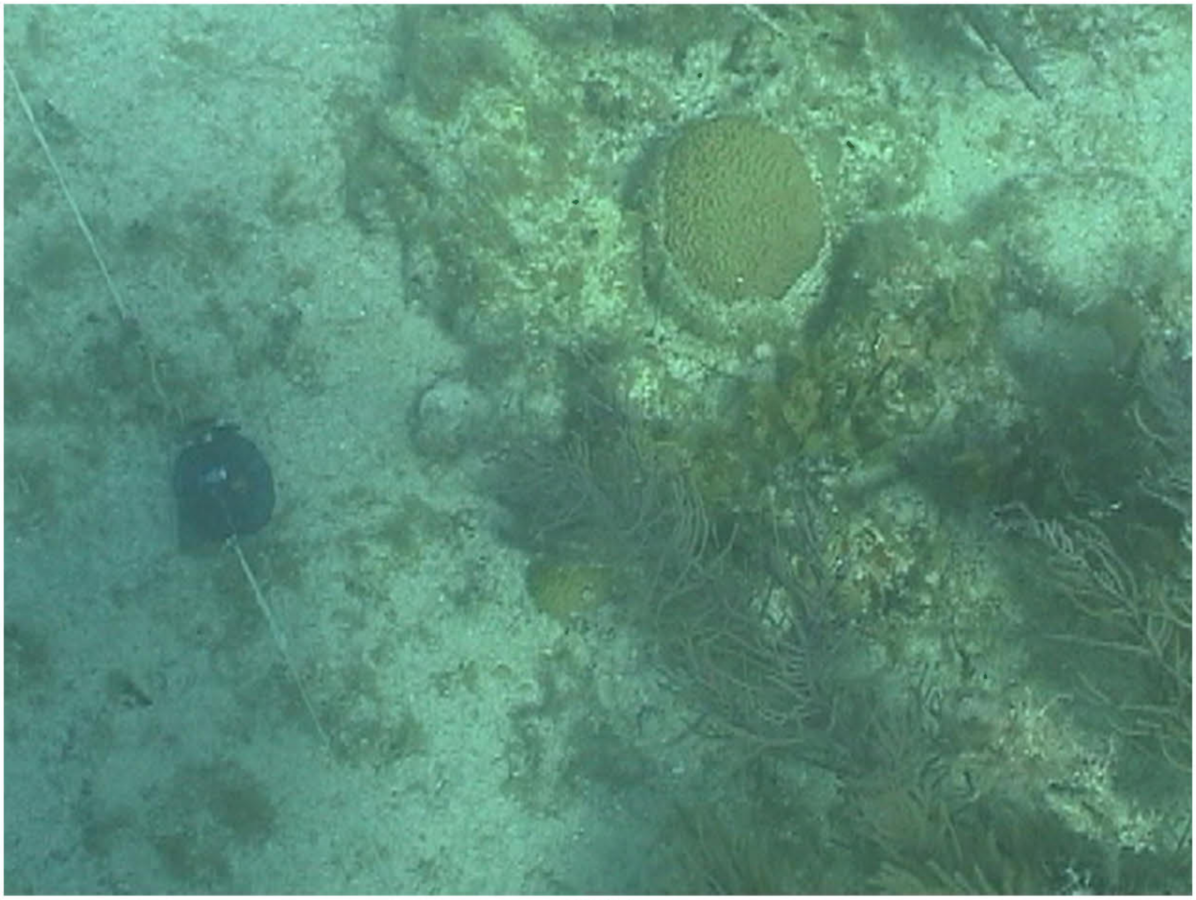
wp_132.bmp

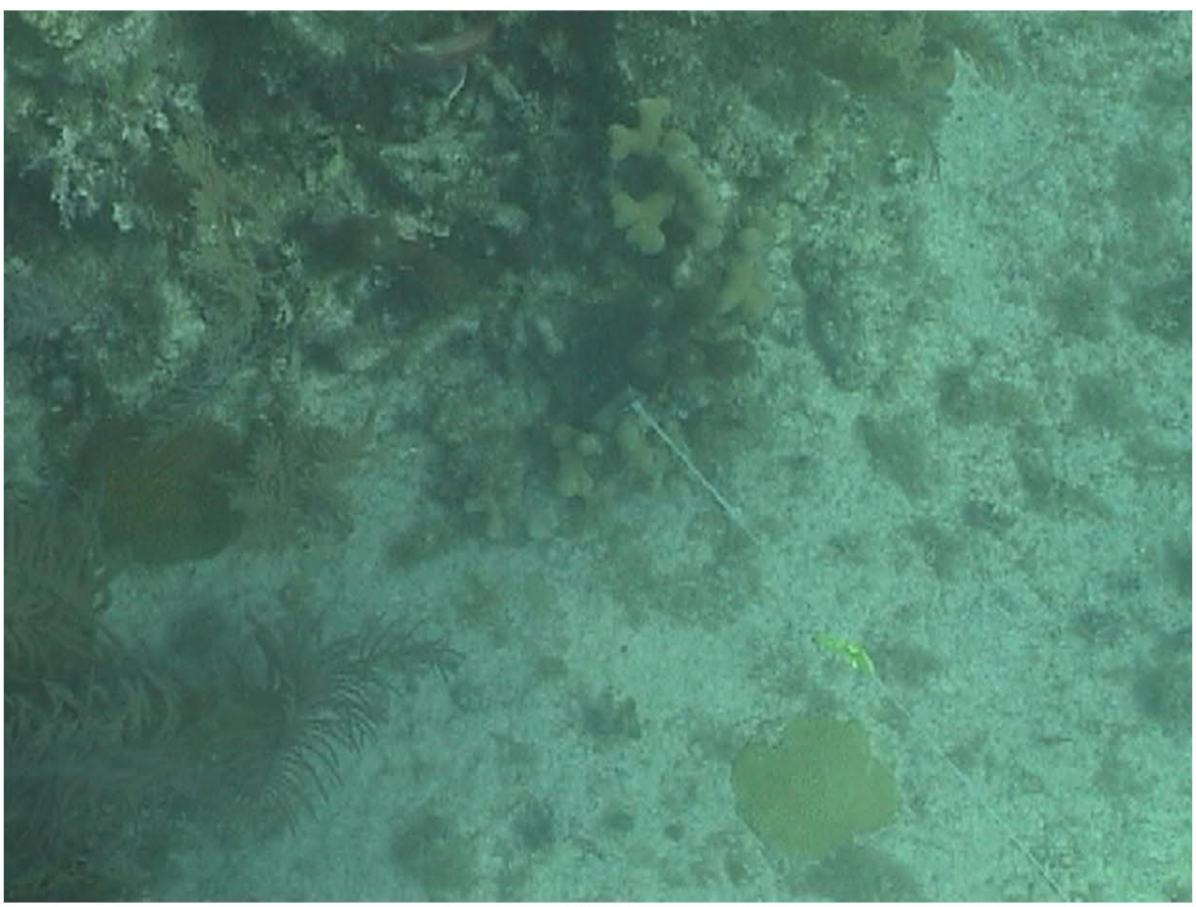
wp_133.bmp

wp_134.bmp

wp_135.bmp

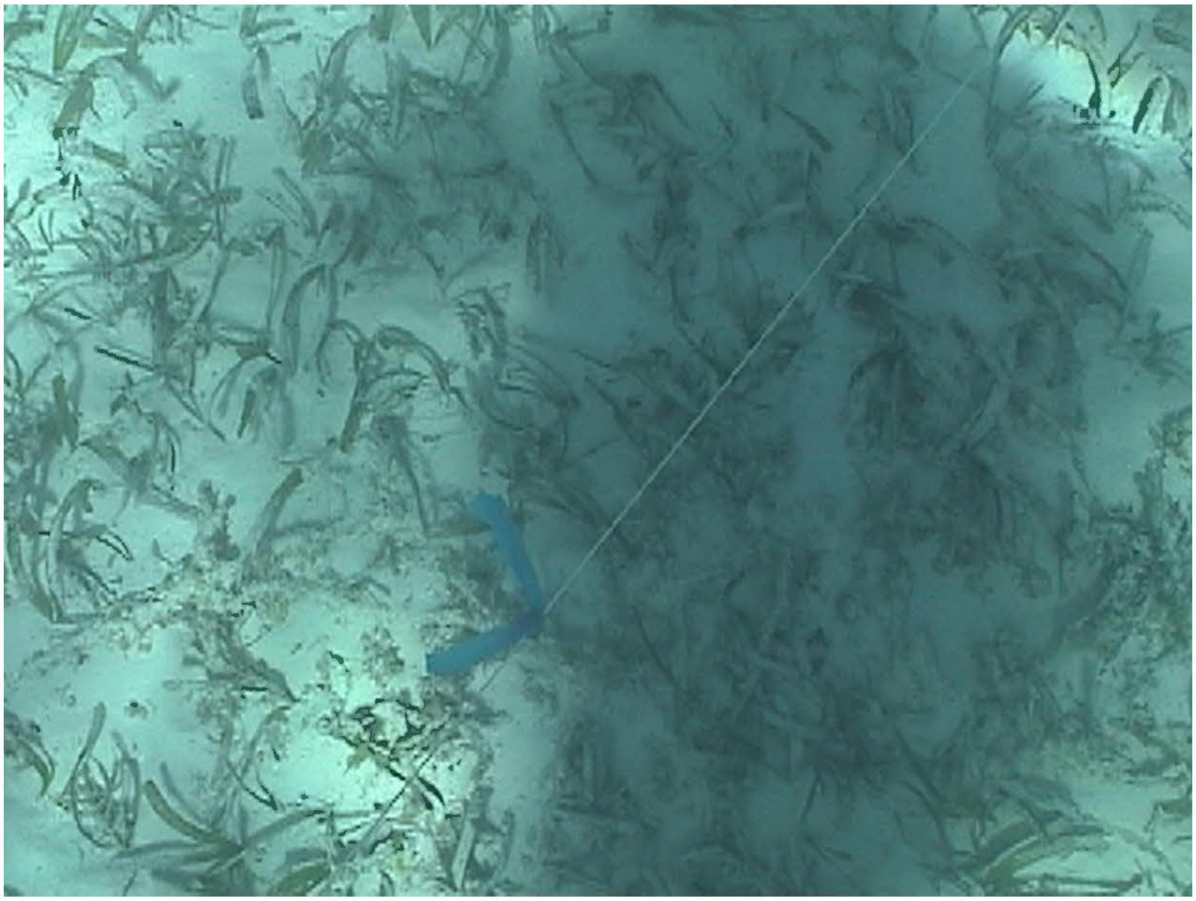
wp_136.bmp

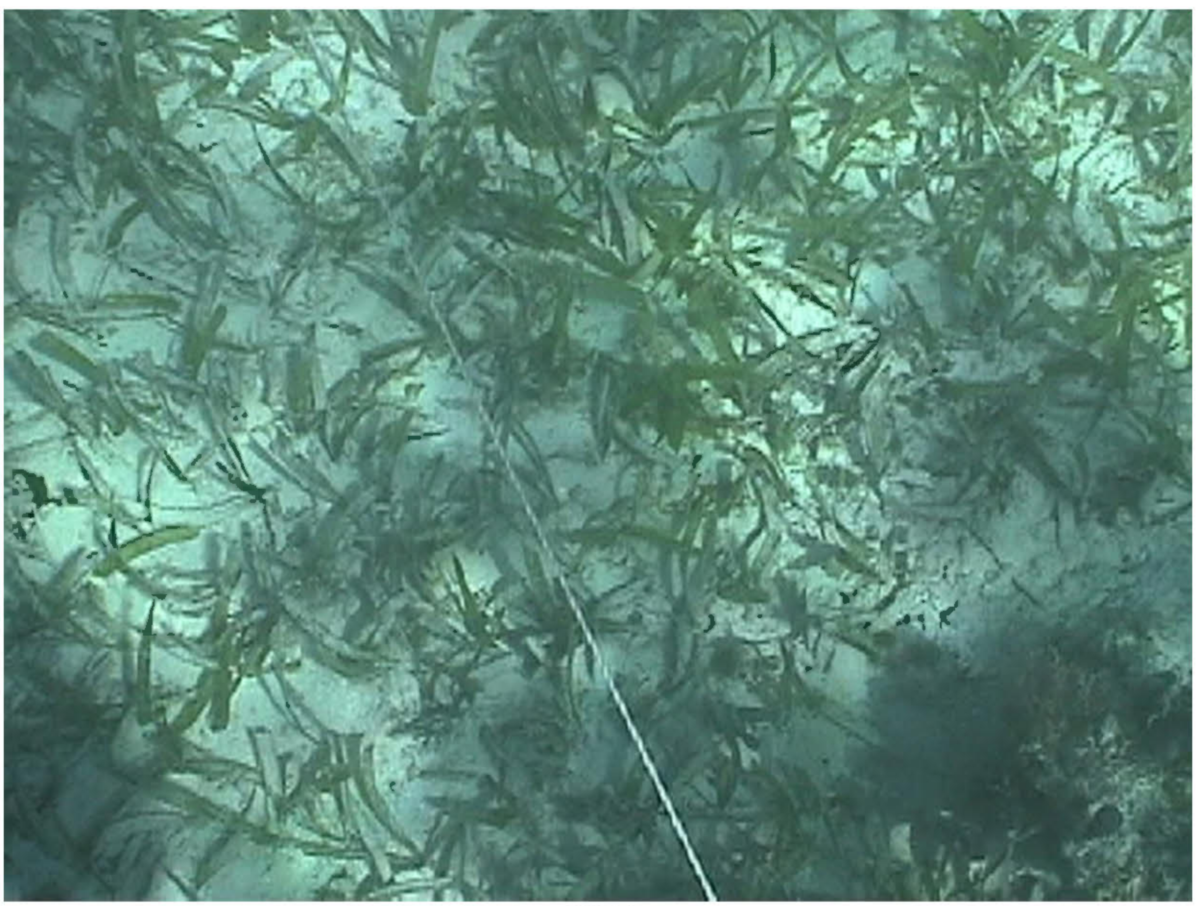
wp_137.bmp

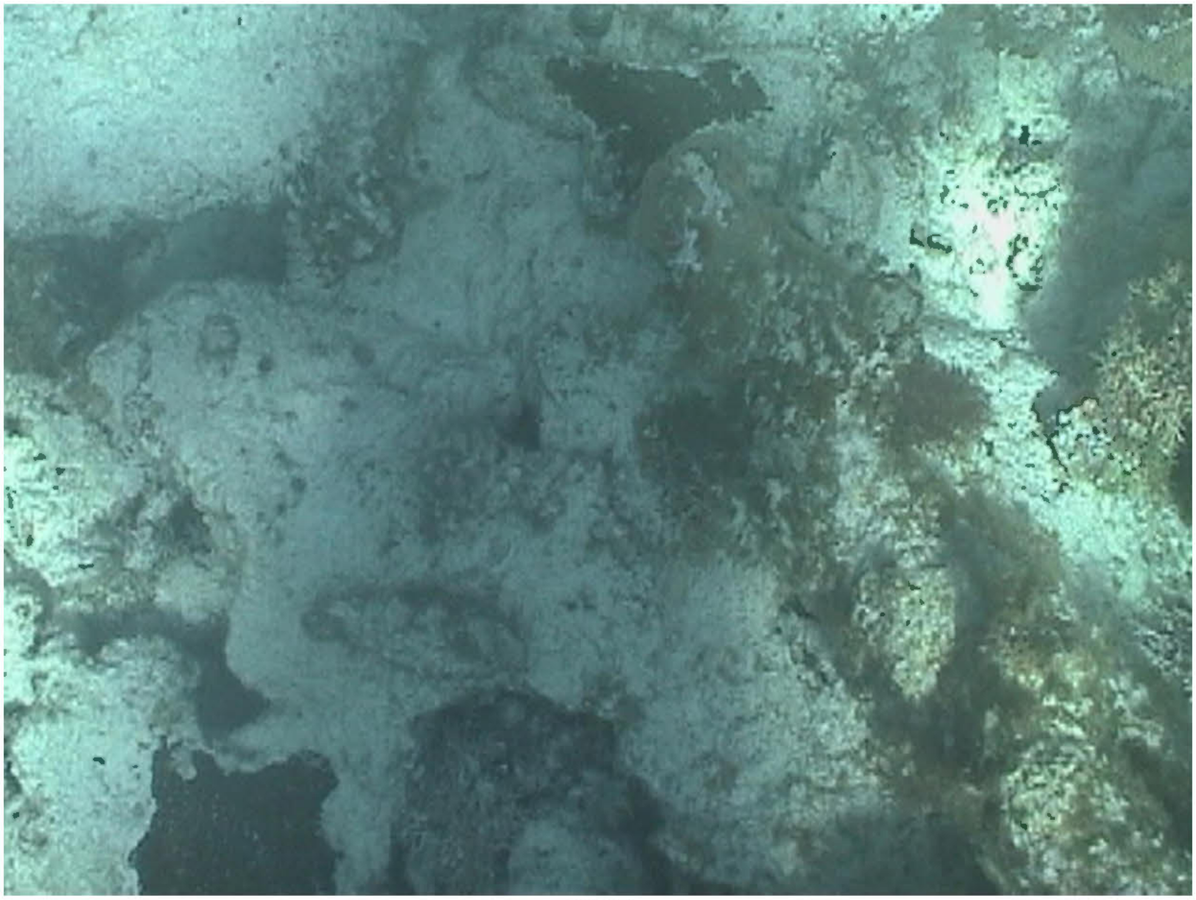
wp_138.bmp


wp_139.bmp

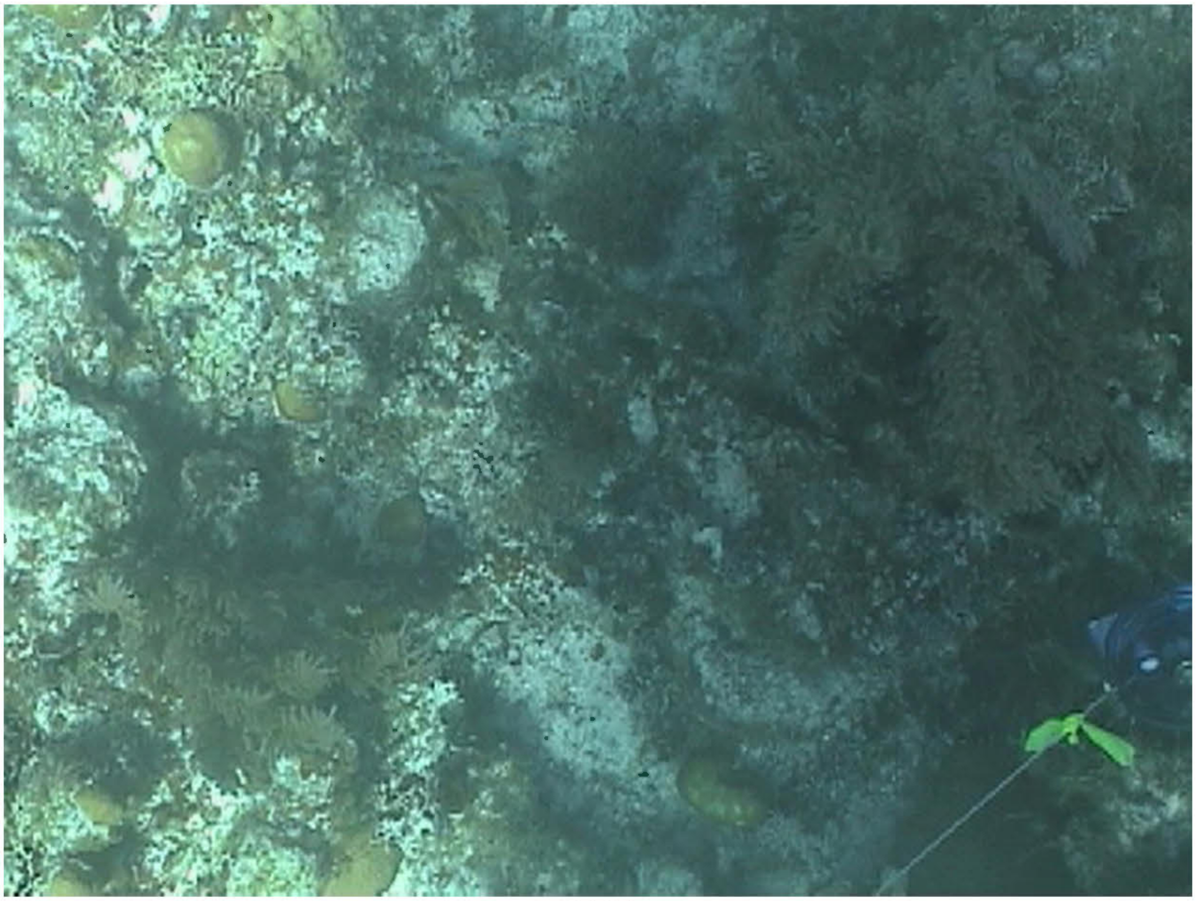

wp_140.bmp

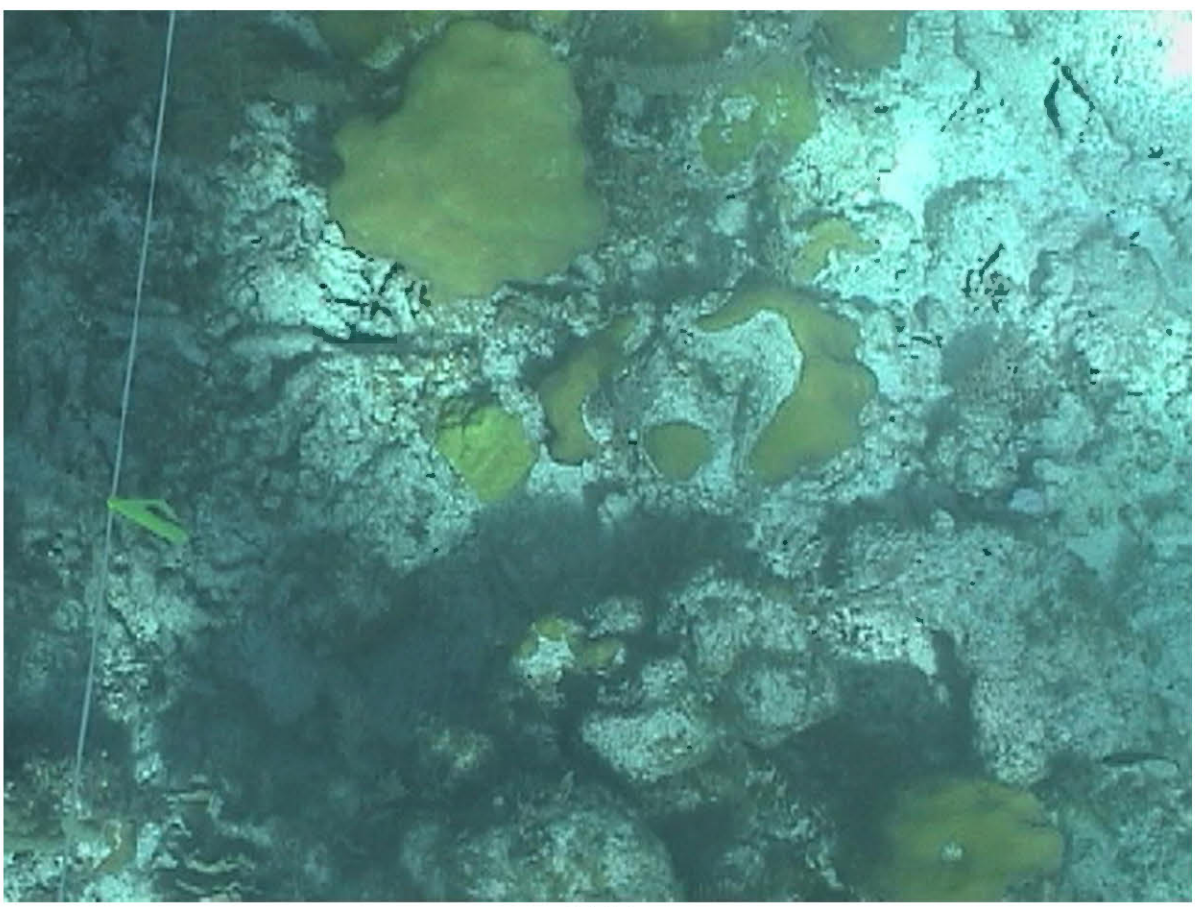

wp_141.bmp

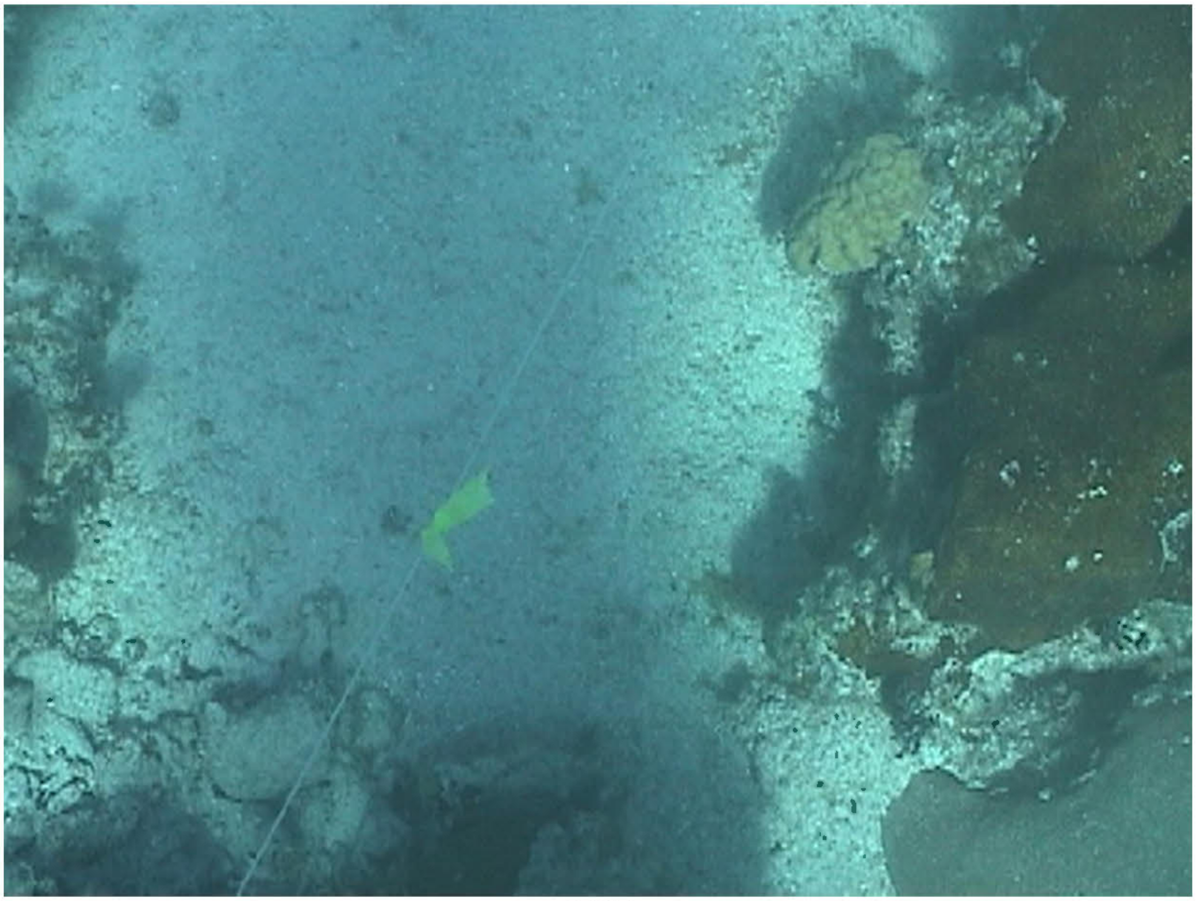

wp_142.bmp

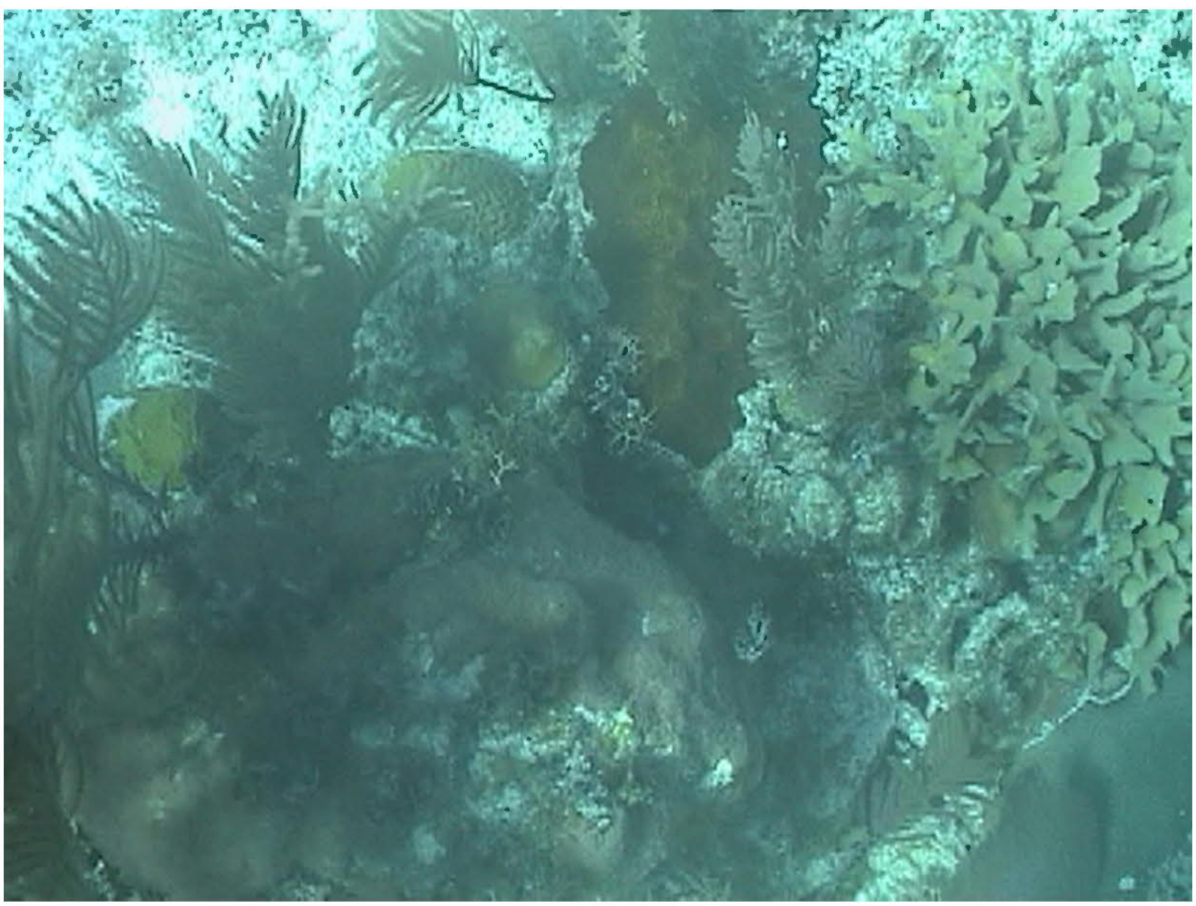

wp_143.bmp


wp_151.bmp

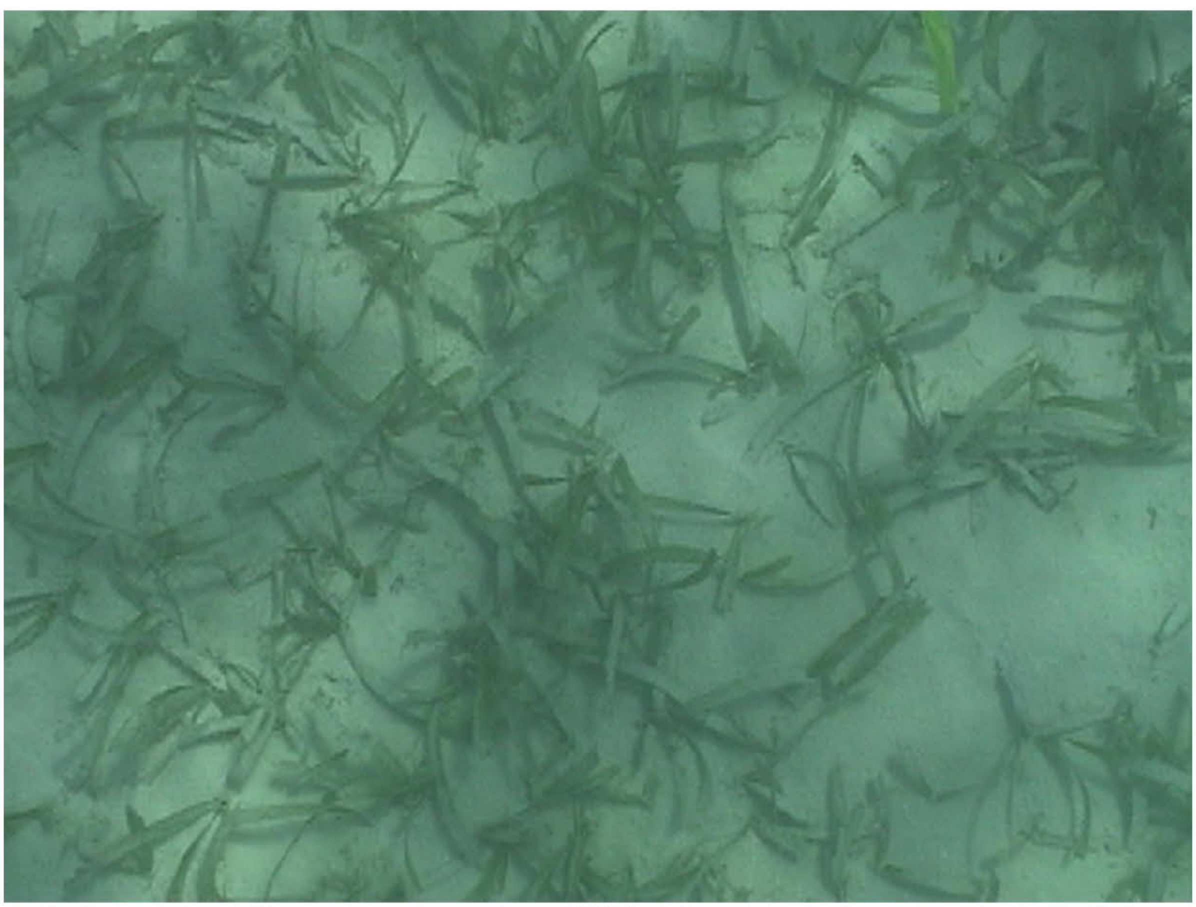
wp_152.bmp

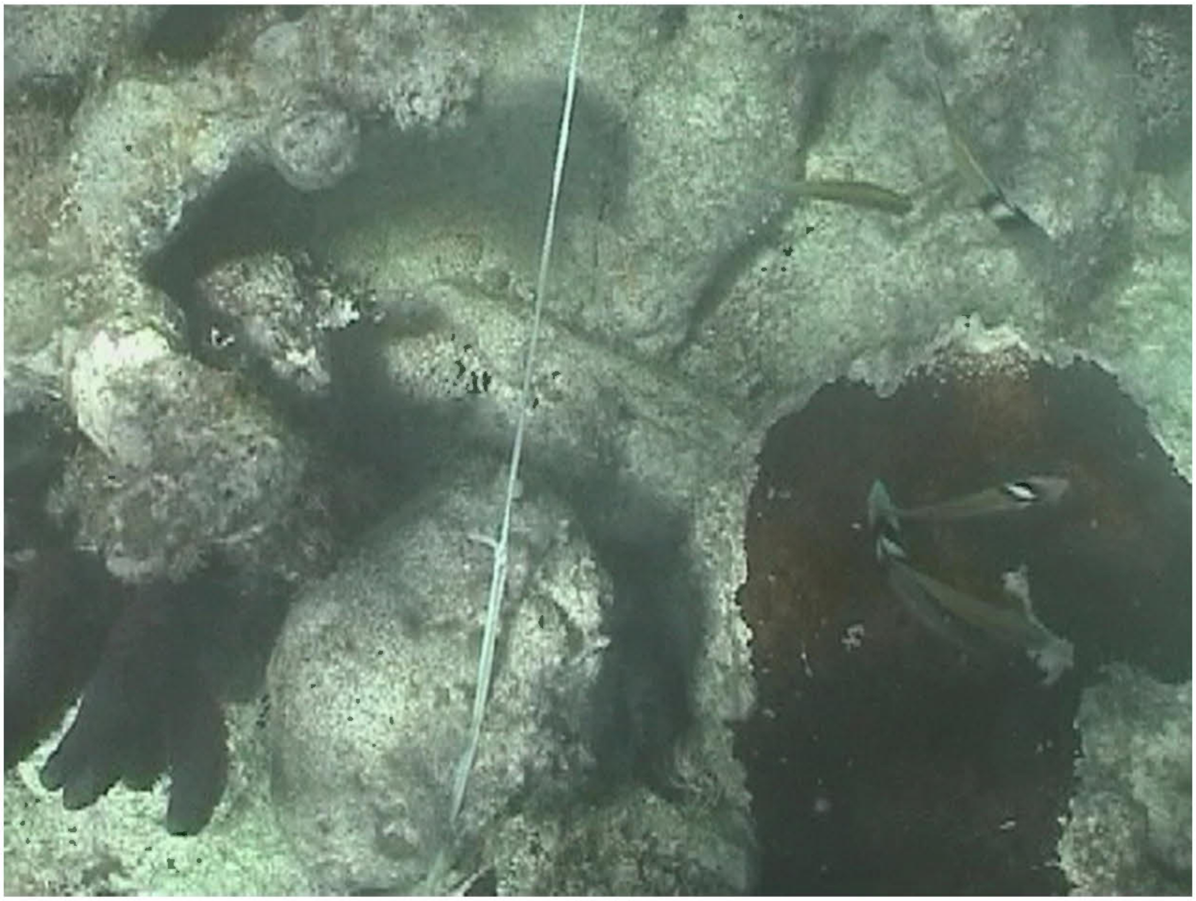

wp_153.bmp

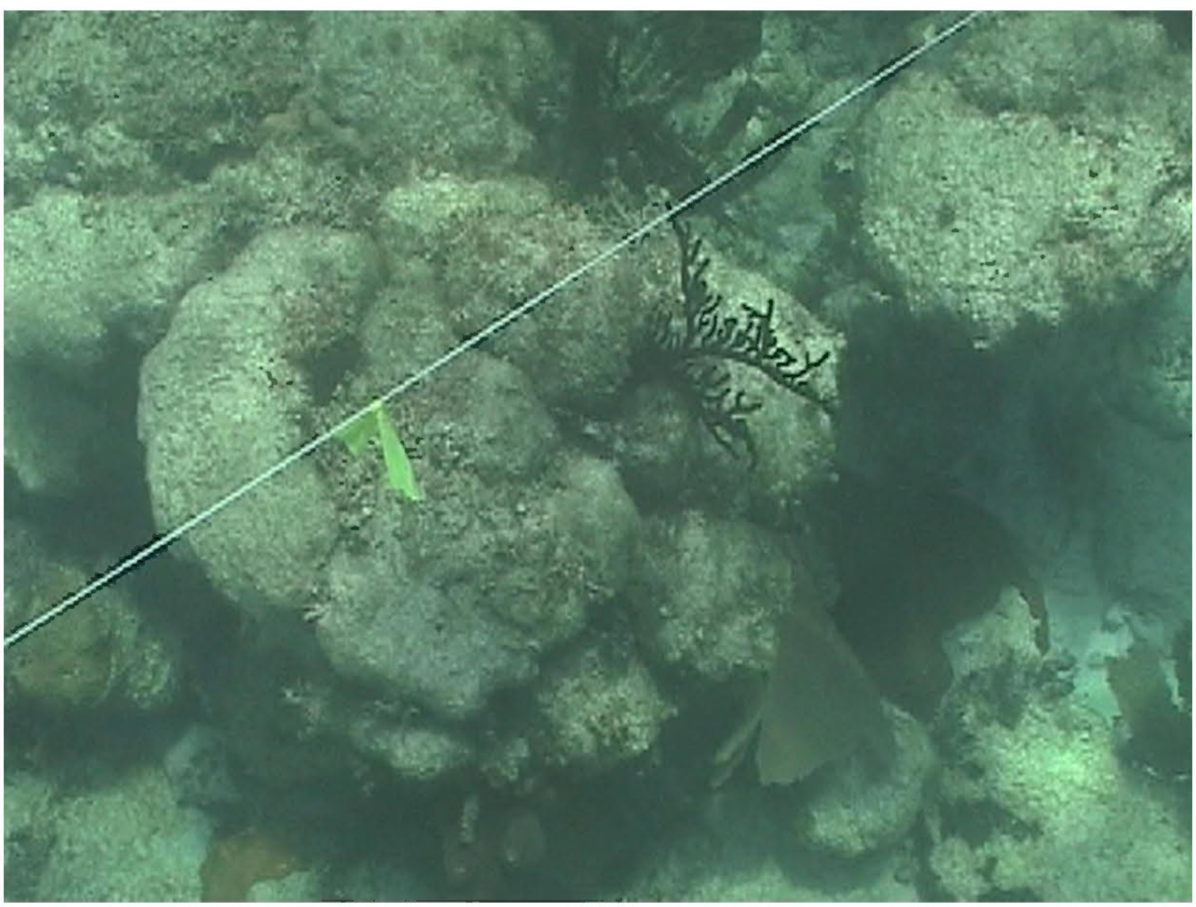

wp_154.bmp

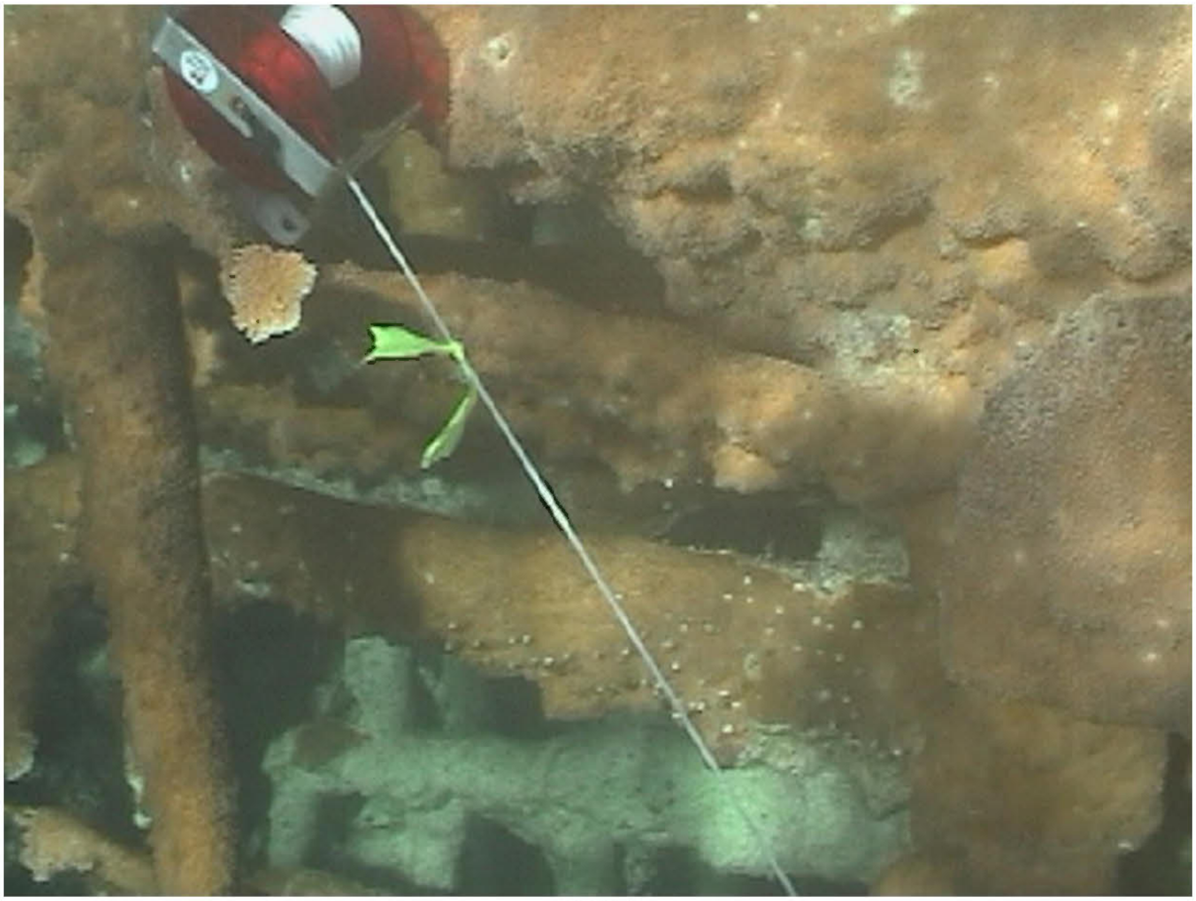

wp_155.bmp

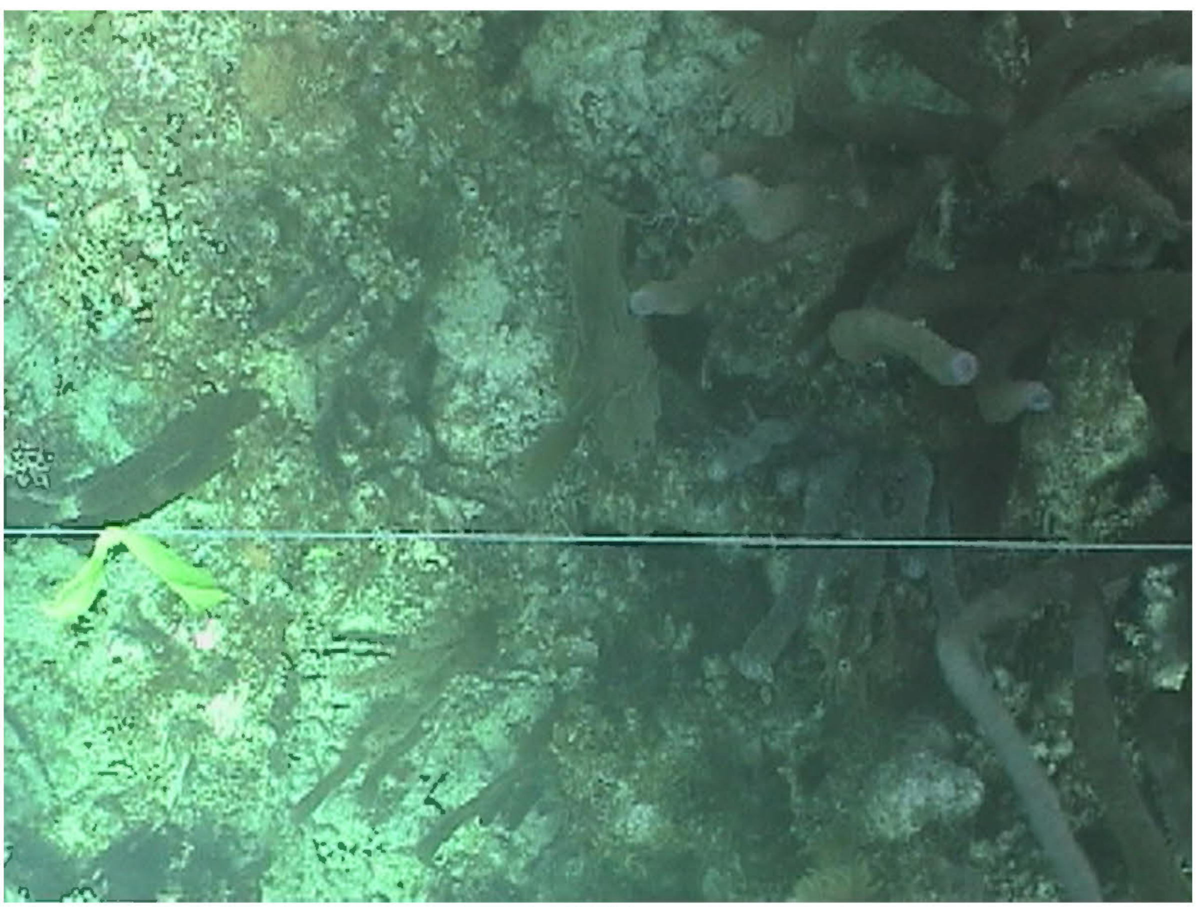

wp_156.bmp

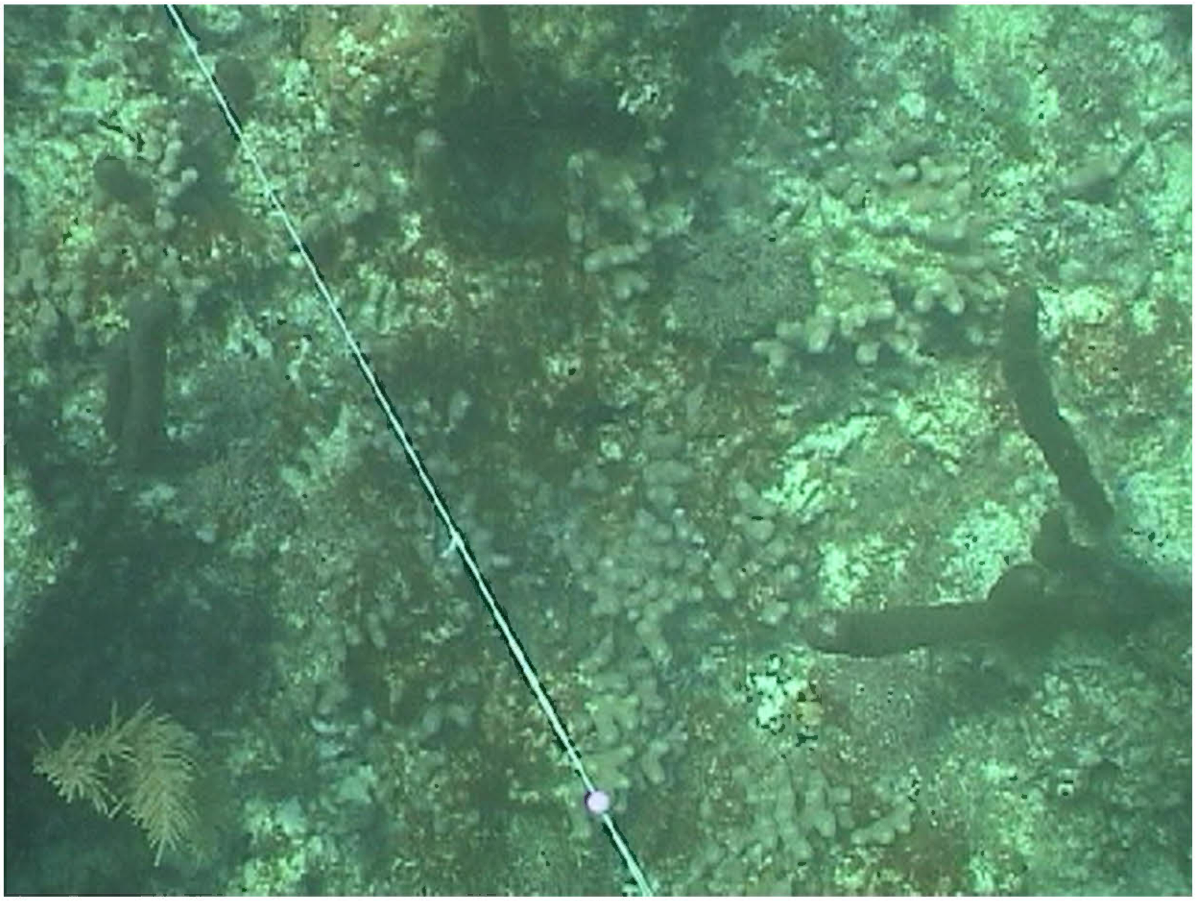

wp_157.bmp

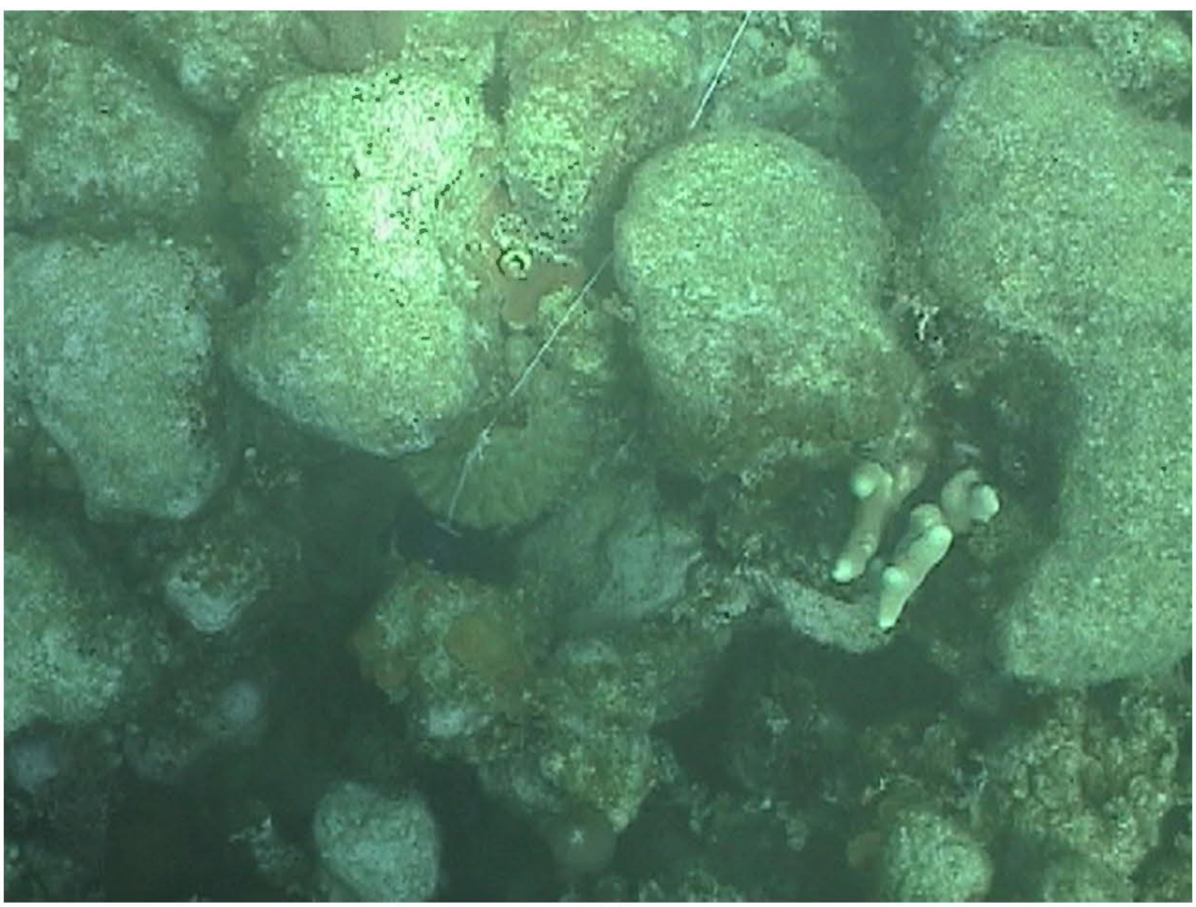

wp_158.bmp

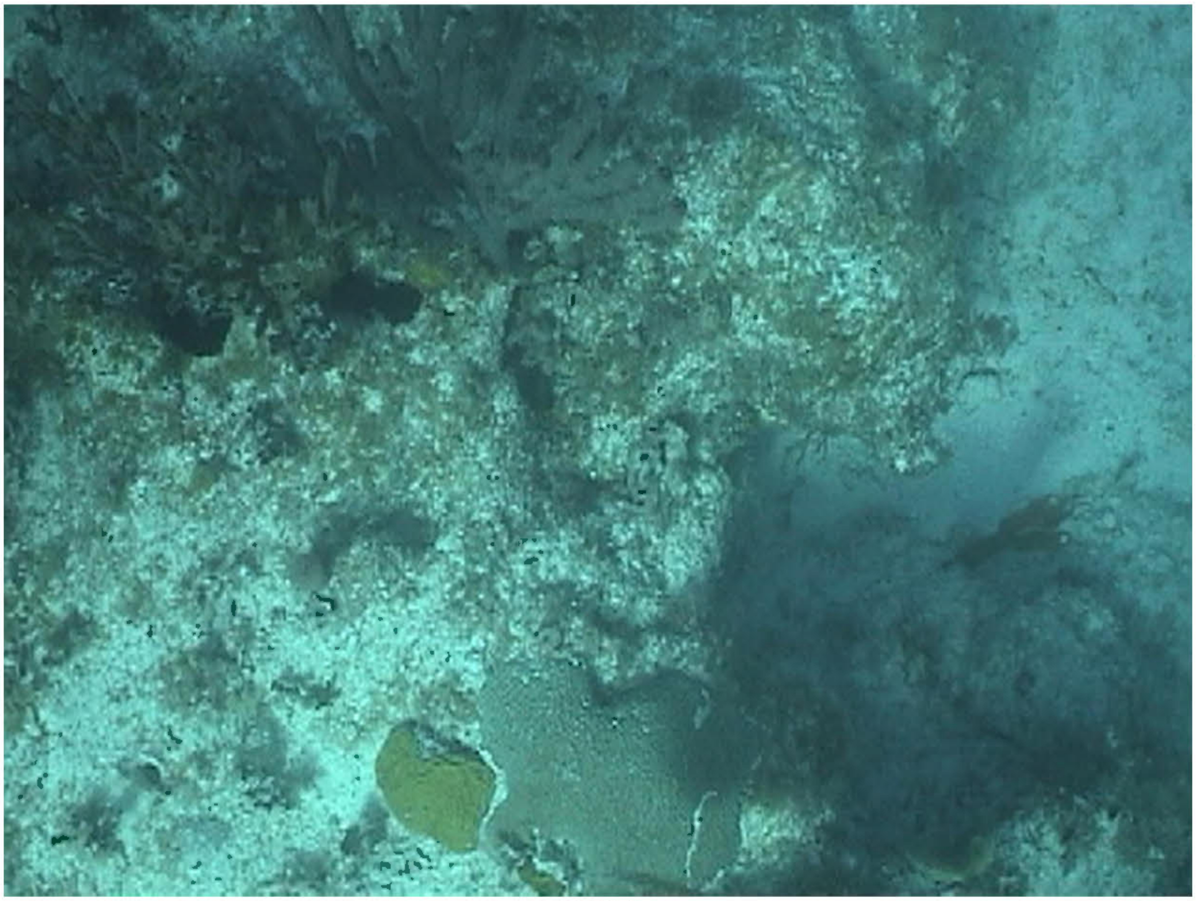
wp_159.bmp


wp_160.bmp

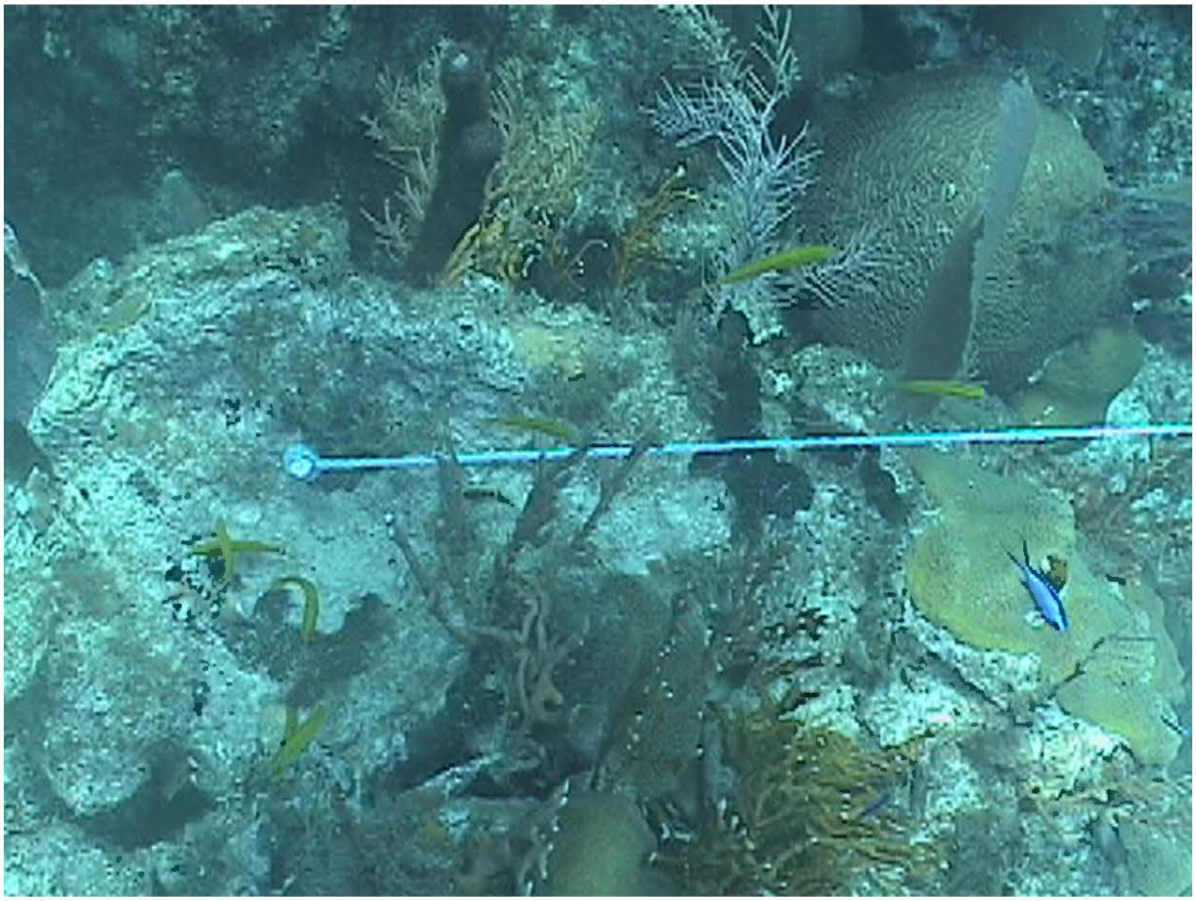
wp_161.bmp

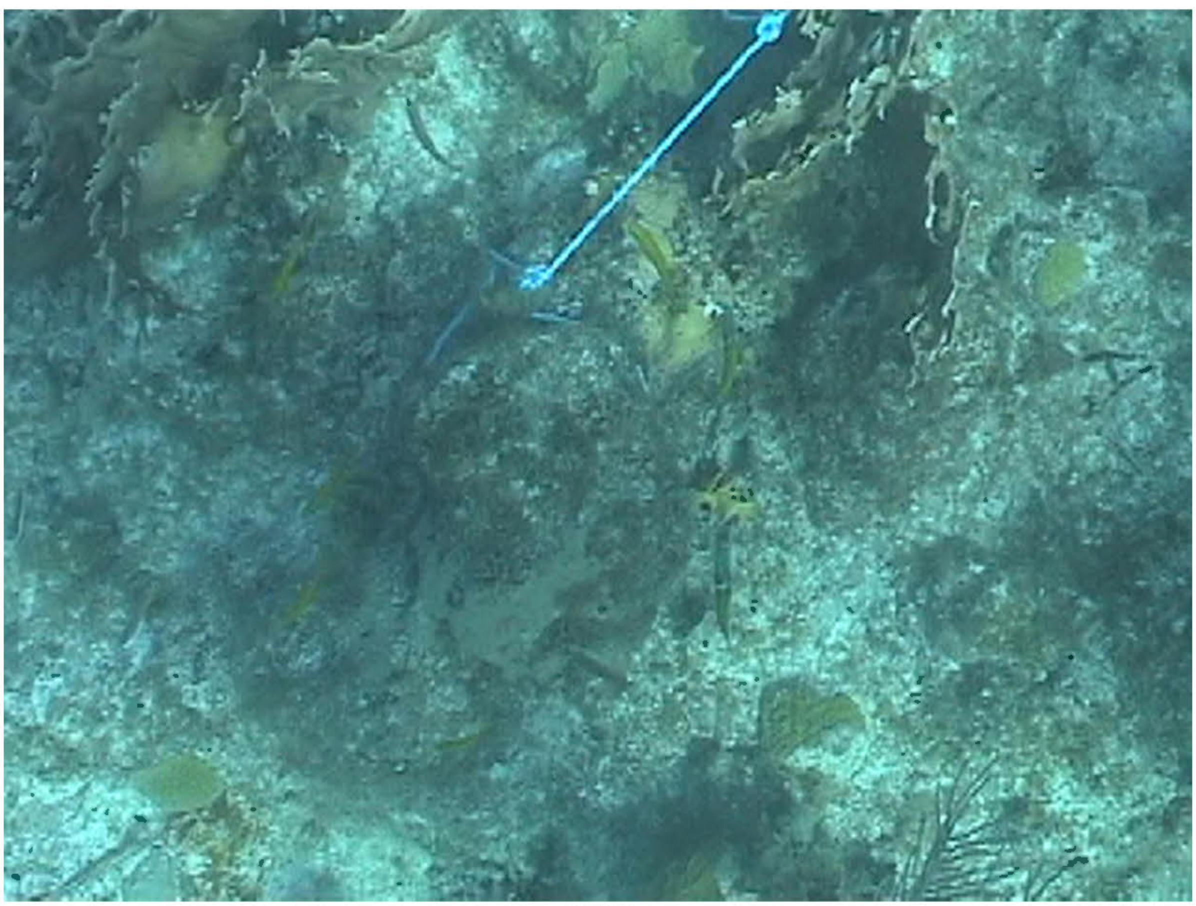
wp_162.bmp

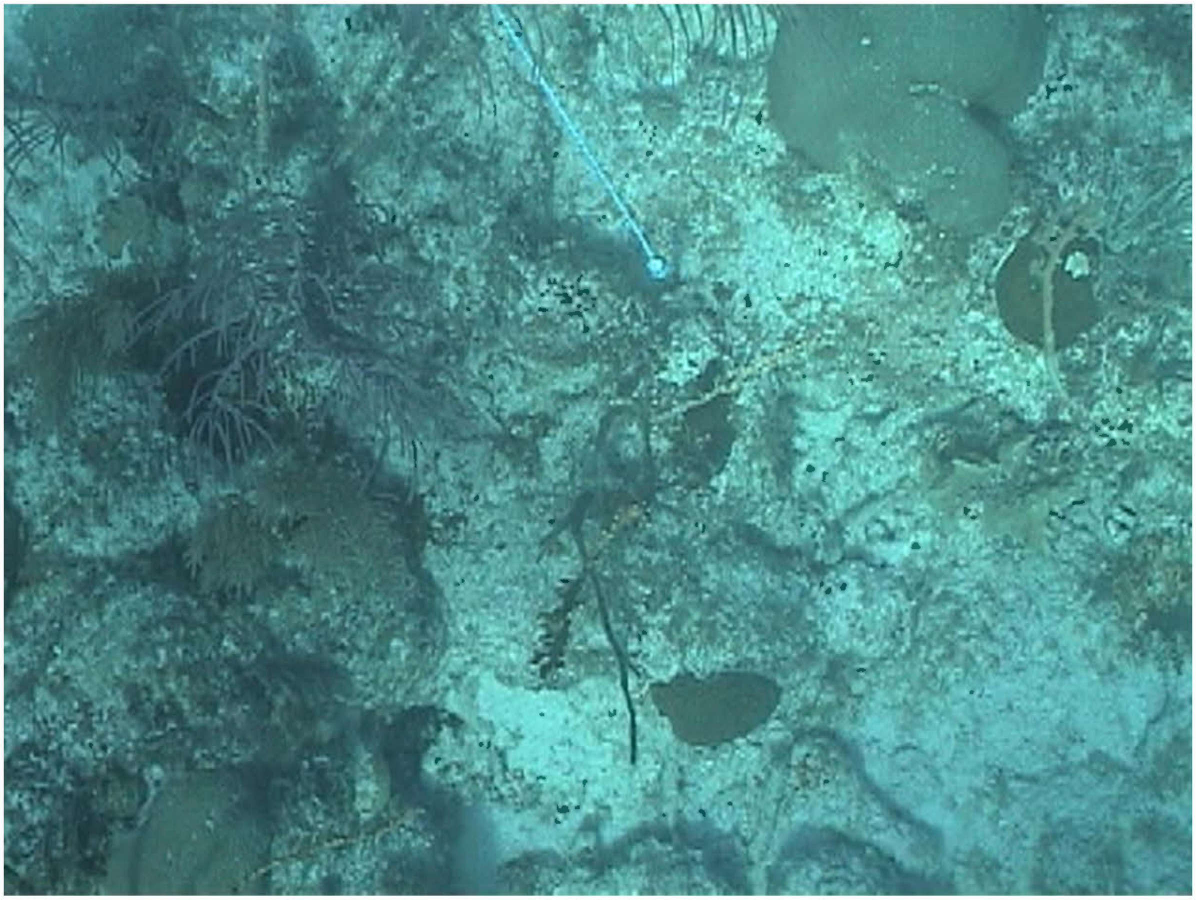

wp_163.bmp

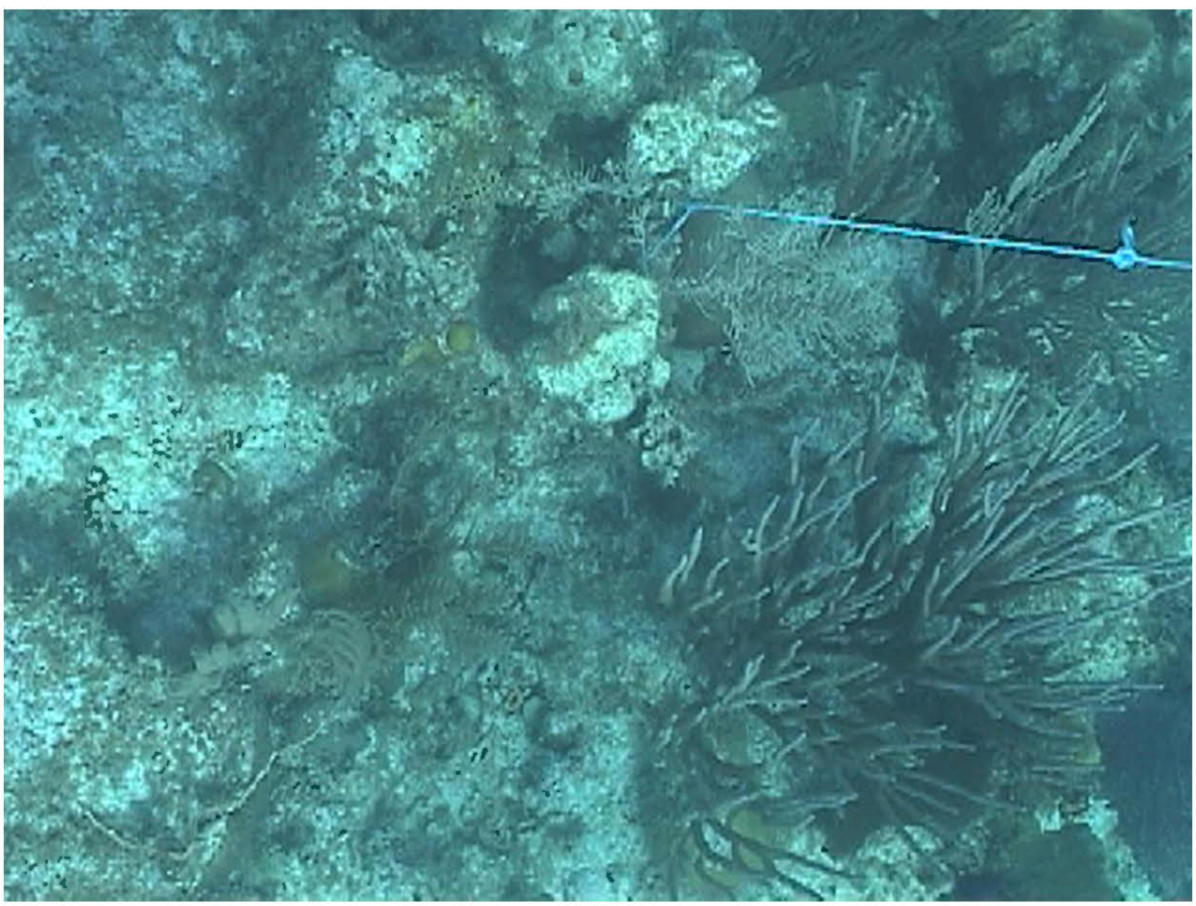

wp_164.bmp

wp_165.bmp

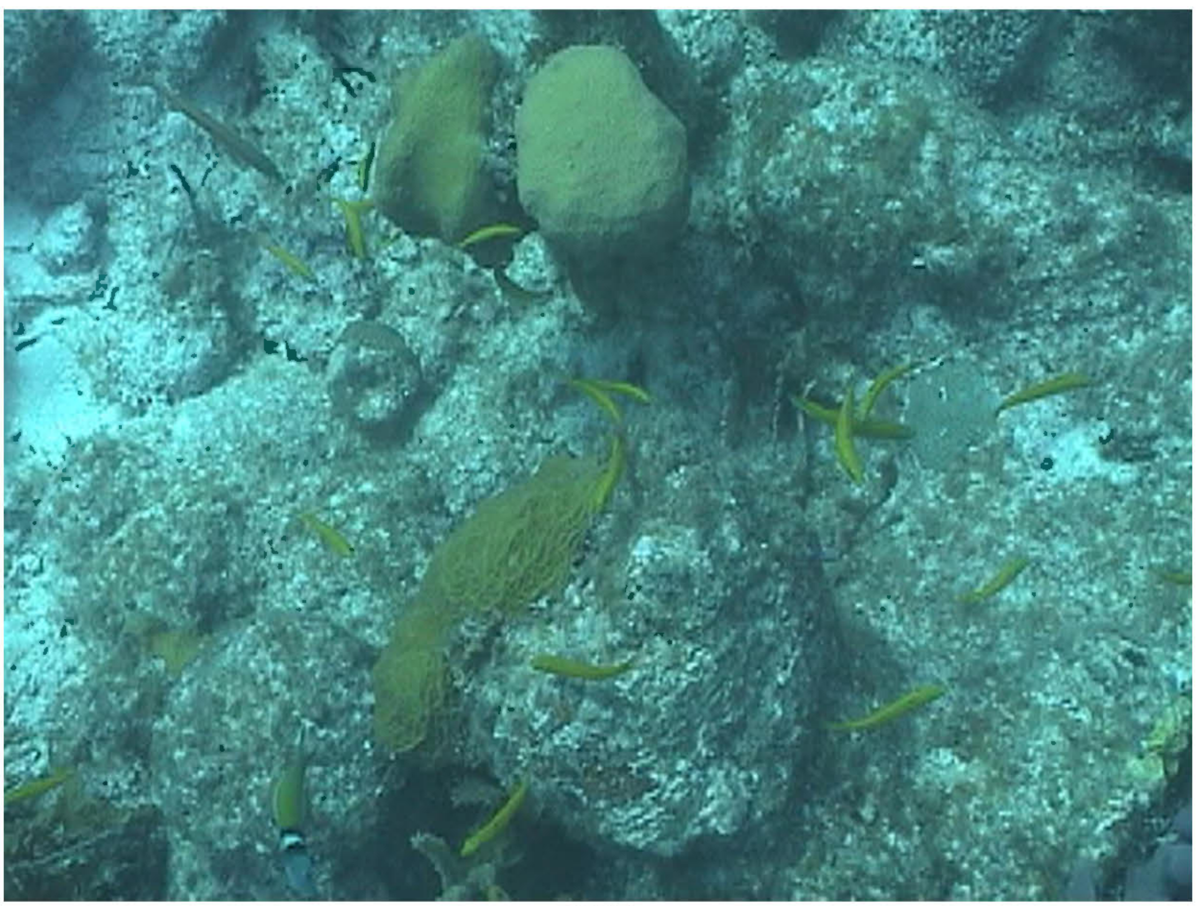

wp_166.bmp

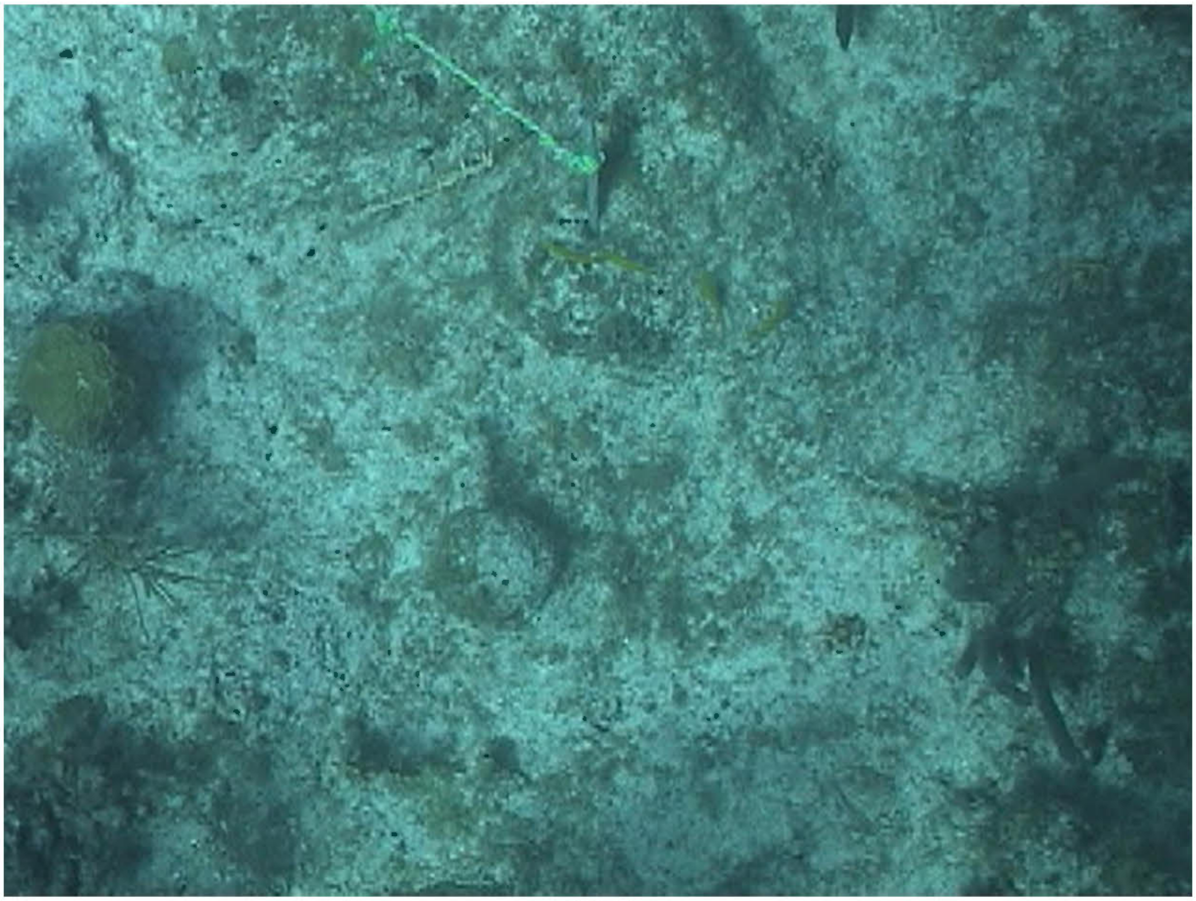
wp_167.bmp

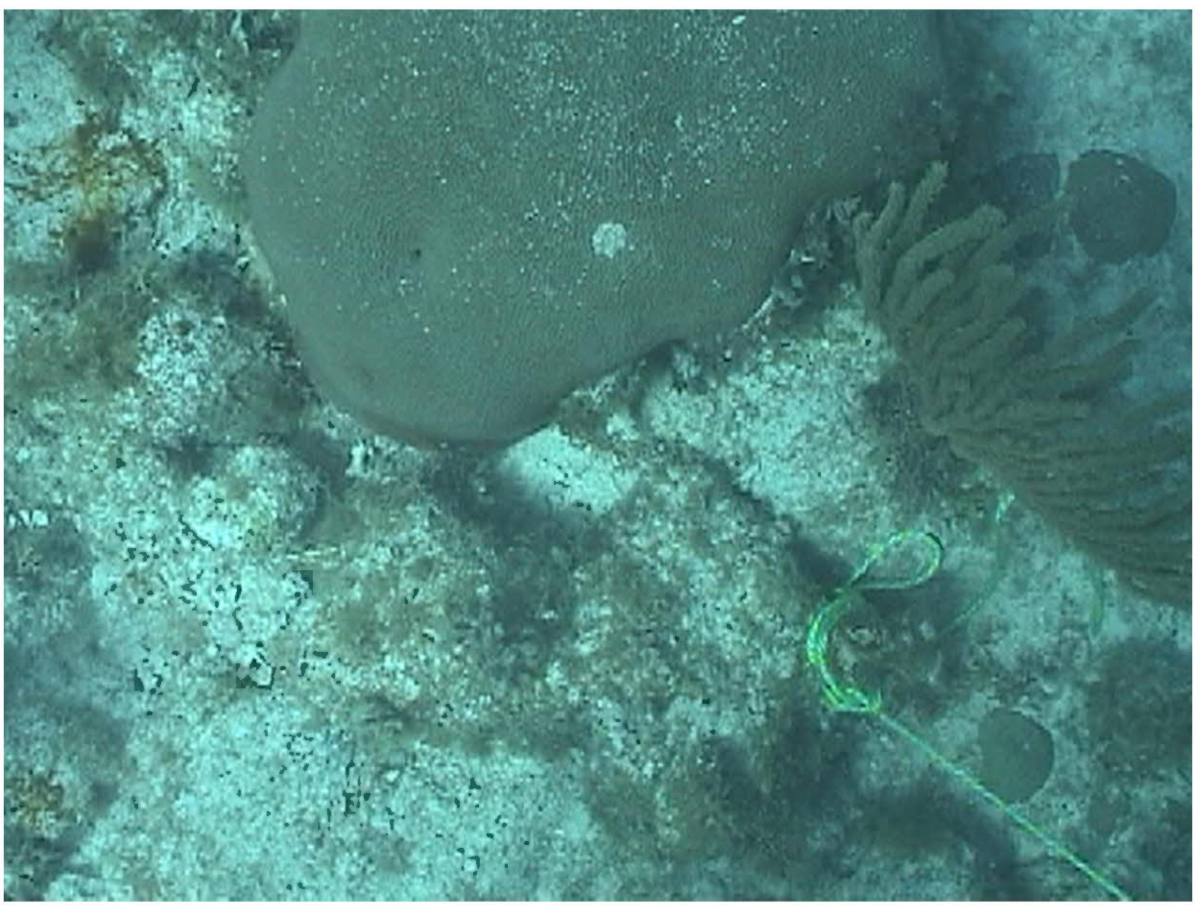
wp_168.bmp

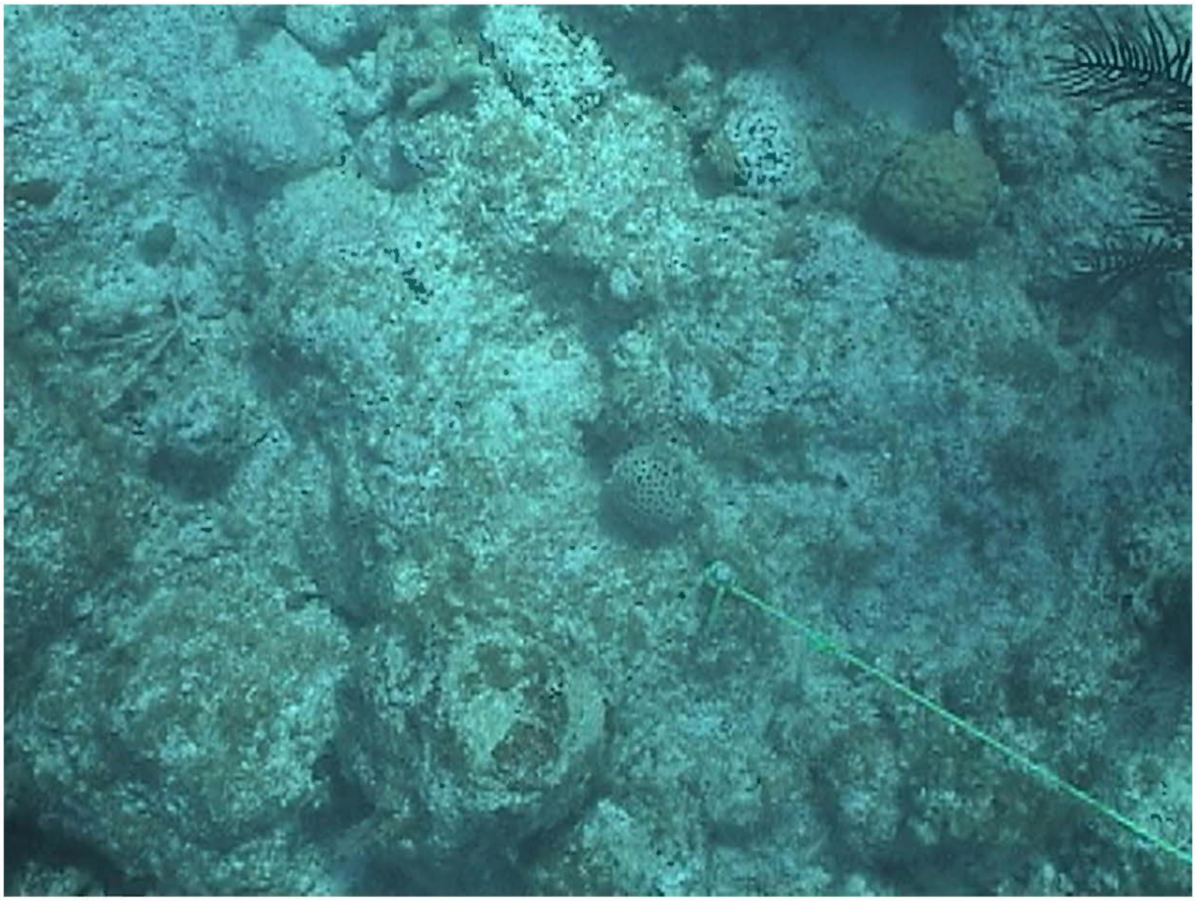
wp_169.bmp

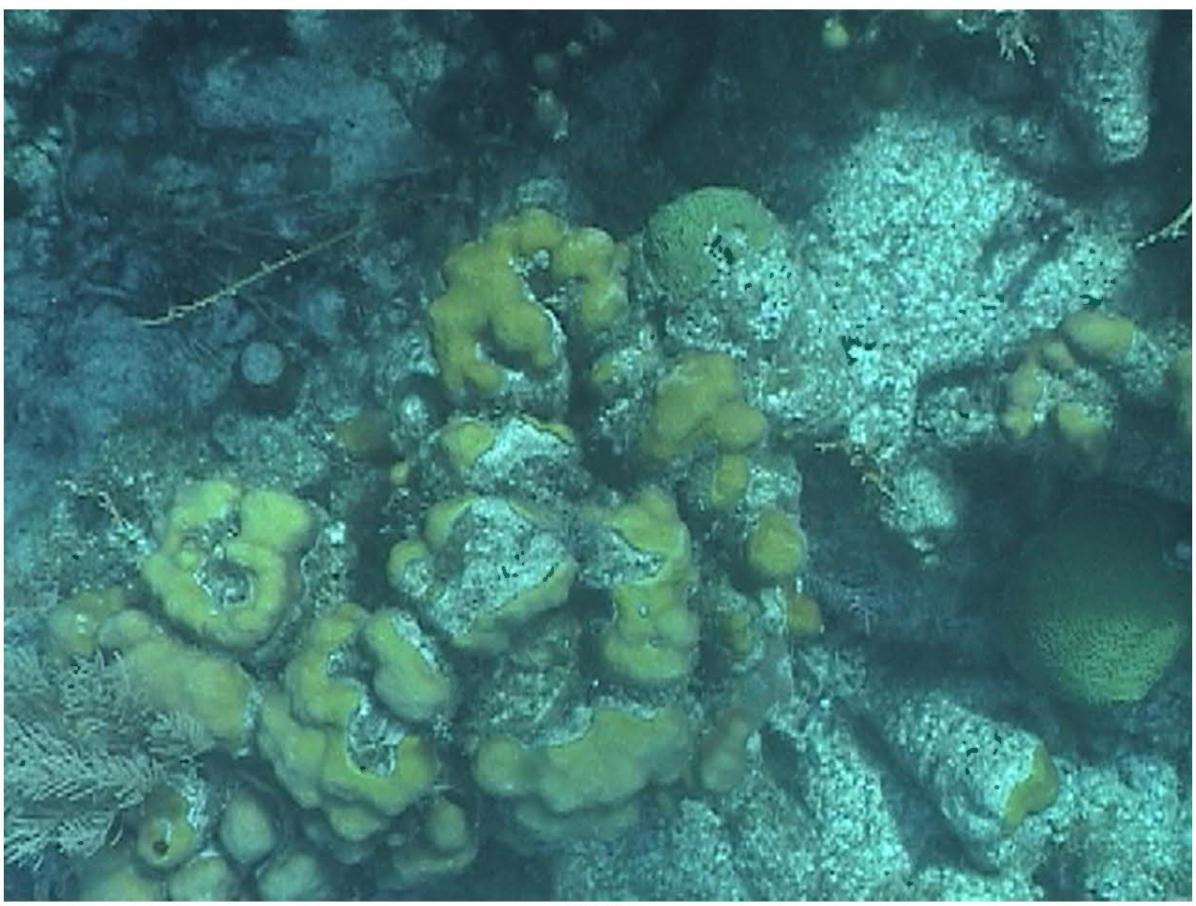
wp_170.bmp

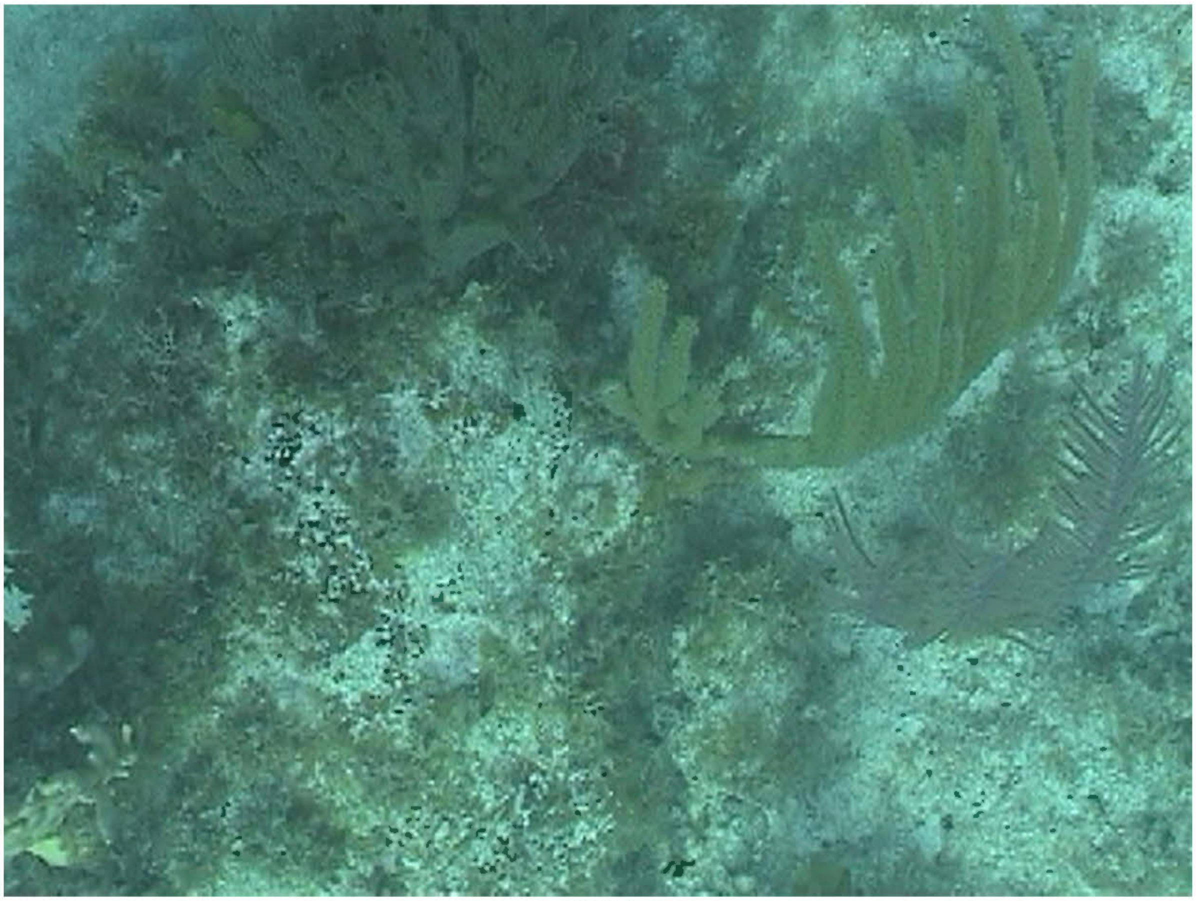

wp_171.bmp

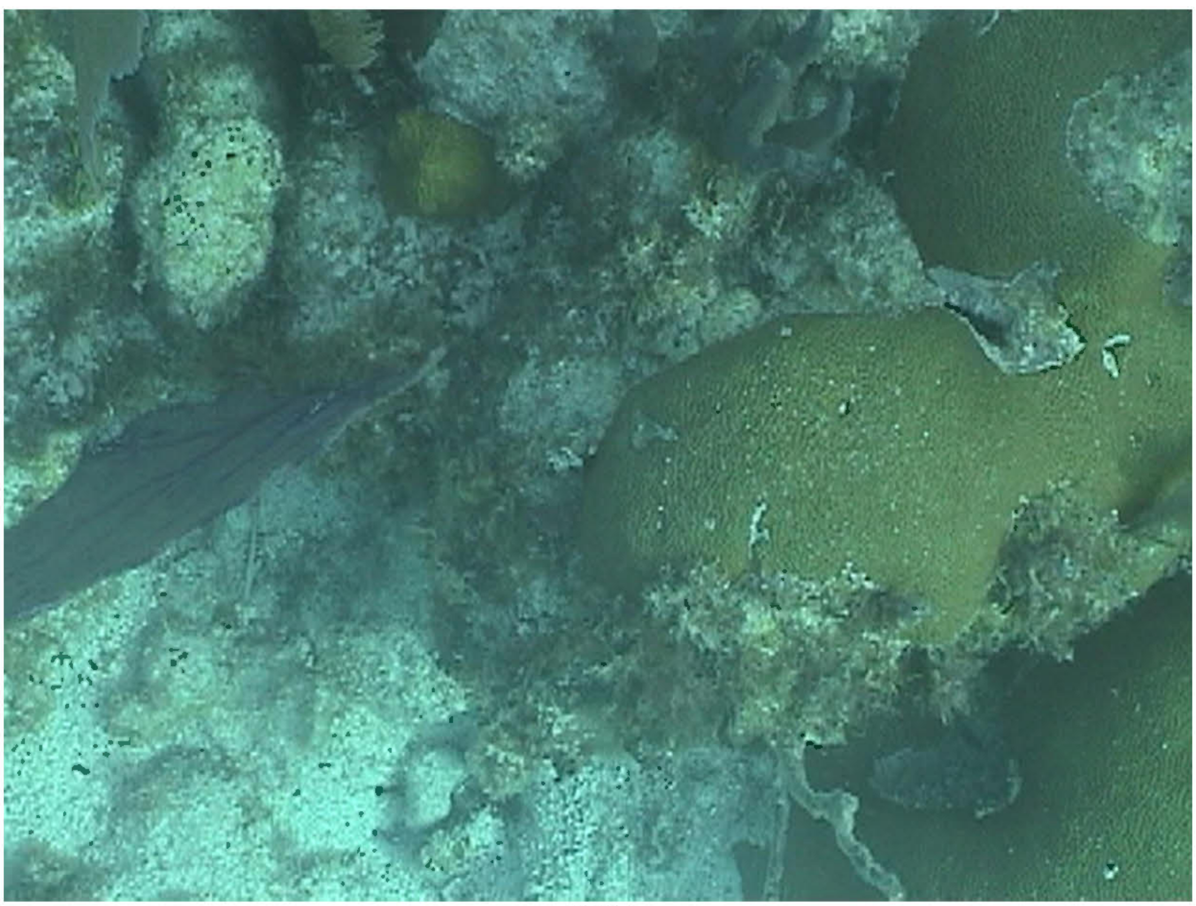

wp_172.bmp

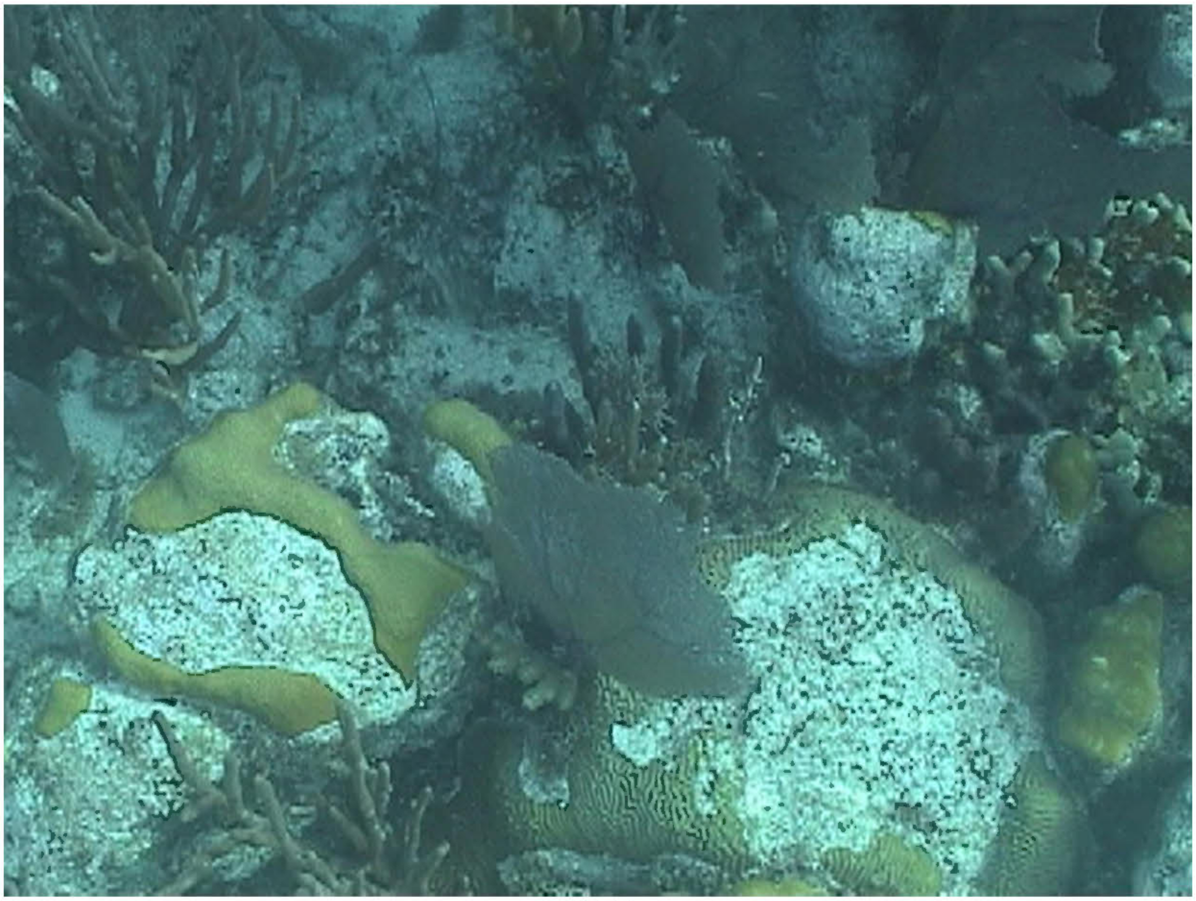
wp_173.bmp

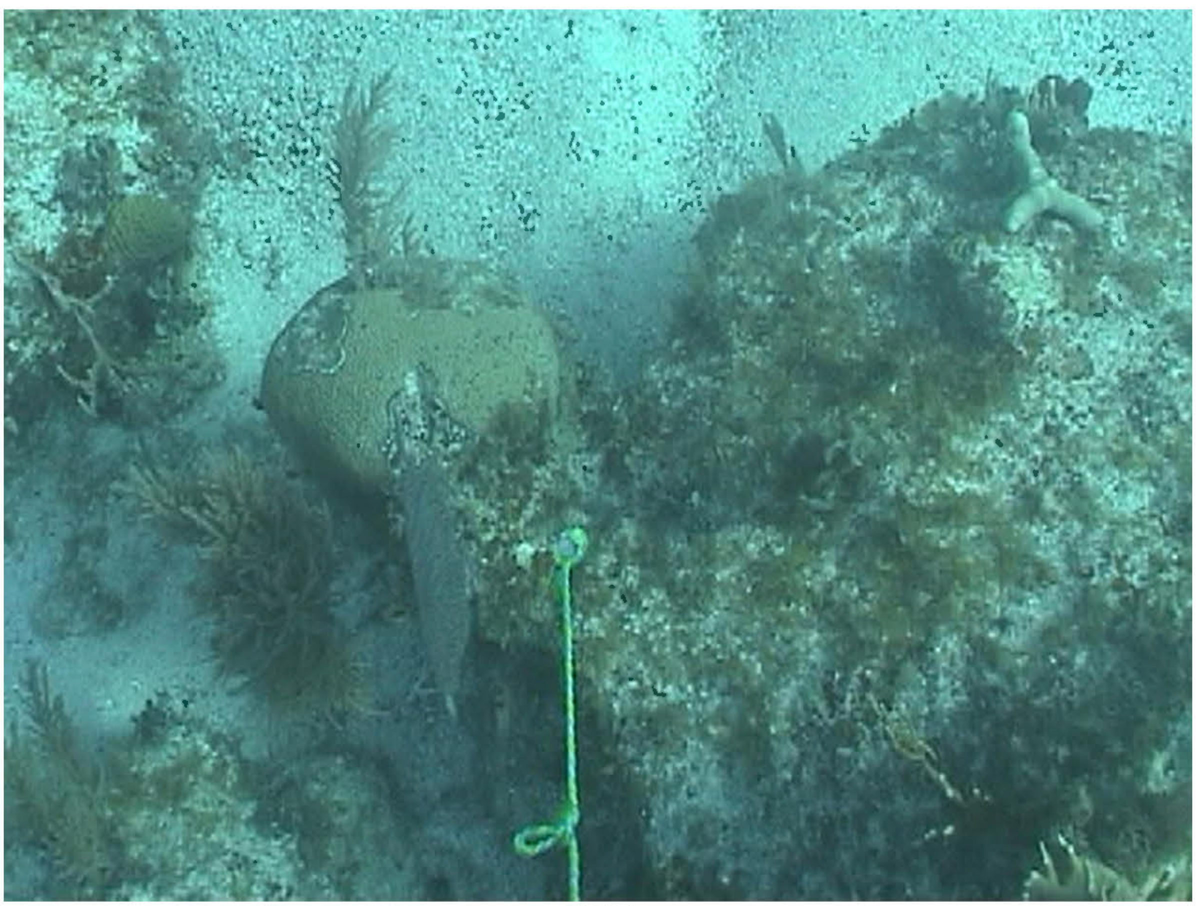
wp_174.bmp


wp_175.bmp

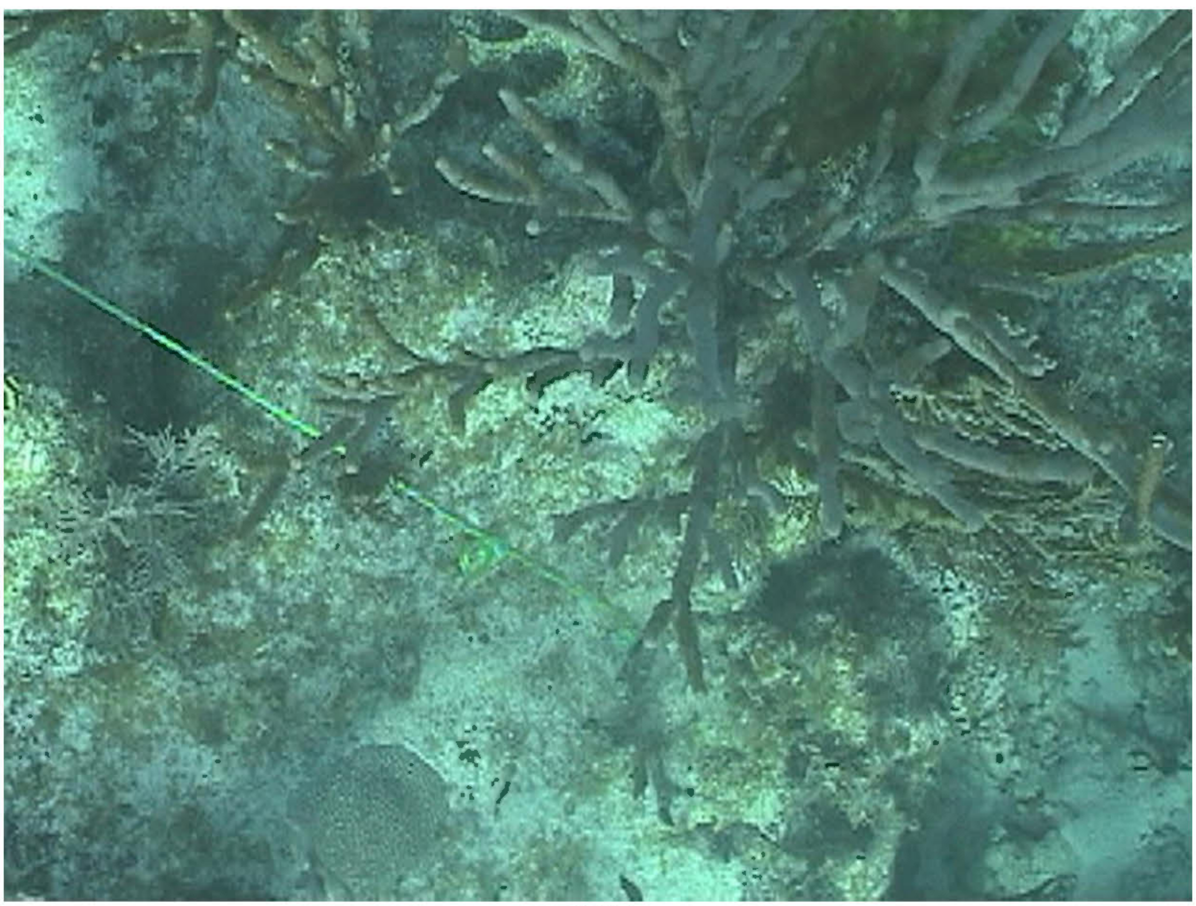
wp_176.bmp

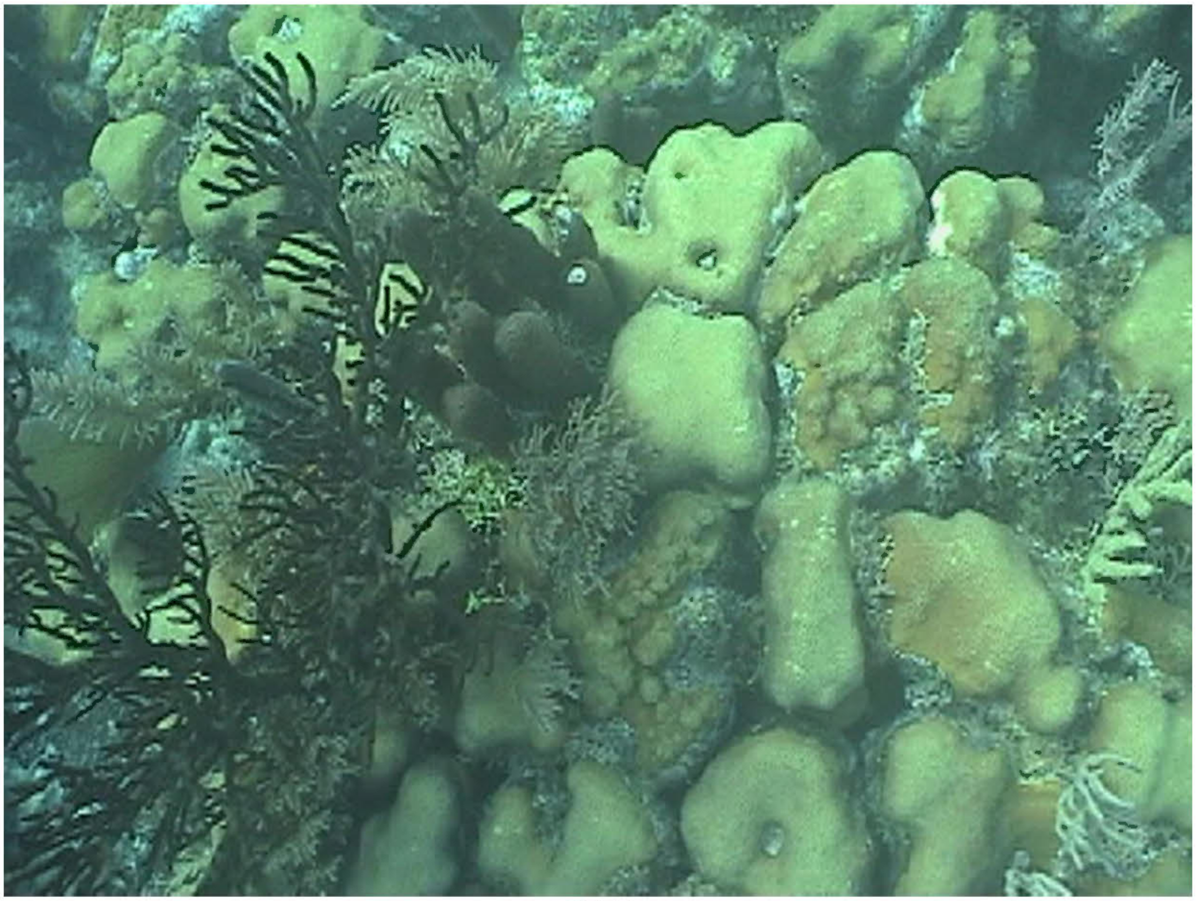

wp_177.bmp

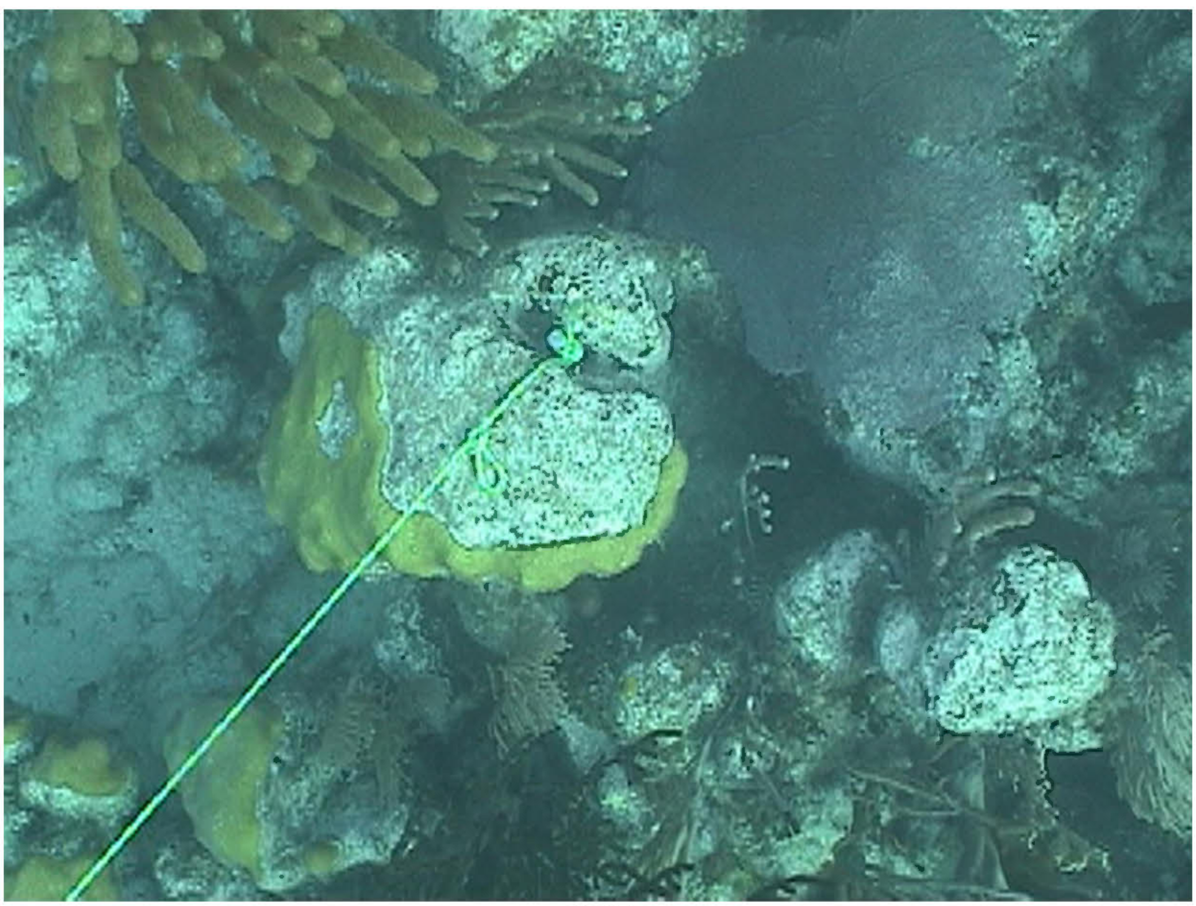

wp_178.bmp


wp_179.bmp

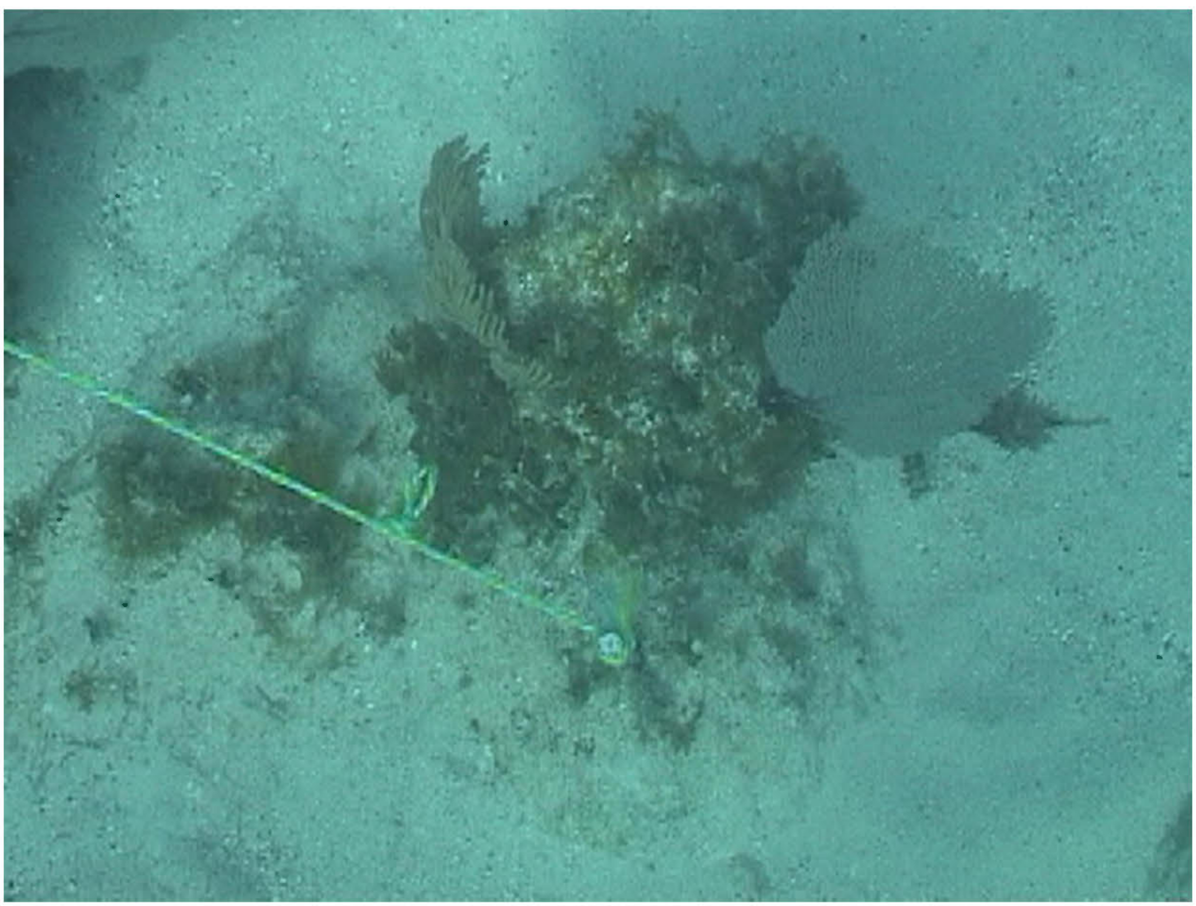
wp_180.bmp

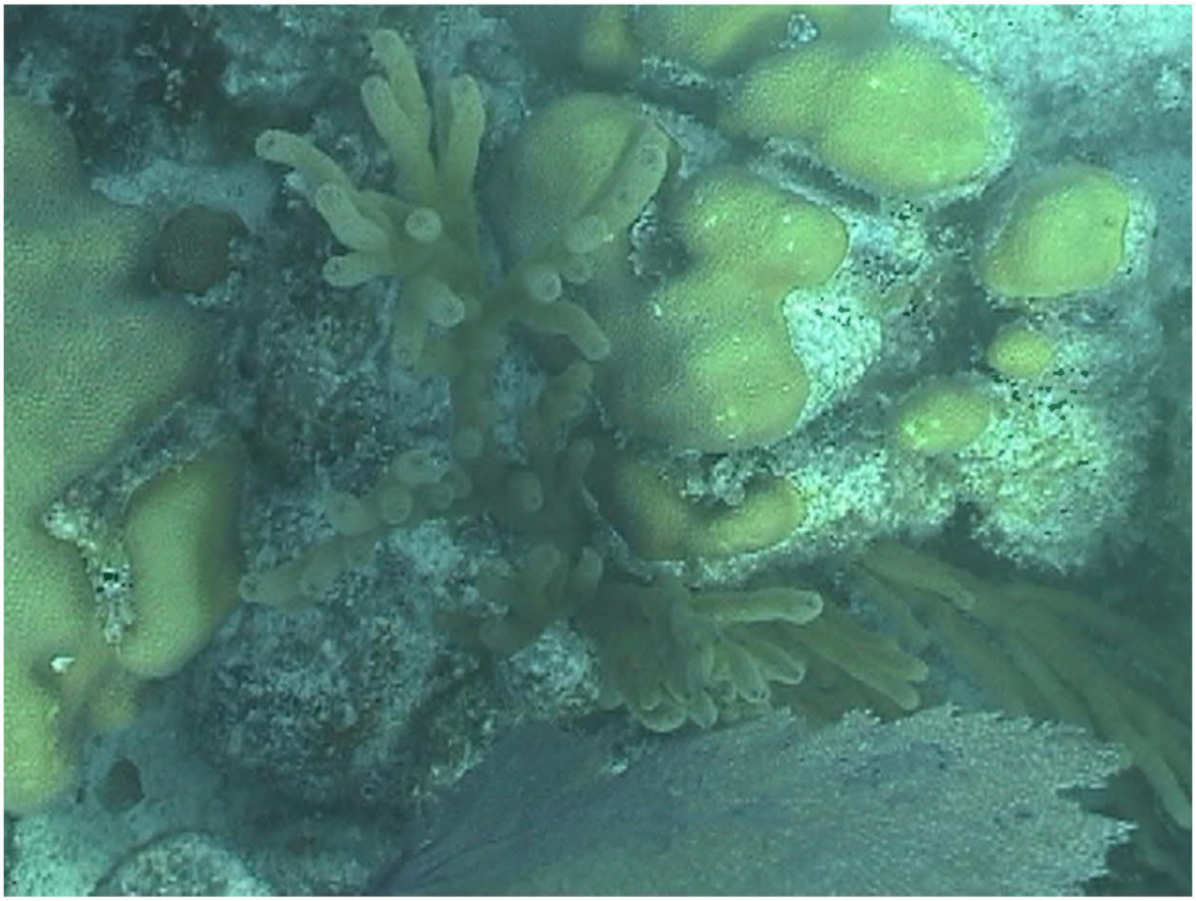
wp_181.bmp

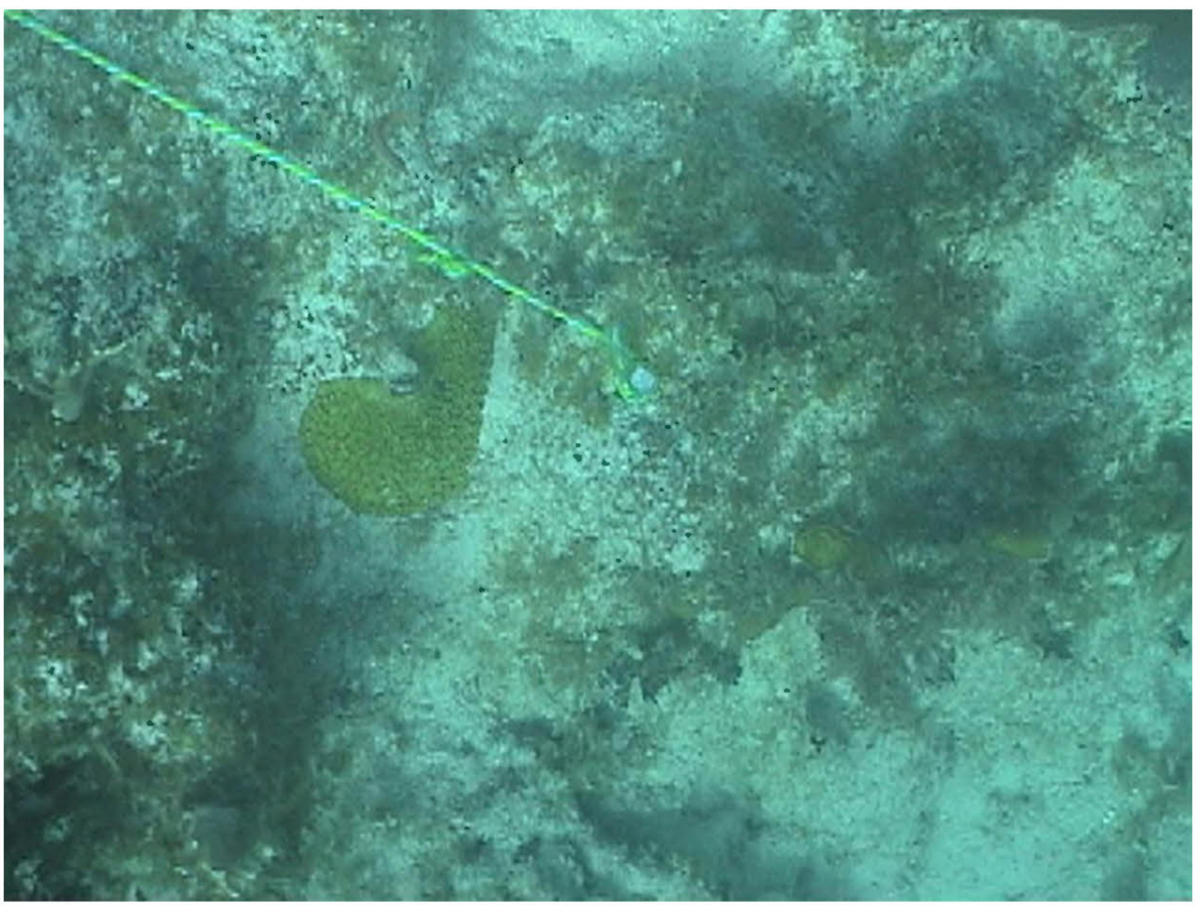
wp_182.bmp

wp_183.bmp

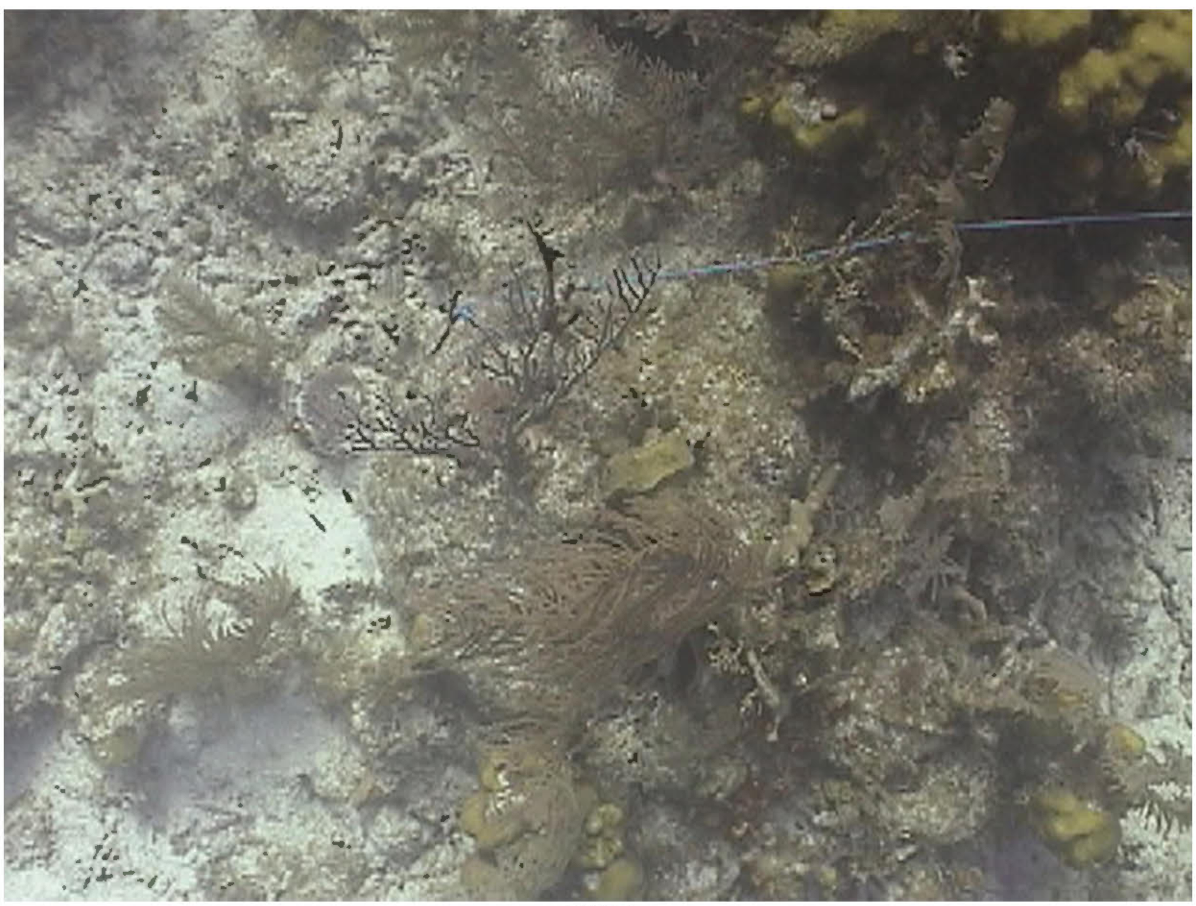

wp_185.bmp

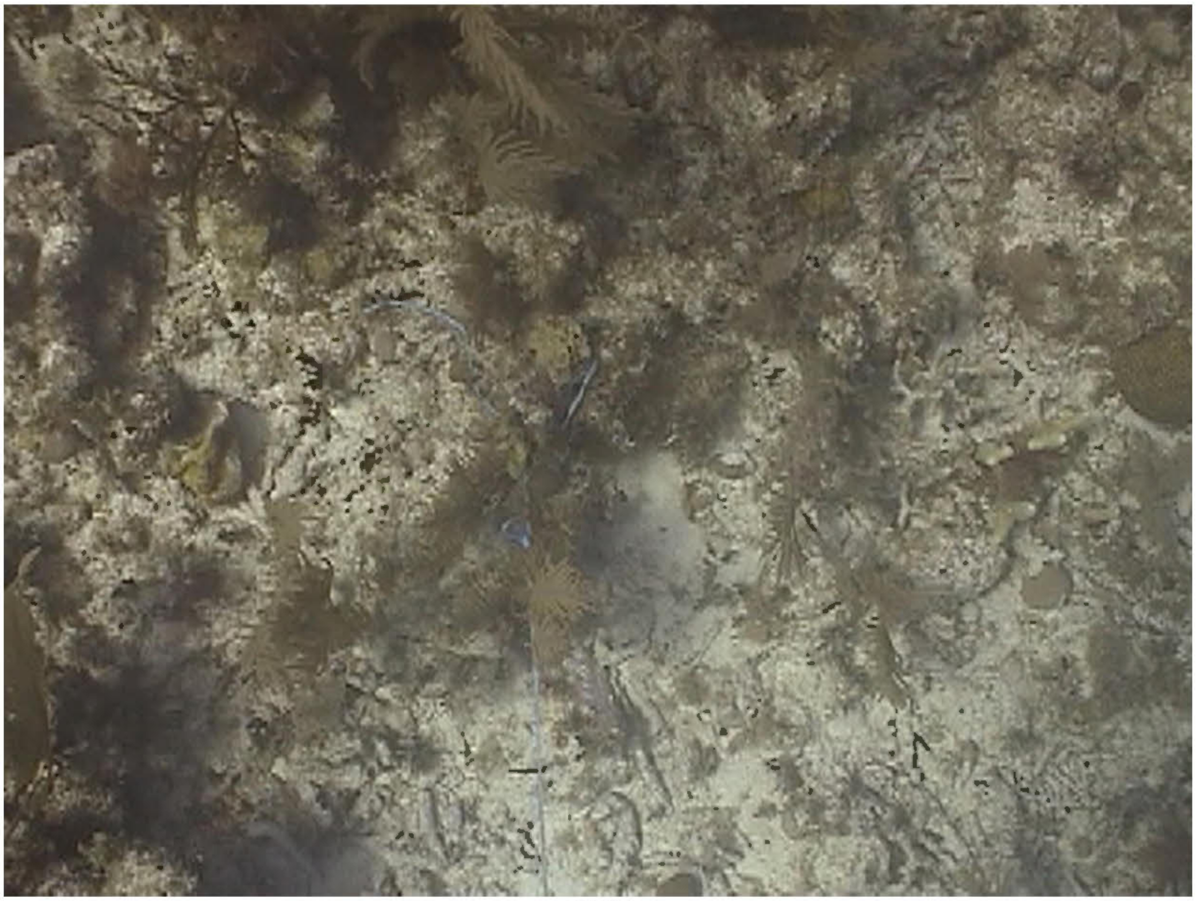
wp_186.bmp

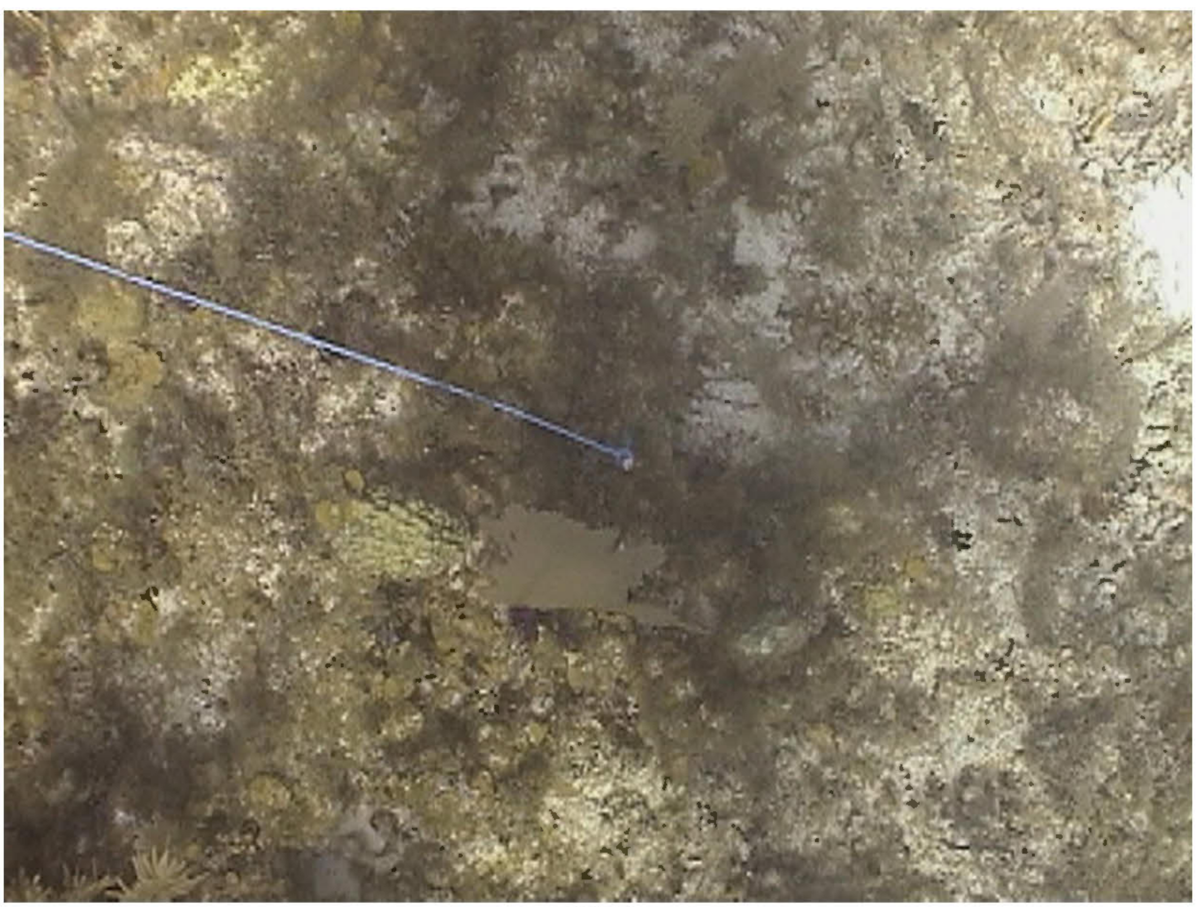
wp_187.bmp

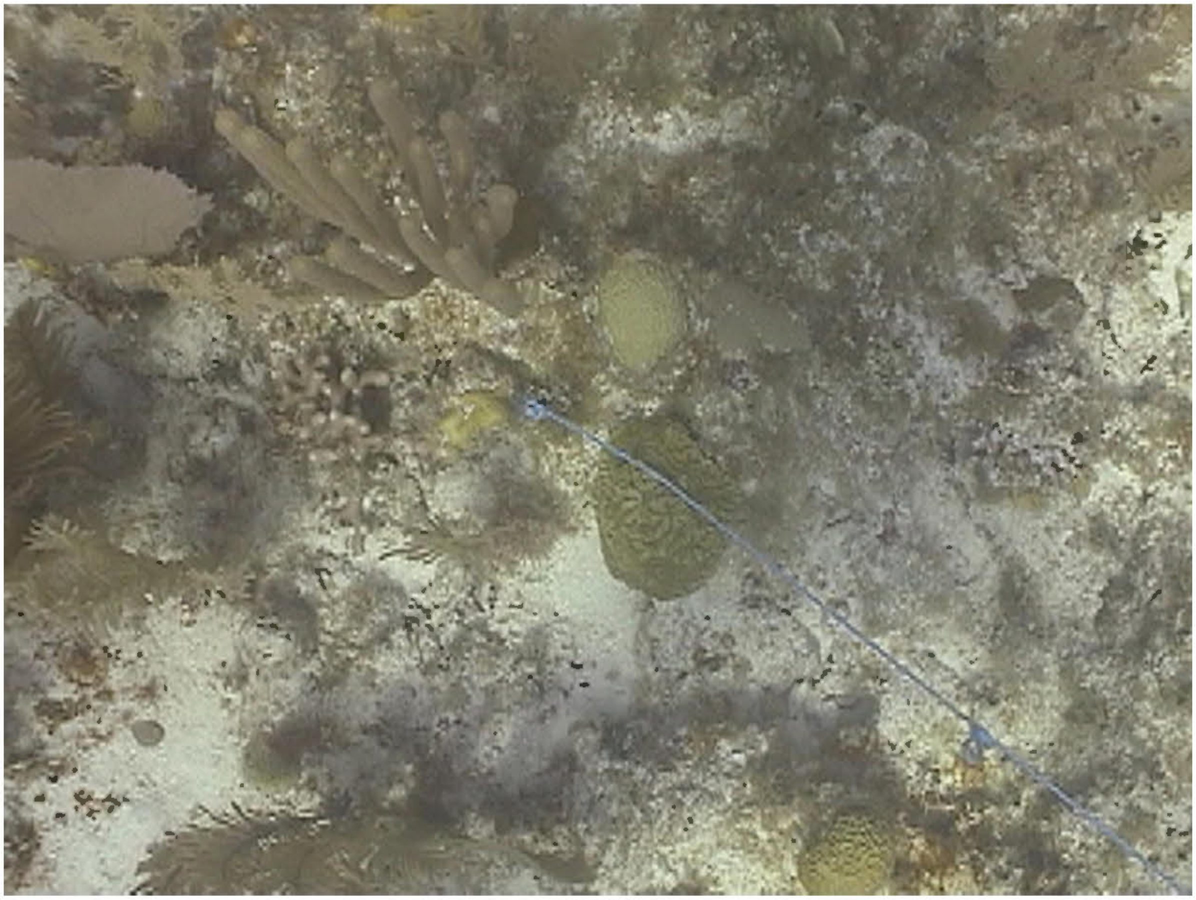
wp_188.bmp


wp_189.bmp

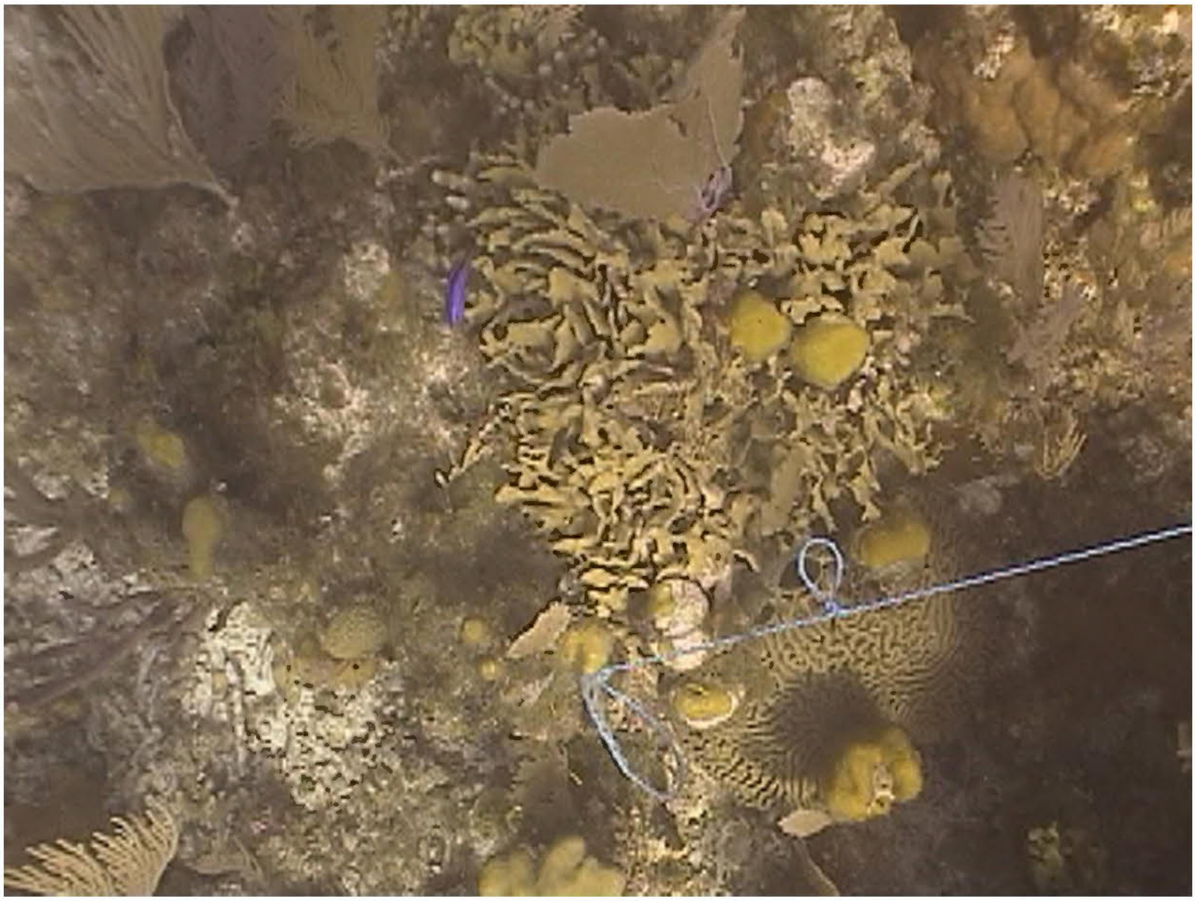

wp_190.bmp

wp_191.bmp


wp_192.bmp

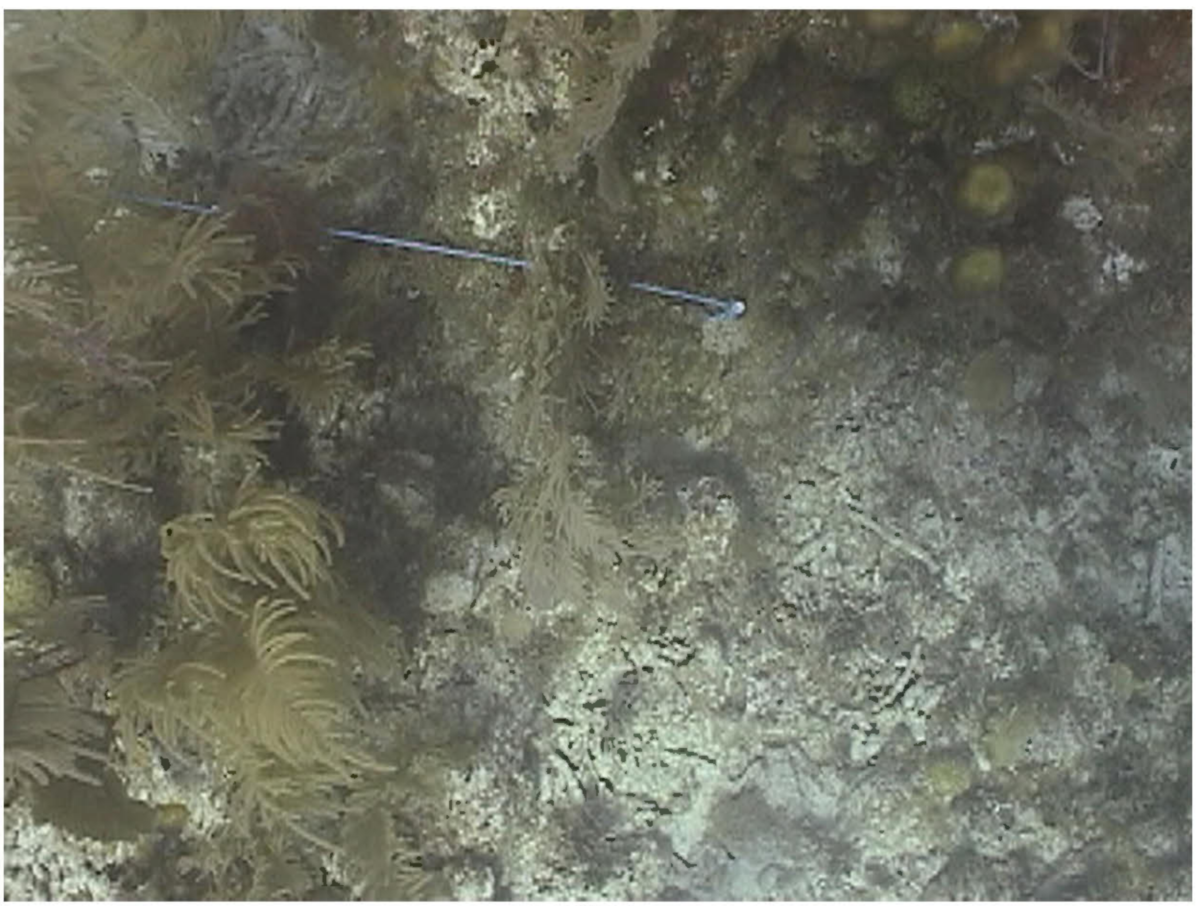
wp_193.bmp

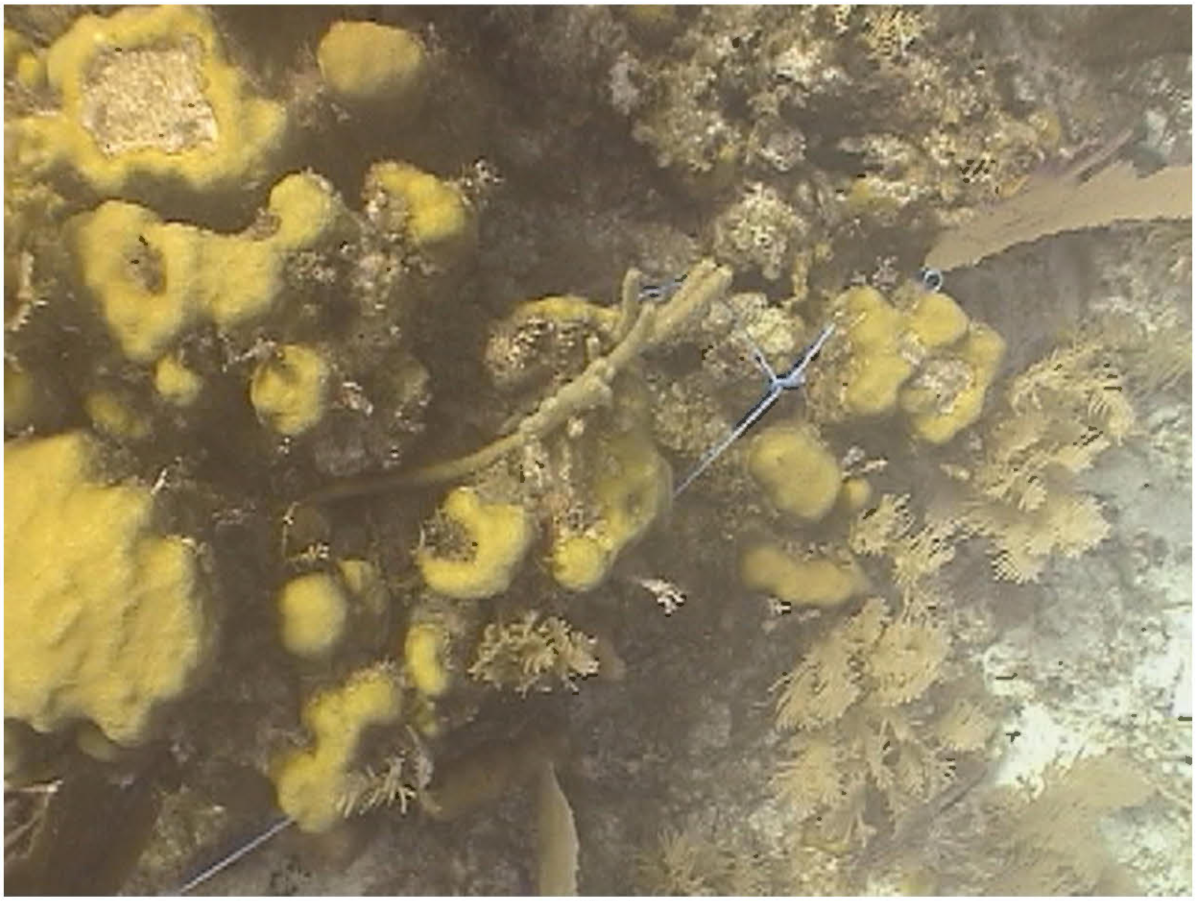
wp_194.bmp

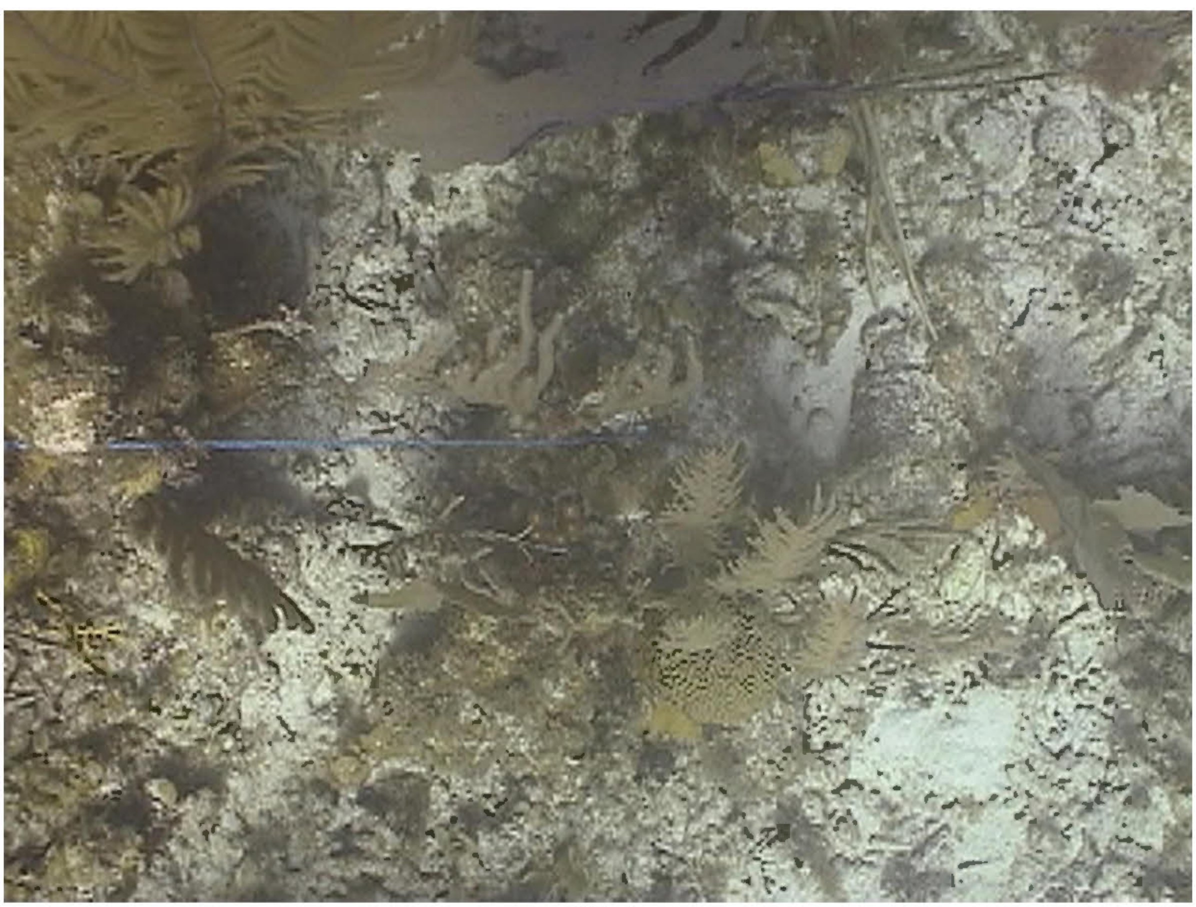
wp_195.bmp


wp_196.bmp

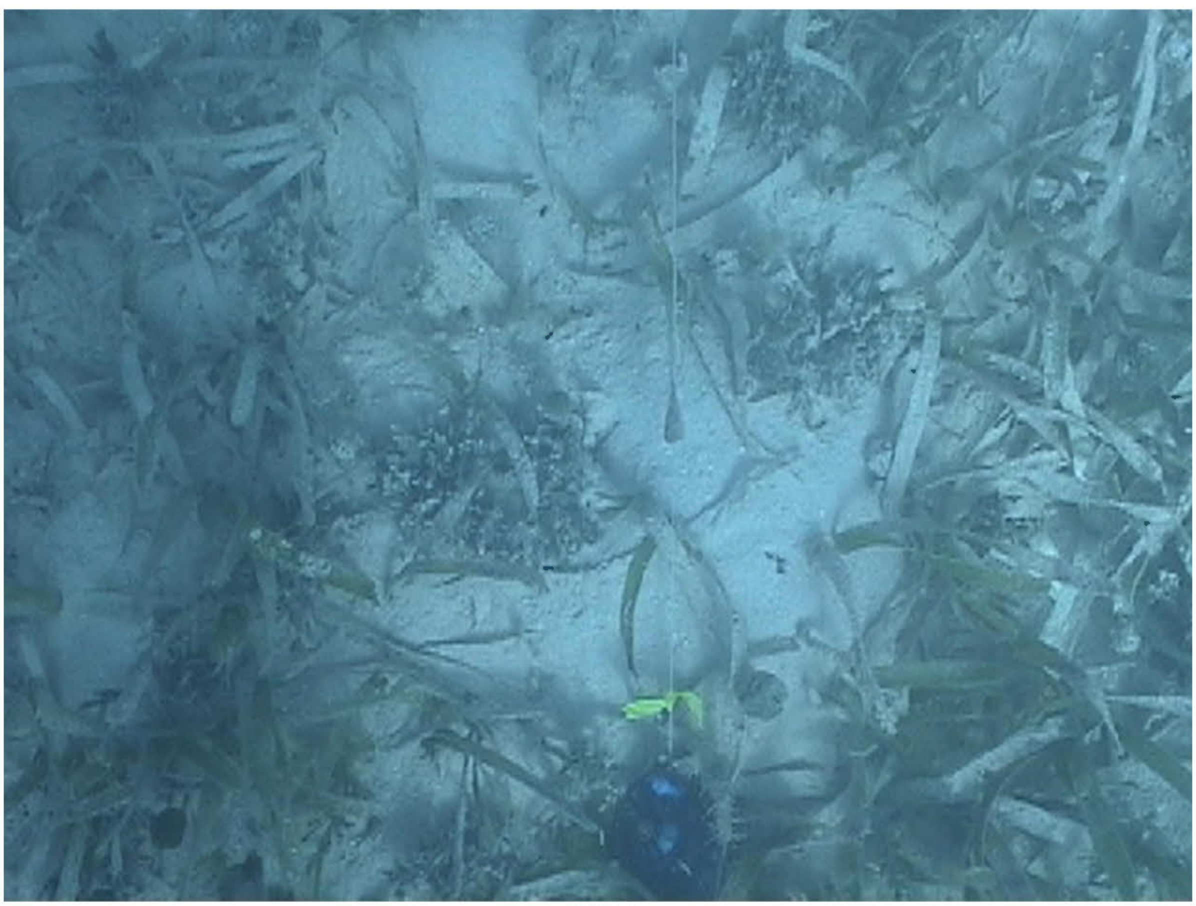
wp_197.bmp

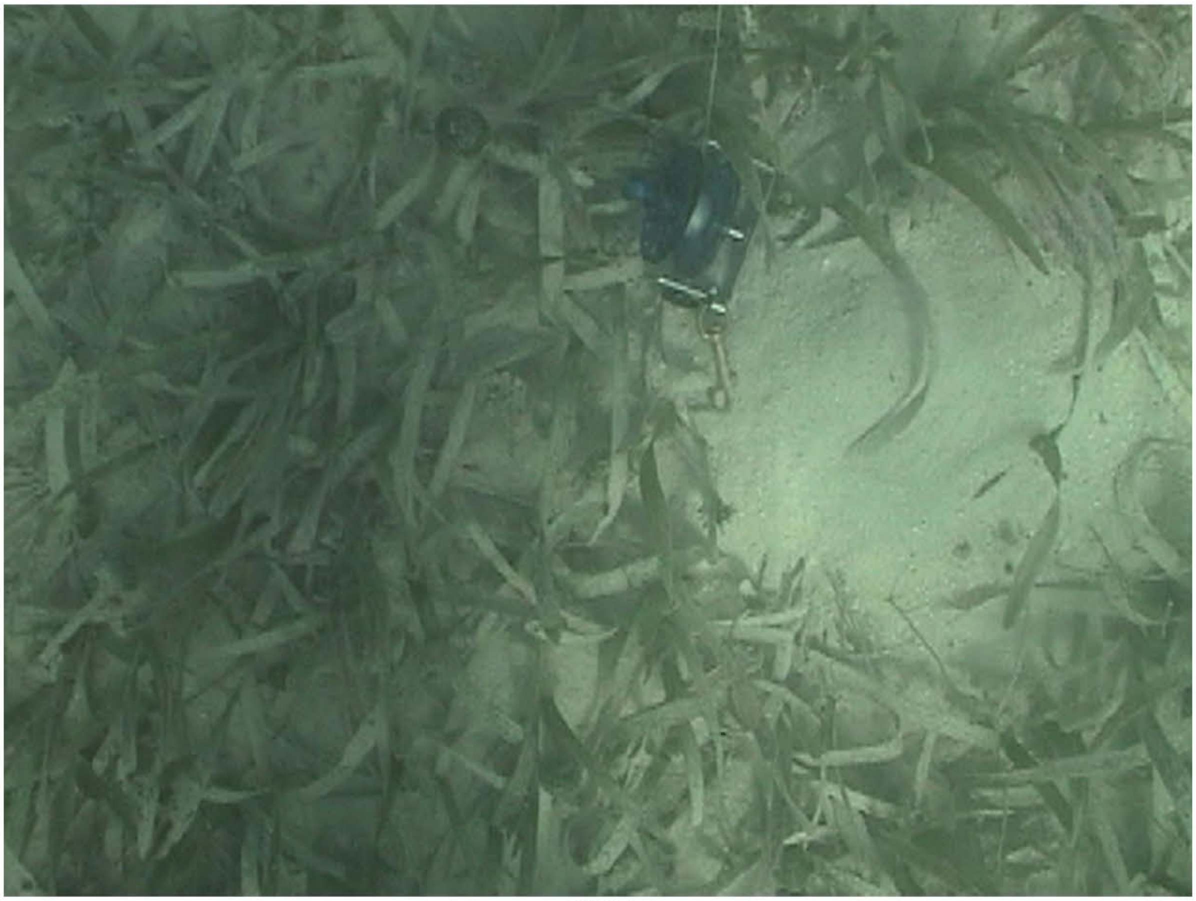

wp_198.bmp

wp_199.bmp

wp_200.bmp